Master's Thesis

Performance Analysis of a Savonius Rotor for Wave Energy Conversion

Supervisor: Prof. Dr. Young-Ho LEE

2010 - 06 - 21

Graduate School of Korea Maritime University

Department of Mechanical Engineering

Submitted By:

Mohammed Asid Zullah

In partial fulfilment of the requirements for the degree of Master of Mechanical Engineering

본 論文을 李珍雨의 工學碩士 學位論文으로 認准함

We certify that we have read this thesis and that, in our opinion, it is satisfactory in scope and quality as a thesis for the degree of Master of Mechanical Engineering.

THESIS COMMITTEE

Chairperson: Prof. Dr. Young-Ho LEE
Division of Mechanical & Information Engineering, Korea Maritime University.

____

Co-Supervisor: Prof. Dr. You-Taek KIM
Marine System Engineering, Korea Maritime University.

____

Co-Supervisor: Prof. Dr. Kweon-Ha PARK
Division of Mechanical & Information Engineering, Korea Maritime University.

____

June 2010

Graduate School of Korea Maritime University

Department of Mechanical Engineering

본 論文을 李珍雨의 工學碩士 學位論文으로 認准함

위원장: 공학박사 이 영 호

위 원: 공학박사 김 유 택

위 원: 공학박사 박 권 하

2010년 06월 21일

한국해양대학교 대학원

기 계 공 학 과

TABLE OF CONTENT

Abstract...I

List of Tables..VII

Lit of Figures..VIII

Nomenclature...XIII

Chapter 1 INTRODUCTION...1

1.1 General...1

1.2 Ocean Waves..2

1.2.1 Power Rating..6

1.2.2 Wave Energy Availability..9

1.3 Reasons for a Renewed World

Interest in Wave Energy..11

1.4 Wave Energy Converters...16

1.4.1 Advantages...16

1.4.2 Factors When Applying WECs...............................16

1.5 Classification of a Wave Energy Device....................17

1.5.1 Location..17

1.5.2 Operating Principles...18

1.5.3 Directional Characteristics.....................................19

1.5.4 Potential and Kinetic Energy..................................20

1.6 WECS Electric Power Generation................................23
1.7 Challenges..25
1.8 Numerical Analysis of Savonius Type
Turbine for Wave Energy Conversion........................29
1.8.1 OWC Type Wave Devices.......................................32
1.8.2 Savonius Rotor...34

CHAPTER 2 NUMERICAL ANALYSIS..................................37
2.1 Introduction..37
2.2 Modeling..38
2.3 CFD Analysis Setup..42
2.3.1 Domain Setup...42
2.3.2 Numerical Results..44
2.2.3 Mesh Generation...45
2.3.4 Boundary Conditions...47
2.3.5 Wave Generation...48
2.3.6 Multiphase...49
2.3.7 Solver Controls...50
2.4 Turbulence Modeling...52
2.4.1 k-ε model..54
2.4.2 The Shear Stress Transport Model.......................55

CHAPTER 3 RESULTS AND DISCUSSION..........................57
3.1 General..57
3.2 Numerical Tank...58
3.2.1 Numerical Wave Tank with OWC...........................63
3.3 Reflector in the Rear Bottom of the OWC..................66
3.4 Rotor Angle and Helical Blade Analysis......................73
3.4.1 3 Bladed Savonius Rotor Angle Analysis..............74
3.4.2 3 Bladed Helical Savonius Rotor Angle Analysis..82
3.5 OWC Inlet Section Analysis...88
3.6 5 Bladed Savonius Rotor Analysis...............................95

CHAPTER 4 CONCLUSION...99

ACKNOWLEDGEMENT...103

REFERENCES...104

APPENDIX A...112

Performance Analysis of a Savonius Rotor for Wave Energy Conversion

Mohammed Asid Zullah

Department of Mechanical Engineering
Graduate School of Korea Maritime University

Abstract

Ocean wave energy is rapidly becoming a field of great interest in the world of renewable energy. Significant advancements in design and technology are being made to make wave energy a viable alternative for our growing energy demands. Ocean waves are a significant resource of inexhaustible, non-polluting energy. Wave energy converters (WEC) provide a means of transforming wave energy into usable electrical energy. The development of these devices is undergoing rapid change. An overview of the various operating WEC is presented, classifying them according to shoreline, near shore and offshore applications. The prior concept of using an oscillating water column (OWC) with a savonius rotor at the bottom of the rear chamber as a potential WEC is of interest. (Under certain conditions and water depth, wave action in the OWC induces a reverse flow. As proposed, this reverse current

could generate electric power by rotating the blades of a savonius rotor turbine).

A numerical study of the savonius type direct drive turbine in typical chamber geometry of an oscillating water column chamber for wave energy conversion was carried out. The research deals with a numerical modeling devoted to predict the turbine efficiency in the components of an oscillating water column system used for the wave energy capture, the flow behavior is modeled by using the commercial code ANSYS CFX (11). Several numerical flow models have been elaborated and tested independently in the geometries of a water chamber with a savonius type wave turbines

Constant periodic wave flow calculations were performed to investigate the flow distribution at the turbines inlet section, as well as the properties of the savonius type turbine. The flow is assumed to be two-dimensional (2D), viscous, turbulent and unsteady. The commercial CFD code is used with a solver of the coupled conservation equations of mass, momentum and energy, with an implicit time scheme and with the adoption of the hexahedral mesh and the moving mesh techniques in areas of moving surfaces. Turbulence is modeled with the k-e model. The obtained results indicate that the developed models are well suitable to analyze the water flows both in the chamber and in the turbine. For the turbine, the numerical results of pressure and torque were compared with each other.

The primary stages of the research effort can be described as follows;

Firstly, a comprehensive literature survey was done to find those articles that deal specifically with wave energy conversion. Gleaned from this is the effect, that variances in technology, location, developments and etc (Appendix).

Secondly, development of a 3D numerical wave tank using CFD that can represent the physical model to an appropriate order of accuracy whilst maintaining realistic computational effort. Furthermore, extend the numerical wave tank to include a detailed OWC to determine energy capture efficiencies.

Thirdly, determine the effect of various 3 bladed savonius geometric parameters on efficiency

Fourthly, A mitigation technique that involves altering the geometry of the OWC chamber inlet section was studied.

Finally, the best geometric models were combined to obtain the highest efficiency for 5 bladed savonius rotor

The results obtained show that with careful consideration of key modeling parameters as well as ensuring sufficient data resolution. The results of the testing have also illustrated that simple changes to the front wall aperture shape can provide marked improvements in the efficiency of energy capture for OWC type devices.

LIST OF TABLES

Table 1.1 List by China New Energy of Active Wave Energy Devices In Each Country of the World [28]..................13

Table 2.1 Fluid Conditions..45

Table 3.1 Reflector Plate Performance Analysis.........................65

Table 3.2 Performance Analyses of the Savonius Rotor............69

Table 3.3 Performance Analyses of Helical Savonius Rotor......69

LIST OF FIGURES

Figure 1.1 OWC Power Curves [14]..5
Figure 1.2 Sources of Wave Energy Generalized
in kW/m^2[23]..10
Figure 1.3 Average Wave Power Availability in kW/m of Wave
Front Source [22]...10
Figure 1.4 Classification of Wave Devices [36]..........................21
Figure 1.5 Configurations of WECS Used to Generate
Electric Power [36]..25
Figure 1.6 The Plan View of Jeju Islands Outer Port................29
Figure 1.7 Power take-off alternatives and steps of wave
energy conversion...33
Figure 1.8 Principles of an OWC Type Wave Energy Device...31
Fig. 1.9 Conceptual Models of the Curtain Type Wall
Breakwater with OWC Chamber..35
Figure 2.1 2D Modeling of Driving Principle of the Savonius
Rotor..39
Figure 2.2 Schematics Diagram of the Numerical Domain.........40
Figure 2.3 Schematic Diagram of Turbine Location...................40
Figure 2.4 Numerical Wave Tank Fluid Models by Parts..........40
Figure 2.5 Bladed Savonius Rotor Fluid Model by Parts...........41

Figure 2.6 Full Model of the Calculation Domain
with 3 Bladed Savonius Rotor at the Rear OWC........................40
Figure 2.7 Schematic Domains with Boundaries.........................43
Figure 2.8 NWT Systematic Schematic......................................44
Figure 2.9 Typical Mesh for the Domains (Refined mesh
near the free surface)..46
Figure 2.10 Numerical Wave-Maker Set-up...............................49
Figure 2.11 Representation of the Control Volume Associated
with Each Mesh Node...52
Figure 3.1 Development of the wave profile in the
numerical wave tank...59
Figure 3.2 Time history of wave elevation of different
turbulence model for t=60s...62
Figure 3.3 Monitor point locations for pressure prediction........63
Figure 3.4 Predicted wave heights at the desired
locations...64
Figure 3.5 Superficial velocity contours in the
numerical wave tank...65
Figure 3.6 Schematic of the reflector plate at the
rear bottom of OWC..67
Figure 3.7 Average torque graph of 3 bladed savonius
rotor with the respective reflector plate...................................70

Figure 3.8 Graphical representation of reflector
plate performance..70
Figure 3.9 Superficial Velocity of Vector Diagram at
Maximum Torque...72
Figure 3.10 Schematics Showing Savonius Rtor with Various
Rotor Angles...74
Figure 3.11 Graphical Representation of the Performance
Analysis of the Savonius Rotor Angle..75
Figure 3.12 Velocity vector around the savonius rotor
during inflow in time increment of 0.53s...................................77
Figure 3.13 Velocity vector around the savonius rotor
during outtflow in time increment of 0.53s.................................79
Figure 3.14 Instantaneous torque of savonius rotors
with numerical time integration for 20seconds...........................80
Figure 3.15 Schematics Showing Savonius Rotor with Various
Rotor Angles...83
Figure 3.16 Graphical representation of the performance
analysis of the helical savonius rotor..84
Figure 3.17 Helical blade 2D flow analysis................................85
Figure 3.18 Instantaneous velocity vectors around 75°
helical savonius rotor at the 3 planes for a full cycle...............86
Figure 3.19 Schematic of various front wall aperture
shapes...89

Figure 3.20 Average velocity for different inlet shapes in XY plane at z = 0..90
Figure 3.21 Average velocity for different inlet shapes in XZ plane at y = 0..91
Figure 3.22 Circumferential average velocities at turbine location..92
Figure 3.23 Velocity vector at the inlet section for the period t=6.4s...94
Figure 3.24 Schematics of 5 bladed savonius rotor with various inlets section..96
Figure 3.25 Instantaneous velocity vectors a 5 bladed savonius rotor for a full cycle of 6.4s...97

NOMENCLATURE

α	wave amplitude	[m]
b:	width of the chamber opening,	[m]
d	water depth	[m]
g	acceleration due to gravity	[m^2/s]
Hi	incoming wave height	[m]
ΔH	change in water height in OWC	[m]
N	rotational speed of the turbine	[RPM]
$P_{\tau ave}$	average torque power	[W]
P_{Wave}	wave energy flux	[W/m]
T	wave time period	[s]
w	wave frequency	[Hz]
Y_{dis}	wave maker plate displacement	[m]
ρ	: density of working fluid	[kg/m^3]
τ	average torque	[N.m]
ω	angular velocity	[s^{-1}]

λ　wave length　[m]

η : total efficiency　[%]

CHAPTER 1 INTRODUCTION

1.1 General

The quest for clean sources of energy is far from the only challenge facing the societies and environments of the world. Poverty, disease, war, hunger, the destruction of natural habitats, eutrophication of water bodies, and the dwindling supply of fresh water are problems that sometimes feel almost forgotten today when most media and societal focus is on global warming and the emission of greenhouse gases. Still, with this imbalance in mind, the utilized energy sources and the energy generating processes tie into many of these problems in addition to the melting of the ice caps, and modern renewable energy technologies avoid a lot of the unwanted effects of traditional energy sources. The road to a future with little but non-polluting energy sources is, however, both long and difficult. Today fossil fuels make up approximately 80% of the gross primary energy used in the world's societies, and the International Energy Agency (IEA) anticipates that the same will be true in year 2030 in addition to a projected increase in global energy consumption by 1.6% per year [1]. The quest for clean sources of energy is therefore both important and urgent, but it is simultaneously hard pressed from competition with fossil fuels. Renewable energy technology that can start to compete with traditional energy sources at an economic level, without subsidies, is greatly needed. That ocean waves carry a vast pool of energy has been known for a long time [2, 3].

Estimates account for power levels in the order of one terawatt descending on the coastlines of the world [4]. Moreover, the potential for a relatively high utilization, in combination with the fact that moving water, due to its high density, is a dense carrier of energy, suggests that ocean waves is a viable source of renewable energy. Still, as wind and solar power industries continue to grow exponentially, wave power technologies are all but absent from the world market. It is an area of multiphysics where conventional solutions do not exist. On the contrary, the lack of them has been a defining characteristic of wave power research over the years, and this is also the case among the larger projects still being researched today [5-13]. Wave power development has faced many difficulties, hence the multitude of solutions. Some of the major challenges are the survivability of parts exposed to the forces of the ocean, investment costs associated with large structures, excessive over-dimensioning needed to handle mechanical overloads, long life mooring difficulties, transmission of energy to shore, and the transformation of wave motion into high-speed, rotating generator motion. Wave power R&D has seen many mechanical solutions to these challenges, and most inventions have had a primary focus on hydrodynamic and mechanics.

1.2 Ocean Waves

Ocean wave energy is generally considered as a fuel-free, clean, renewable energy with a vast resource potential. With mounting environmental concerns about traditional methods of energy production and the ever increasing demand for energy, research into wave energy extraction technologies has experienced renewed interest in recent times. In order to ascertain how much energy a wave energy device will be able to convert to useful energy, the potential power available to the device at the site it is located must first be determined. Also, the estimation of the incident wave power is an important step in the design of wave energy devices because if the equipment is rated too high it will be under utilized most of the time; on the other hand if it is rated too low it will be unable to capture much of the available energy or may be damaged. The potential power is quantified in the form of the annual average incident wave power.

The oceans contain enormous amounts of energy that is dissipated along the world's coastlines. It has been estimated that the practical world wave energy resource is somewhere between 2000 TWh and 4000 TWh annually [14]. To put this into perspective, this equates to a value of approximately 20% of the world's electricity production in the year 2003 [15]. Consequently, energy from waves can be considered on the world stage as a power producing means. Perhaps even more importantly, given recent scientific understanding of the effects and drivers behind the greenhouse effect, wave power has the potential to play an important role as a carbon free energy resource. In general, the research and development for power utility scale wave energy devices is still in the elementary stages such that the net cost of energy is still somewhat higher than conventional or other forms of renewable power generation. Given this cost penalty there has been only limited commercial exploitation of this significant wave energy resource [16]. The net cost of energy can be principally summarized as sum of capital costs, operating and maintenance costs divided by the amount of energy produced reduced to a common cost base by using present value techniques shown in equation (1-1).

$$\text{Cost of Energy} = \frac{\text{Capital Cost} + \text{PV (O\&M costs)}}{\text{PV(Energy Production)}} \tag{1-1}$$

Although all three components to the equation are important drivers, studies such as those by The Carbon Trust (2006) have indicated that significant gains can be made in the short to medium term in the area of energy production, whereas capital and O&M costs improvements are more likely to occur in the medium term [14]. Thus, during this infancy stage in wave energy, it is suggested that design improvements to increase energy production may be an enabling mechanism to raise wave energy from a research area to a mainstream electricity generation discipline.

Energy Production from wave energy devices is a function of a number of areas including:

- The extent to which energy capture device is matched to the wave resource.
- The efficiency of the systems of energy conversion.

◆ The proportion of the time the device is able to generate.

These areas are illustrated in Figure 1.1 which illustrates a typical power conversion multi-dimensional graph that plots power output against axes of wave period and wave height. The feature of prime importance in energy production is the 'Power Captured by Device' which is simply the efficiency with which a device can capture the incoming wave energy. This figure also identifies key operational aspects such as minimum cut-in conditions whereby no power is generated and power shedding conditions whereby the device either moves into a survival mode in large waves or the power absorbed exceeds the capacity of the generating equipment. It is however the accurate modeling and optimization of this power capture efficiency that is the prime motivation for this present investigation.

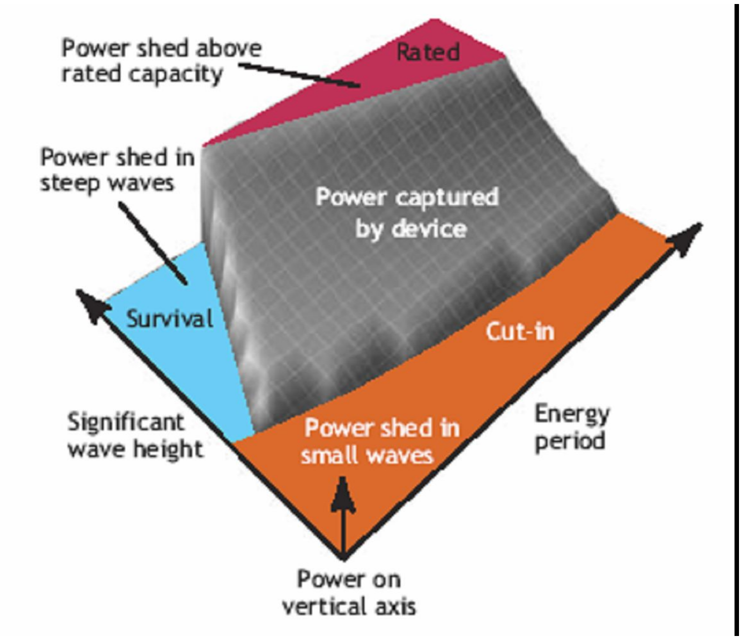

Figure 1.1 OWC Power Curves [14]

1.2.1 Power Rating

Winds are created by the differential heating of the earth's surface by solar energy, and when blowing over water, they transfer their energy into waves. The amount of energy transferred depends on the wind speed, time applied and distance covered ("fetch"). Solar energy of ~ 100W/m^2 is converted into waves typically of 10-50kW/m [17]. Even though the wind may change direction or diminish in magnitude, storm generated irregular waves continue to travel away from their source. Waves generated in deep water can travel great distances with very little loss in energy. They eventually become regular smooth waves or "swell". In linear theory, the total energy of waves in deep water can be determined using equation (1-2).

$$E = E_p + E_k = \frac{\rho g H^2 L b}{8} \qquad (1\text{-}2)$$

Where Ep is the potential energy and Ek is the kinetic energy of the wave. The other parameters are ρ the density of water, g the acceleration of gravity, H the waveheight, L the wavelength and b the width of the wave crests. Wave energy is expressed as total energy per unit crest (E/b) or joules per meter (J/m) or foot-pound per foot (ft-lb/ft).

Power is the total work done per total time interval. The wave energy transferred in the direction of the wave from one point to the other is the energy flux or more commonly known as wave power. Equation (1-3) is defined by linear theory as

$$P = \frac{\rho g H^2 C_g b}{8} \qquad (1\text{-}3)$$

Where C_g is the group velocity. In deepwater; (d>L/2) where d is the water depth, the group velocity is equal to the phase velocity (celerity) divided by; $C_g=C/2$. For shallow water (d<L/2) the group velocity equals the phase velocity; Cg=C [18]. Wave power is expressed as the total power per unit crest (P/b) in units of kilowatts per meter (kW/m).

(Note: 1 watt = 1 Joule/s = 1 Newton.m/s=1kgm^2/sec^3).

In deep water, the power in watts per unit meter of wave width is expressed in equation (1-4, 1-5) [19].

$$\dot{P} = P/b = \frac{\rho g^2 H^2 T}{32\pi} \tag{1-4}$$

Where

$$Cg = \frac{L}{2T} = \frac{1}{2T} = \left(\frac{gT^2}{2\rho}\right)\text{(Deep water)} \tag{1-5}$$

The above expressions for wave power are for regular waves. Ocean waves are irregular in nature and can be expressed by linear theory as the superposition of waves of varying height, period and direction. For a certain length of time, the sea conditions can be considered constant and represented by a directional wave spectrum. Power is expressed by significant wave height H_s and energy (peak) period T_P in seconds, where [20].

$$\dot{P} = 0.42 H_S^2 T_P \tag{1-6}$$

Power P is the estimated power in kW/m, significant height H_S is in meters, and peak wave period T_P in seconds. The significant wave height is the average height (trough to crest) of the one-third highest waves valid for the wave spectrum. “The 0.42 multiplier in the above equation is exact for any sea state that is well represented by a two-parameter Bretschneider spectrum, but it could range from 0.3 to 0.5, depending on the relative amounts of energy in the sea and swell components and the exact shape of the wave spectrum” [20].

Bretschneider and Ertekin provide four different methods for estimating the amount of wave energy around the Hawaii an Islands [21]. Hagerman and Bedard describe how to estimate the annual average incident wave power at a selected location [20]. For a given measurement record, the estimated incident wave power recorded was sorted into sea state bins of H_S and T_P. The 8 percentage of time that a given sea state bin occurs can be determined by dividing the number of records in the bin by the entire number of records in the measurement period. When multiplied by the hours in a year [8766 hrs - 29 days in February every 4th year] results in the number of hours that sea state occurs. Multiplying the hours the sea state occurs by the wave energy contribution (kW/m) gives the wave energy contribution for that bin (kWh/m). The annual average incident wave power is calculated using the equation (1-7) which is the summation of wave energy contribution of all bins divided by the number of hours in a year [20]:

$$\overline{P} = \sum\left(\frac{\text{records}}{\text{totalrecords}}\ x\ 8766\text{hrs}\ x\ \dot{P}\,\frac{\text{kW}}{\text{m}}\right) \tag{1-7}$$

To obtain performance data from various WEC manufacturers, Hagerman and Bernard send out templates to various vendors to fill out bins of H_S and T_P with the respective capture width ratio (CWR) of their device;

$$CWR = \frac{P_{abs}}{(JD_y)} \tag{1-8}$$

where "Pabs = Absorbed power or modeled sea state (before losses in conversion in electric power) J is the incident power in simulated or modeled sea state and D_y is the cross-wave dimension of the simulated device or test model" [20]. Each template covers approximately 85% of the annual available wave energy. Hagerman and Bernard mention that test results determined from the mean zero-crossing period (T_Z) for the Pierson-Moskowitz Spectra can be converted to peak period by using equation (1-9):

$$T_P = {T_Z}/{0.710} \tag{1-9}$$

1.2.2 Wave Energy Availability

Wave energy availability and concentration varies with the locality. Not all coast lines are good candidates for a WEC installation. Figure 1.2 gives an overview of world average available wave energy. Graw (2002) generalized the wave energy into zones as shown in Fig. 1.3.

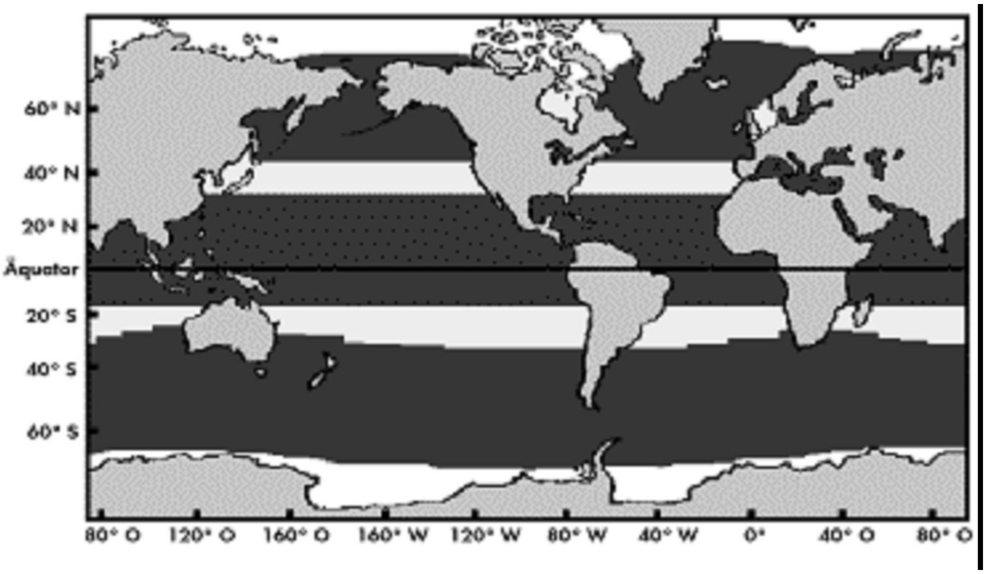

Figure 1.2 Sources of Wave Energy Generalized in kW/m^2 [23]

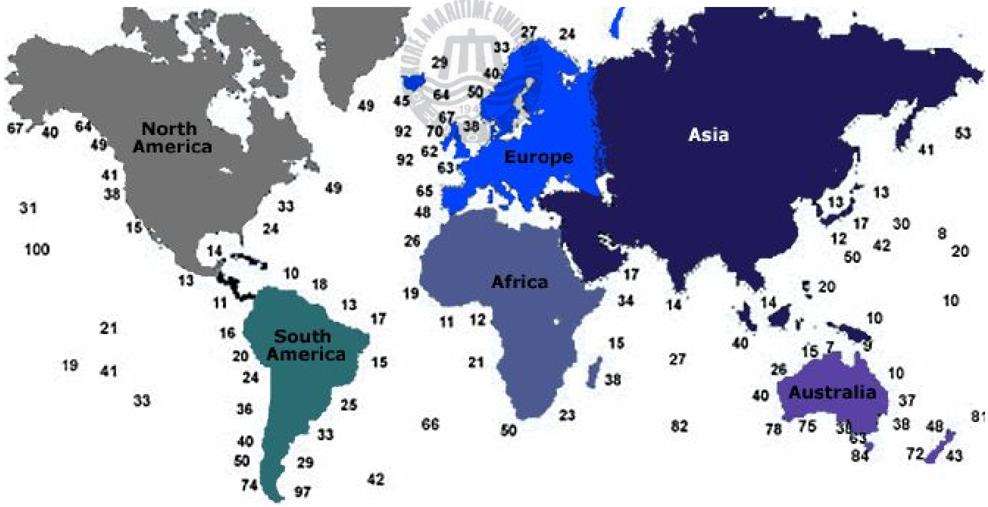

Figure 1.3 Average Wave Power Availability in kW/m of Wave Front Source [22]

Large wave densities are experienced on those coasts that have prevailing winds and long fetches such as the western coasts of Americas , Europe and Australia / NewZealand Coasts. Hagerman and Ertekin et. al. determined the available wave energy around the islands of Hawaii [24, 25].

To maximize the capture of wave energy by a WEC, the location of the device is important. Convex bathymetries such as headlands and submarine ridges can concentrate wave energy while the seabed and bays disperse wave energy. As waves approach the shore they are altered by refraction, diffraction and reflection when the water depth is less than one half the wavelength ($d < L/2$) or in depths in most cases less than 100m. For this phenomenon, energy is conserved. Wave energy is dissipated by wave breaking and bottom friction. Thus as WECs are installed in depths less than 100m and closer to the shore they will experience a decrease in the available wave energy that can be captured depending on the slope and roughness of the sea floor. Wave breaking can be important to limit wave forces on devices during storm conditions. Refraction is important for WECs that are directional dependent or that weather vane into the direction of the waves.

1.3 Reasons for a Renewed World Interest in Wave Energy

- The price of oil continues to increase. The output of existing oil fields is decreasing due to depleted supply and water or air is being pumped down to extract more oil. New sources of readily available oil are becoming more costly to find and develop because the remaining oil reserves are located deeper in the earth's crust. The demand for oil has increased with the economic growth of

Asia, especially India and China. Also many of the sources of oil are located in countries with unstable regimes.

- WECS have benefited from the oil industry, as offshore platforms have been operated successfully in rough sea environments. Placing wave energy devices further out to sea increases the available wave energy that can be captured. With the significant advancement of electronics, costs of components have plummeted and the power output and efficiency of electronic devices have improved. Dynamic systems using electronics can respond better to variances, i.e., changes in wave conditions. Converter technology has improved such that off the shelf units are readily available to convert the low frequency of a wave system and match it the higher frequency of the power grid. They also permit coupling of power grids of different frequencies, i.e., 50 Hz to 60 Hz system.
- Undersea cables have improved with the development of offshore platforms for oil and wind applications, paving the way for transmission of energy from offshore WECs.
- Advances in industrial control are providing new control systems that can be applied to WECS in a changing wave environment.
- With the development of population centers near coastal areas, the power grid is more readily accessible for coupling to wave energy devices.
- Advances in wind turbine technology have raised public awareness to the advantages of alternative sources of power. Many of the wind turbines are being installed

offshore. The wind is of a more constant steady flow rather than the turbulent flow which occurs over an irregular land surface. Wavegen has proposed making a wave energy device that is mounted on the same platform that the wind turbine is built on [26]. Wind turbine technologies uses the same power generation auxiliaries as wave energy, i.e., submarine cables, converters, transformers, power grid, etc.

- Hydro technology is a well-established field. Many of the wave energy devices using the tapered channel concept, that is storing elevated water through wave action, use a hydro-turbine to convert the potential wave energy into electrical energy.
- The Kyoto Treaty in 1997 has encouraged signatory governments to set targets for renewable energy [27].

Table 1.1 List by China New Energy of Active Wave Energy Devices In Each Country of the World [28]

Location	Technology	Capacity	Status
Norway	Multi Resonance Oscillating water Column	0.5	Operated in 1985 to 1989
Norway	Wave Convergence Reservoir	0.35	Put into operation in 1990
Japan	Wave Embankment Oscillating Water Column	0.06	Put into operation in 1988
Japan	On-Shore Oscillating Water Column	0.03	Put into operation in 1988
Japan	Swing Plate Type	0.005	Put into operation in 1983
Japan	Moored Barge Oscillating Water Column	0.125	Pilot operation in 1978 to 1980

Japan	Moored Backward Bent Duct	0.12	Started to pilot operation in 1998
India	Offshore Fixed Oscillating Water Column	0.15	Completed in 1991
Portugal	Onshore Oscillating Water Column	0.5	Completed the civil engineering, planned to run in 1999
England	Offshore Fixed Oscillating Water Column	2	Failed to operation in 1995
Scotland	Onshore Oscillating Water Column	0.0075	Put into operation in 1990
Scotland	Onshore Oscillating Water Column	0.5	Under the construction
Sweden	Undulating Buoy	0.03	Pilot Operation in 1983 - 1984
Denmark	Undulating Buoy	0.045	Pilot in spring 1990
Wanshan Island, China	Onshore Oscillating Water Column	0.02	Pilot in 1996
Shanwei, China	Onshore Oscillating Water Column	0.1	Under the construction
Daguan Island, China	Swing Plate Type	0.05	Under the construction
Nanhai, China	Moored Backward Bent Duct	0.005	Pilot in 1995

- The price of generated electricity by WECs is becoming more competitive as device efficiency has improved. Like wind turbines, WECs need to be placed where the energy density is high in order to be efficient. Improvements in wind technology have resulted in taller towers making available higher wind velocities. The wind power increases as the cube of the wind speed, so significant gains in power are obtained for each incremental increase in wind velocity and the return on investment improves [29, 30, 31]. The same is true with wave energy: the further offshore the devices are installed, the greater the available wave energy to be captured and the better the return on investment, assuming the device can withstand the wave conditions.

- Devices are becoming modularized; so many devices can be woven together into an integrated power system. This simplifies the device construction, reduces the cost as duplicate units are manufactured and increases the reliability as failure of one device does not bring the power system down.

1.4 Wave Energy Convertors

1.4.1 Advantages

- Utilizes an unlimited source of power
- Dissipation of wave energy can help protect the coastline
- Modular design means relatively short time period to receive a return on investment
- Can be part of harbor development - wave protection or aeration of water
- Applications applied to desalination
- Minor visual impact from the shore
- Potential for aquaculture
- Local economic development
- Generation of hydrogen with electrolysis of water

1.4.2 Factors When Appling WECs

- The longer the wavelength, the greater the wave power
- Wave power is greatest for deep water conditions and is reduced for depths less than half a wavelength
- Waves are difficult to harness as they vary in direction, wave height, wavelength and are able to withstand impact (durable)
- Extreme wave conditions can occur. The device must be robust enough to withstand or avoid (submerge etc.) these

extreme conditions.

- Distribution of power may require submarine cables, and grid extension
- Navigational, fishing regulations need to be considered
- Tidal variations can affect mooring and efficiency of the device
- Visual impact from the shore must be considered

1.5 Classification of a Wave Energy Device

Harris et al. provides a good overview of how to classify the various wave energy converters [32]. Three principle areas are mentioned: location, operating principles and directional characteristics. Devices can also be classified according to size relative to incident wavelength. WavePlane International A/S differentiates their over topping device from other Wave Energy Converters (WECs) by comparing how the devices capture kinetic and potential energy of the wave [34]. The following is a summarization of these classifications.

1.5.1 Location

WECS were initially developed on the shoreline and thus are defined as first generation devices. Later, near shore or seabed anchored second generation devices resulted. Utilizing concepts from first and second generation devices, third generation or offshore WECs evolved. The time to develop third generation devices is longer due to the harsher sea environment these WECs have to contend with resulting in higher installation costs.

1.5.2 Operation Principles

The operation principles of WECS can be broken into three main areas: Oscillating Water Columns, Overtopping Devices and Wave Activated Bodies.

1. Oscillating Water Column (OWC) -These devices use wave action to expand and compress air above a water column, to rotate an air turbine / generator, i.e., Wells Turbine.
2. Overtopping Devices (OTD) –For OTD devices, waves spill over into a reservoir, elevating the water above the sea level so that it can be used to run a low-head hydro turbine, i.e., Kaplan turbine.
3. Wave Activated Bodies (WAB) - WAB devices oscillate due to wave action relative to a fixed reference or to other parts of the body. For an oscillating body, the primary hydrostatic restoring forces are proportional to the amplitudes of heave, pitch and roll. Surge, sway and yaw require a restoring force to bring them back to equilibrium and for many of the devices are of less interest for wave energy capture. Many of the WAB devices use a hydraulic system to turn a

hydraulic/generator combination. For the mooring of WECs, nearshore devices generally use a gravity anchor where the device rests or is fixed to the seabed. Offshore mooring is much more complex and the sea environment is much harsher. The mooring must take into account the direction of the device relative to the incident waves as well as the loading and energy extraction of the device.

1.5.3 Directional Characteristics

Directional characteristics of WECs are in three main areas, point absorbers, terminators and attenuators.

1. Point Absorbers - These floating devices have dimensions that are small relative to the incident wave length. They can capture wave energy from a wave front that is larger than the dimensions of the absorber and WECs capture energy from waves varying from 40 to 300 meters in length [35]. These devices absorb energy from all directions.
2. Terminator - The principle axis of this device is aligned perpendicular to the direction of wave propagation and in essence “terminates” the wave action. An Efficient terminator will create waves that are exactly in anti-phase with incident waves. An inefficient terminator will reflect and transmit some energy, and capture the remainder.
3. Attenuator - The principle axis of this device is aligned parallel or in the direction of wave propagation and in

essence “attenuates” or reduces the amplitude of the wave. Both the terminator and the attenuator devices have length dimension equal to or greater than a wavelength. The efficiency of these devices is directionally dependent, thus they must weather vane relative to the direction of wave propagation. Stresses are less on the attenuator device as compared to the terminator, as the attenuator’s are a normal to the wave direction is smaller.

1.5.4 Potential and Kinetic Energy

WECS can also be classified as to their principle of operation, which is how they convert available potential and kinetic wave energy into useable electrical energy. WavePlane International A/S (2005) conveniently outlined these differences on their web site. This is summarized below and shown in Fig. 1.4 [36].

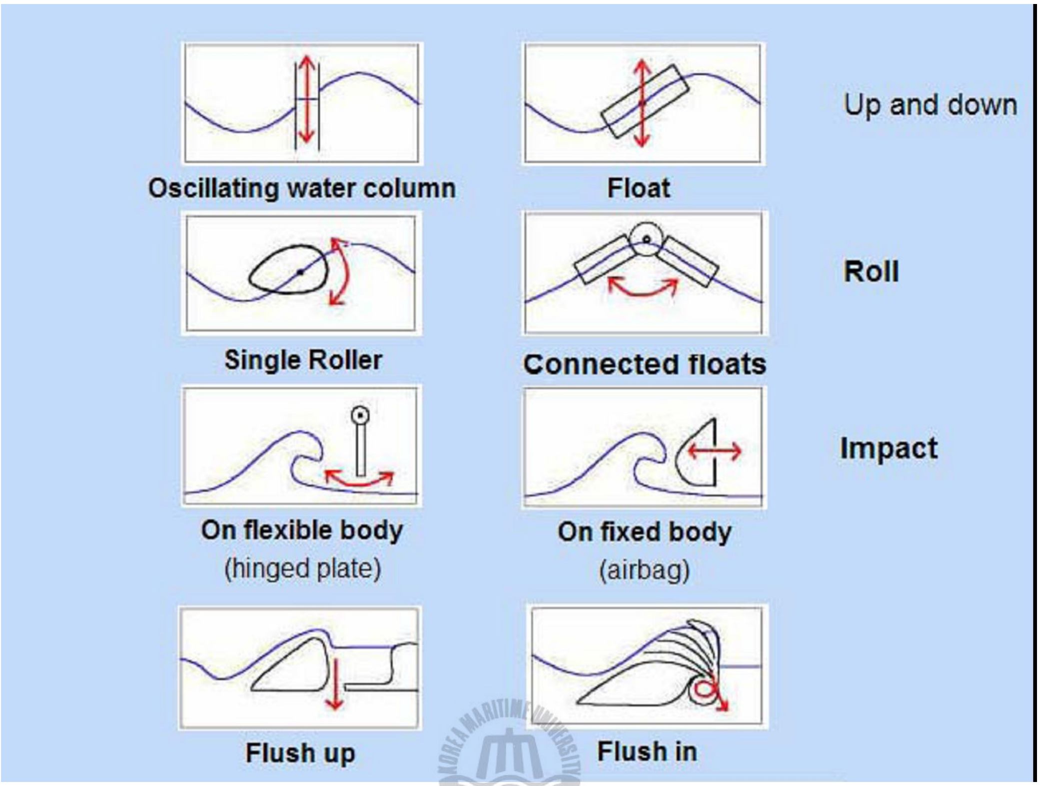

Figure 1.4 Classification of Wave Devices [36]

1. *Up Down Motion* - Many of the WECS use afloat, which undergoes an up/down or heave motion to push or pull against a fixed point, i.e., a block anchor, damping plate or large inertia to capture the potential energy of the wave. The efficiency of the device depends on its relative size to the incident wavelength. If the horizontal distance of the float in the direction of the incident wave is greater than $\frac{1}{4}$ of the wave length of the incident wave, the efficiency of the device decreases as the float tends to roll on its center of gravity. If its horizontal distance is greater than a wavelength, it tends to ride out several wave crests rather than moving downward into a wave trough. As the vertical

dimensions of the float increases, the center of gravity of the device is placed further beneath the wave, reducing the potential energy that can be captured. Smaller floats (point sources) use latching mechanisms to alter the phase relationship of the device relative to the wave, delaying its movement relative to the wave motion so that it over shoots the crest or trough of the wave, to capture more energy from the wave by being more in phase with the wave. Water in an OWC column also has an up down motion and its efficiency drops significantly if the column is smaller than $\frac{1}{4}$ of a wave length and goes to zero if the column reaches a width of one wave length. Heat energy is lost in the expansion and compression of air molecules.

2. *Roll* - Devices that roll with the waves extract both the kinetic and potential energy of the wave. To be efficient, they must oscillate at the same phase and amplitude of the wave. Generally one of the two parts moves relative to one another. Often multiple pontoons (raft) have a hydraulic cylinder placed across hinged sections, where the cylinder is expanded or compressed by the rolling action of the wave. The hydraulic cylinder moves a hydraulic motor to generate electricity. Energy is lost due to friction.
3. *Impact* - Waves impacting on a fixed or flexible structure capture the kinetic and potential energy of a narrow band of wave energy spectrum. Energy is lost due to the uneven surging action.
4. *Flush Up and Flush In* - WavePlane International A/S (2005) describes their WavePlane overtopping device as

incorporating both a flush up and flush in concept. Many shoreline devices like TAPCHAN use the flush up concept to store the wave's potential energy. This is accomplished through first channeling of the wave to increase its amplitude as it moves up a ramp before spilling over into a basin where the water is stored. The increased water elevation is then used to generate electricity, by rotating a hydro-generator as it returns to the sea. The WavePlane, in addition to capturing potential energy by the flushing up of the wave, applies the flush in concept, where it uses the kinetic energy of the wave to create a spinning vortex of water to turn an electric generator.

1.6 WECs Electric Power Generation

Wave energy conversion systems convert variable, low frequency wave energy (1 cycle/sec or less for wind generated waves) into electric power, which is transmitted to the stable electrical power grid (50/60 cycles/sec). As previously mentioned, WECs are classified according to three main operating principles: OSC, OTD and WAB, and are shown in Fig. 1.5.

An OSC device uses air as the active medium to drive an air turbine. Wave action in a water column, expands and compresses air which passes through an orifice, to increase its velocity. This bidirectional air flow is often applied to a Wells Turbine, as its blades are adjusted so that it turns in only one direction even though the air flow is in two directions. As the wav energy source varies in its magnitude, an AC/DC/AC converter is often used to provide an adjustable link between the variable generator output and the relatively fixed frequency and voltage of the grid. These converters phase their electronic devices forward or back depending on the power generation requirements.

The OTD device stores elevated water that it has captured from waves spilling over into a reservoir. This WEC has a more constant source of energy as it can regulate the flow of water through a hydro-turbine. Generally, an AC/DC/AC converter is not used for this wave energy converter.

Some of the WAB devices move a hydraulic cylinder, which pumps hydraulic fluid to turn a hydraulic motor coupled to a rotary generator. Newer WECs use linear generators, which generate electricity by moving a magnetic assembly within a coil. These magnets are connected to a shaft, which is attached to a float that moves up and down due to wave action. As this source of energy is variable, an AC/DC/AC converter is used to interface with the relatively fixed power grid. To reduce transmission losses when generating power to the grid, the voltage is raised and the current is lowered by means of a transformer.

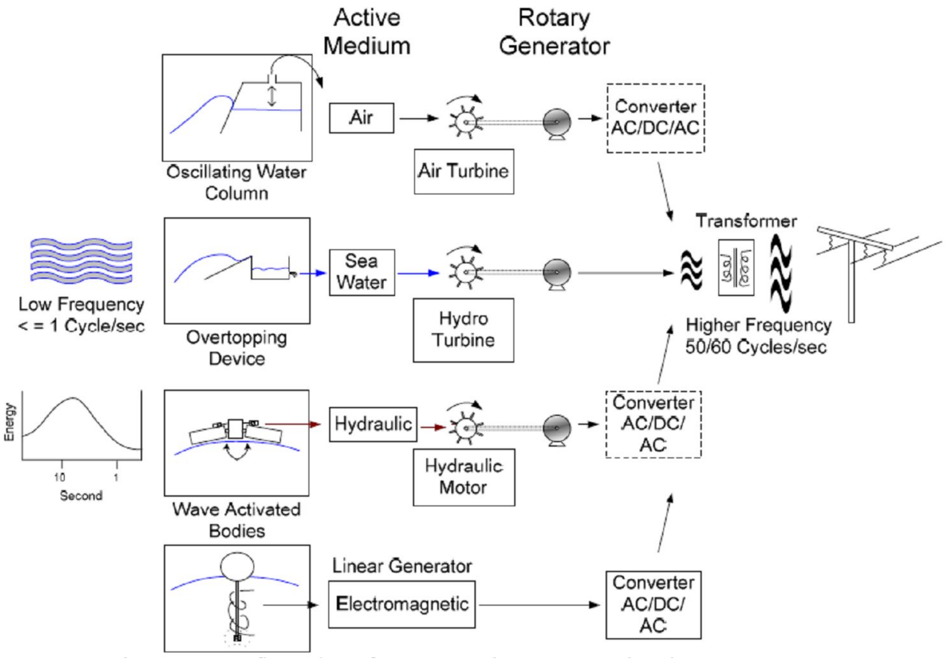

Figure 1.5 Configurations of WECS Used to Generate Electric Power [36]

1.7 Challenges

Some of the positive features of wave energy have been discussed above, and there are several more that all together seem to make wave energy an obvious choice as a source for renewable energy. Some of the features are: the relatively high utilization; the magnitude of the resource in the world; the slow variations in energy flux noted above when compared to wind power; the high energy density; that the energy is free in contrast to fuel based energy sources; installations are likely to have positive artificial reefing effects; and the degree to which wave energy would pollute the environment or add to greenhouse gas emissions is potentially insignificant compared to for example fossil fuels. If all of this is true then why is wave power, unlike the closely related wind power, hardly noticeable in the global energy system? The reason is that although research has been carried out since the 70s, similar to wind power, wave power has received less funding and fundamentally faces bigger challenges:

Extreme forces: Although the energy density in waves is high on average, it often reaches really great proportions during storms. Average power levels of storms may reach 50 times higher than the overall average. The consequences of this are large mechanical loads on the WECs, stress levels that need to be considered in the design stage. A standard practice in offshore constructions is to design the device so that it will survive the statistical 50 or 100 year wave. In general, however, it is not the extreme power levels that produce the energy, i.e. the revenue, for a WEC. Depending on the strategy used to avoid particularly high stress levels (requiring a device to hold for a 50 or 100 year wave) a heavy burden may be placed on the economy of the device. With this in mind, if possible, it is desirable to choose wave energy sites that naturally exhibit relatively small peak power levels in relation to the average power level.

Fatigue: One year of waves may easily result in over a million load cycles on the WEC. Although storm load levels will be relatively few the total number will be significant and the WECs resistance to fatigue needs to be carefully considered if the structure is intended to survive for years in the ocean.

Corrosion: Metal objects are sensitive to corrosion in the saltwater environment. Its weakening affects on the durability of a structure, together with fatigue, can have dire consequences and some form of cathodic protection is often warranted.

Working environment: The ocean is a difficult place to work. Unless it is a calm day it may be difficult to reach the WEC for the purpose of performing research, repairs, or maintenance. This plays a big role in the large development costs associated with wave energy.

Intermittency: As noted previously in Section 1.2.1 the intermittency of modern renewable energy sources such as wind, wave and solar is an unwanted characteristic of these energy sources. It makes them practically incapable of constituting the sole electric energy sources used in a society, at least as long as there is no capability for electric energy storage large enough to store energy from the time it is supplied, at the whim of nature, to when it is needed in society, at the whim of humans.

Marine life: Although biological life in the oceans may enjoy offshore structures to live on and around, they may hinder the operation of WECs. This problem is, however, likely to decrease with depth.

Societal conflicts: Fishermen, military, commercial ships and private boats all make use of the ocean. There is potential for conflicts of interest which can make the process of receiving permits for a wave energy installation very lengthy. *Energy price*: The cost of energy produced by the WECs has to be able to compete with other energy sources, and this is difficult for an immature technology. A few countries, Ireland, Portugal and the UK in particular, have implemented policies that promote the development and market introduction of ocean energy technologies [37]: In March 2007 the Irish government launched a target deployment of 500 MW of ocean energy by the year 2020. The Portuguese government has launched a feed-in tariff of up to 26Cc per kWh supplied to the electric grid depending on the development stage of the technology.

Harnessing ocean energy is truly a challenge spanning over many areas of physics, e.g. hydrodynamics, mechanics, solid mechanics, fatigue, electromagnetism, electrochemistry, electronics, power electronics, marine biology etc. If all of the above challenges are to be met, then a holistic perspective is critical to the designers of wave energy converters. Wave energy is an unforgiving field of engineering, and a smart solution at one end of the path, from energy in ocean waves to electricity on the national grid, may create great challenges at the other end.

1.8 Numerical Analysis of Savonius Type Turbine for Wave Energy Conversion

The typical period of waves in the ocean is about 10s or a frequency of about 0.1Hz. However, conventional electric generators operate at frequencies of about 60Hz. In order to connect the slow moving waves to high speed generators, most of the devices that have recently been proposed have used hydraulic or pneumatic intermediate power conversion systems. Under this arrangement, the slow motion action of the waves is used to pump a high pressure working fluid through a hydraulic motor. The motor then spins a generator at the required speed. A direct drive device couples the slow motion of the waves to the electric generator, which is usually a specially designed linear generator or a rotary generator with some kind of mechanical or magnetic form of thrust transmission and amplification of speed [38].

This study was carried out to develop a Jeju island piston-shaped wave-power generation system with Guanodong University, Korea Maritime University and Dae-lim Industry as shown in Fig. 1.6. The numerical analysis had been performed to evaluate the rotational performance and generated efficiency, which are the principal condition for wave-power generation, of a rotating turbine. Previously, 3 three types of analysis had been performed to decide the location and the size of turbine. A numerical analysis of a 2D cross-flow hydro turbine and wave flume which are precedent had also been performed [39].

Figure 1.6 The Plan View of Jeju Islands Outer Port

As shown in Fig. 1.6, Jeju Island outer port which has the western break water of 1,425 meters and the eastern break water of 390 meters is blocking waves from outside. Future plans are to develop a wave-power generation facility with water chamber-shaped installed in the break water like a curtain wall style, in the section of 46.5 meters after head section among the eastern break water of 390 meters.

There are three steps of wave energy conversion; primary energy conversion also known as first stage energy conversion, secondary energy conversion and tertiary energy conversion shown in Fig. 1.7. However, only secondary and primary energy conversion is part of the present study. Design modifications was made to the OWC for instance varying the OWC chamber and the inlet section as the primary energy conversion perfection and for the improvement of the secondary energy the turbine design was altered with respect rotor angles and number of rotor blades.

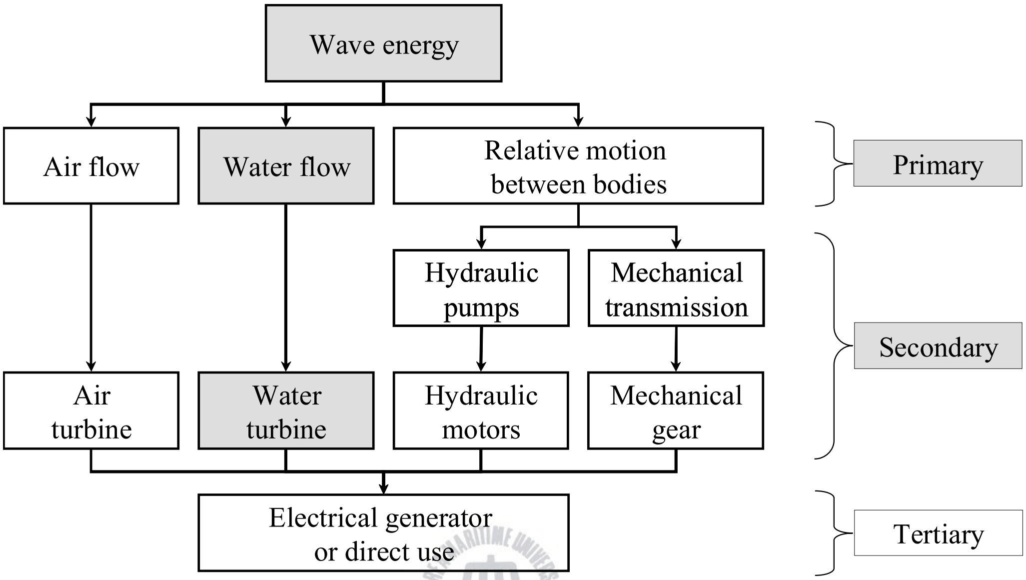

Figure 1.7 Power take-off alternatives and steps of wave energy conversion

The area of interest is highlighted in Fig. 1.7. The energy extracted from the waves can be converted through air, water or oil. This is called the working fluid. To make use of this energy we need a converting machine. Mechanical conversion equipment was typical of the nineteenth-century proposals. Hydraulic motors, water turbines and air turbines are typical components of modern proposals. The water turbine technology is well known, and provides a very high efficiency, as water turbines have been used in hydro power plants for a long time. Hydraulic pumps and motors are also well known and used all over today. However, off-the-shelf equipment does not have sufficiently high efficiency to be used with advanced methods of wave-energy conversion.

Research and development are therefore presently being carried out by wave power enthusiasts in order to improve the efficiency of high-pressure hydraulic equipment. Air turbines have been the most common power take-off device so far for OWC. Conventional turbines with a flap system to rectify the air flow have been used, but now a self-rectifying turbine called the Wells turbine is the dominating type. Energy storage is desirable before conversion to electricity if the WEC is to be connected to the grid, because the wave energy is strongly variable while the grid prefers a stable delivery. This can be obtained e.g. by pressure tanks, water reservoirs, or flywheel.

1.8.1 OWC Type Wave Devices

Vantorre et. al. [40] categorize wave energy devices into two main groups: "Active devices where the interface element responds to the wave action and produces mechanical work, and Passive devices where the device remains stationary and the water movement relative to the structure is made to work". The Oscillating Water Column device can be considered the closest to maturity of the latter group. This type of device consists of a land-backed chamber in which the front wall has an opening to let waves pass into the device whilst the rear wall extends down to the seabed. The wave action makes the water level in the chamber oscillate causing the air in the chamber to flow in and out through a turbine to generate electrical energy shown in Fig. 1.8.

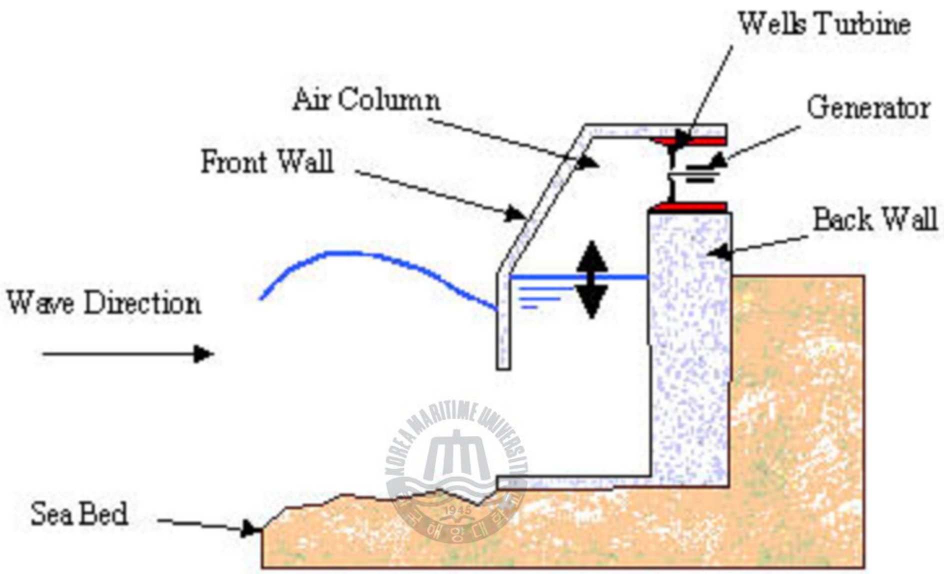

Figure 1.8 Principals of an OWC Type Wave Energy Device [14]

These types of device are the most common type of wave energy device currently in operation with at several prototype plants currently operating worldwide (for example, in Scotland, Portugal, Sweden, Australia and India).

The optimum design of an OWC is based upon the idea of inducing resonant motion of the water chamber oscillations by tuning the device parameters to the ambient waves. This is a complex phenomenon and involves the energy transfer between the incoming wave and the hydrodynamic, pneumatic, aerodynamic and electrical power take-off attributes of the device.

A novel designs had been researched in this paper on a savonius turbine incorporated at the rear bottom of the OWC and extract the energy directly from the fluid.

1.8.2 Savonius Rotor

Savonius rotor is of "S-shaped" cross-section constructed by three semi-circular buckets developed by Savonius [41]. It is simple in structure, has good starting characteristics and operates at relatively low operating speeds. According to studies carried out by Menet [42] and Reupke et. al. [43], Savonius rotors spin due to the differential drag on the curved surfaces. These rotors develop high torque at low rotational speeds, but have a low power coefficient. Ocean currents can be used to drive vertical axis Savonius rotors submerged in water. The geometry of the blades is such that any flow of water will produce a positive force on the rotor. The rotors depend on the force of the current on the blades to create torque. Savonius rotors have also been tried to extract wave energy. Savonius obtained power by using rotors with their axis horizontal and perpendicular to the direction of wave propagation. Also Khan et. al. [44], and Jabb [45], Merriam [46] and Faizal et. al. [47] suggested that the kinetic energy of the water particles' orbital motion should be used to drive small Savonius rotors, and that the diameter of the rotors should be less than the length of the rotor and the wave height. For the current study the Savonius rotor was incorporated at the rear bottom of the OWC as shown is Fig. 1.9. There was no reported work on the design and testing of such rotors.

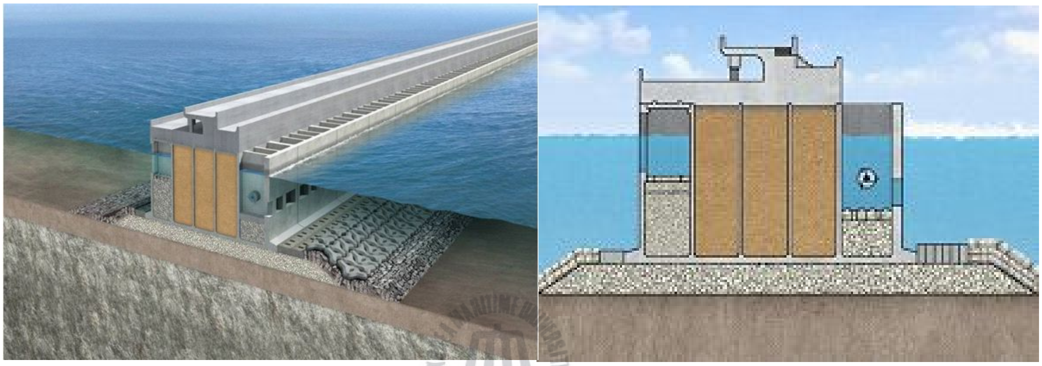

Fig. 1.9 Conceptual Models of the Curtain Type Wall Breakwater with OWC Chamber (Birds-eye View and Cross-Sectional view)

The present study is related to increasing the efficiency of the system by design evaluation of the turbine, chamber inlet and OWC. The primary stages of the research effort were to develop of a 3D numerical wave tank using CFD that can represent the physical model to an appropriate order of accuracy whilst maintaining realistic computational effort. Water wave motion motions are complex and irregular on the ocean surface. So in the NWT it is easier to study 2-dimensional waves with parallel sidewalls where the boundary layer effect is very small almost negligible. The numerical wave tank was then extended to include a detailed OWC with 3 bladed savonius rotor to determine energy capture efficiencies.

Furthermore, the effect of various 3 bladed savonius geometric was determined via the generated torque. Also, the effect of various OWC inlet geometric parameters was studied to find the influence on efficiency. The best geometric configuration was then simulated with 5 bladed savonius rotor to obtain high efficiency. Lastly, simulations were carried out for different turbulence model.

CHAPTER 2 NUMERICAL ANALYSIS

2.1 Introduction

Computational Fluid Dynamics is an important tool to recreate phenomena such as ocean wave and thus aids in understanding the hydrodynamics of it. As the increasing use of CFD in engineering analysis is evident it is important to make sure that the results from the simulation are in tandem with the theoretical or published results. CFD is a computer-based mathematical modeling tool that incorporates the solution of the fundamental equations of fluid flow, the Reynolds-averaged Navier-Stokes equations, using turbulence models to compute the averaged turbulence stresses. The Navier-Stokes equations represent the laws of conservation of mass, momentum and energy in differential form. These partial differential equations in integral form are then approximated as finite-volume expressions and reformed into algebraic equations to allow for numerical computation within a specified domain. The ANSYS CFX software used for this study uses the finite volume method to solve the Reynolds-averaged Navier-Stokes equations and has several features for multi-phase flows applicable to the problem at hand. Among these features is the ability to implement the VOF method to track the air-water interface within the domain. This is not only important as a means to delineate the interface but is also critical for the correct modeling of the hydro-pneumatic interaction within the

OWC chamber

As with any numerical modeling, simplifications and approximations need to be made to allow finite analytical durations or to explain phenomena not yet fully understood (eg turbulence). It is therefore prudent to perform systematic validation of any numerical work against either known theoretical or experimental solutions prior to acceptance as a valid method. Experimental validation is of particular importance as it may reveal real-world conditions that were not envisaged during the numerical development that may require incorporation into the chosen modeling tool.

This chapter is concerned with the CFD modeling of OWC type wave energy devices with particular focus on the energy absorption ability of the device. The development of a CFD model involves the creation of a domain i.e. modeling, generation of waves and the hydrodynamic and pneumatic modeling of the interaction of these waves with the OWC. The work in this chapter firstly details the development of a Numerical Wave Tank (NWT) with the OWC and turbine.

2.2 Modelling

As discussed in the introduction, this study is carried out to develop a Jeju island piston-shaped wave-power generation system. Fig. 2.1 shows the planed setup of the wave energy conversion system in the curtain wall type breakwater.

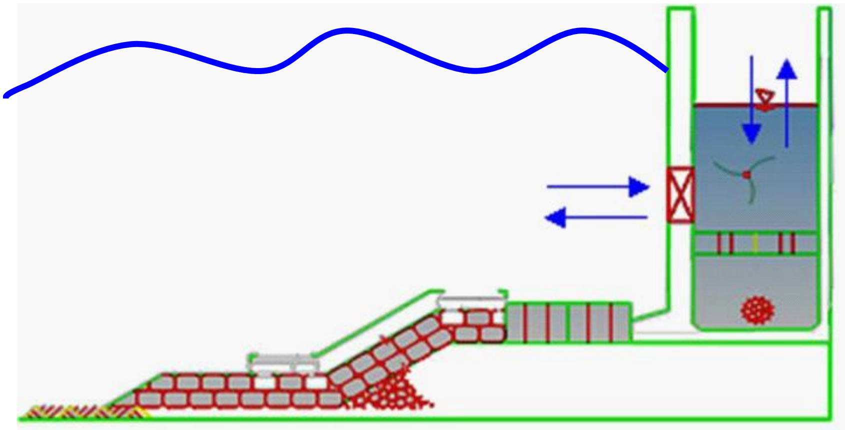

Figure 2.1 2D Modeling of Driving Principle of the Savonius Rotor

The above schematic diagram has been used for the base model study which shows the cross-sectional diagram and operating principles of wave energy converting system. The inflow and outflow can be achieved by reciprocating motion of the waves. As the water oscillates in the oscillating water column the turbine rotates in a unidirectional way efficiently. The numerical analysis has been done to practical dimensions of the wave energy converting system at Jeju island outer port east breakwater as shown in Fig. 2.2 and Fig. 2.3. Modeling of geometry was done in Unigrapics 4.

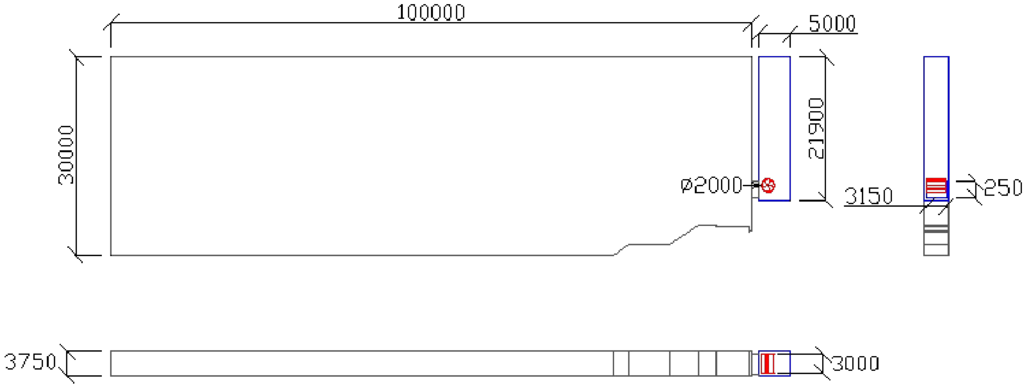

Figure 2.2 Schematics Diagram of the Numerical Domain

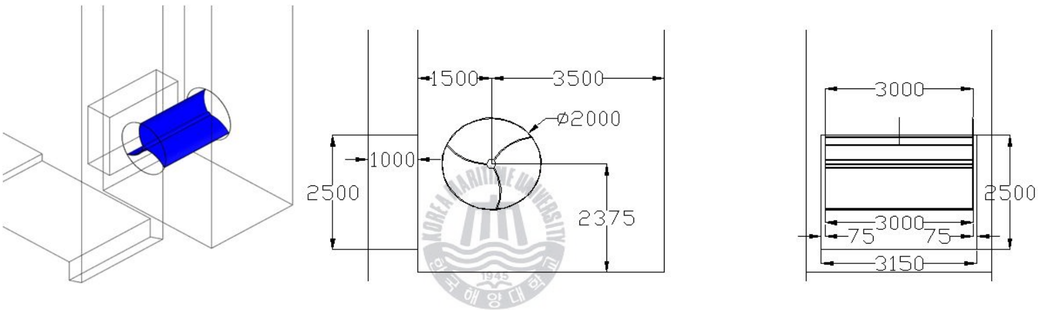

All Dimensions are in mm

Figure 2.3 Schematic Diagram of Turbine Location

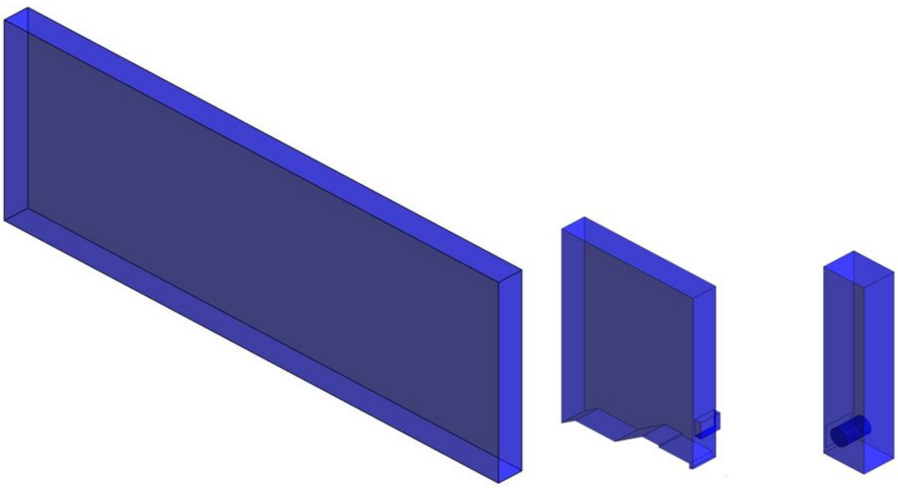

(a) Numerical wave tank part 1 (b) Numerical wave tank part 2 (c) Oscillating water column chamber

Figure 2.4 Numerical Wave Tank Fluid Models by Parts

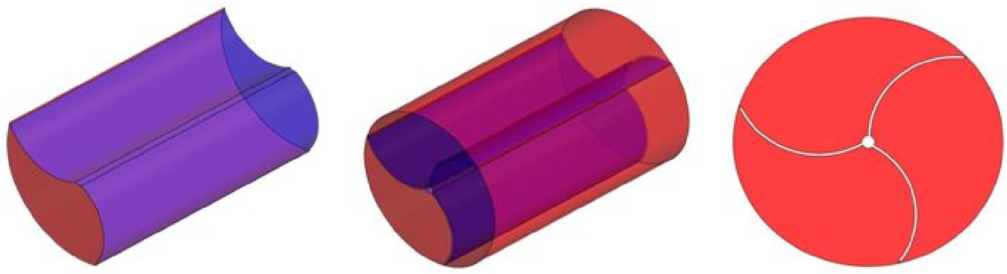

3 bladed savonius rotor by parts

Figure 2.5 Bladed Savonius Rotor Fluid Model by Parts

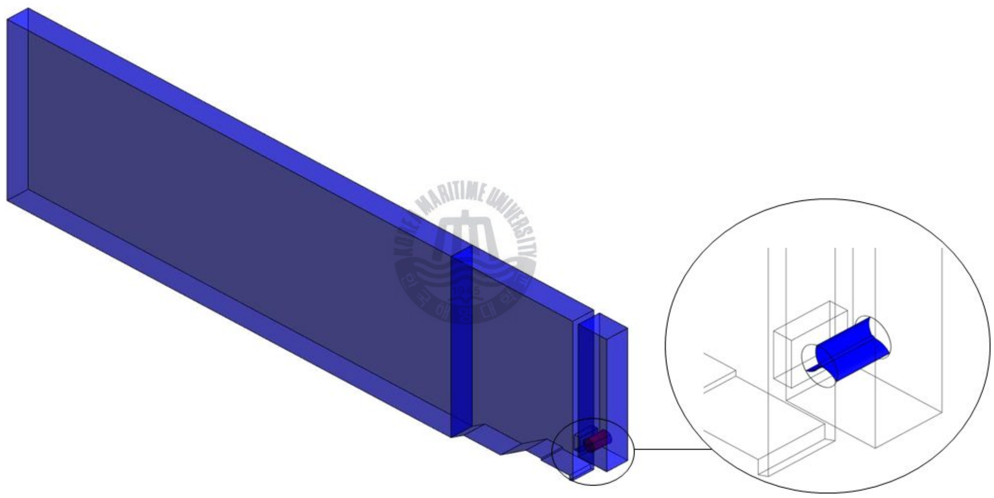

Figure 2.6 Full Model of the Calculation Domain with 3 Bladed Savonius Rotor at the Rear OWC

The NWT is the basic building block to which various features that warrant consideration (eg an OWC) may be added. It is thus of fundamental importance that the NWT provide results with an appropriate degree of accuracy to ensure that results from subsequent modeling are not distorted or diminished.

2.3 CFD Analysis Setup

The analysis of any fluid flow using CFD is an iterative process consisting of three basic steps:

1. Numerical Domain Setup
2. Modeling and Computation
3. Evaluation of the Results

These steps applied to the development of the basic model calculation are described in the following sections.

2.3.1 Domain Setup

As part of the pre-processing, one must define a geometry to which the CFD will be applied. The geometry chosen needs to take into account the size of the device and the surrounding volume that needs to be modeled in order to create a realistic response without significant 'boundary effects' (e.g. reflection). This model setup also includes the generation of the mesh to define the individual volumes that make up the computational domain. In addition to the creation of the mesh, boundary conditions such as a wave generator need to be carefully considered in order to accurately reproduce real world situations.

A schematic of the NWT proposed is presented in Fig. 2.2 and Fig. 2.3. In this model, the tank size is L=1000m and

H=30m with a width of 3.75m. At the right hand side of the tank a wave generation boundary is created by the reciprocating movement of the plate whilst the bottom and left hand side of the tank are represented by walls.

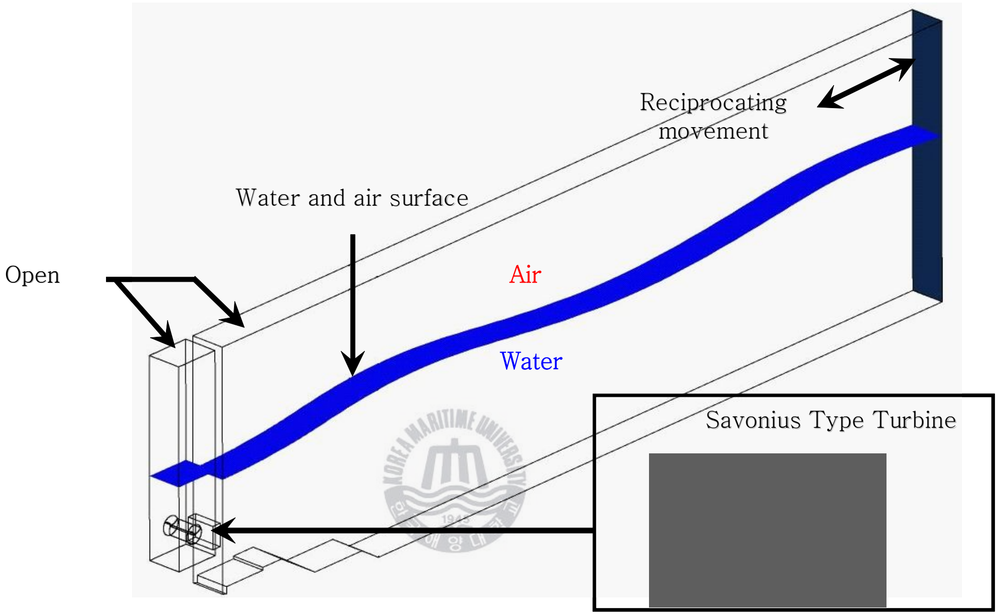

Figure 2.7 Schematic Domains with Boundaries

As with experimental testing, techniques to allow a sufficient number of waves to be analyzed prior to potential contamination from reflected waves is required. Numerical techniques such as numerical damping or active wave absorption paddles may be applied to minimize the domain size but both require considerable effort to calibrate and ensure satisfactory application [47, 48].

2.3.2 Numerical Results

The calculation of wave profiles and OWC device efficiency require a number of parameters to be monitored, however these are only some of the many variables, data sets and graphical representations can be extracted both during analysis and post processing.

Free surface elevations are determined at particular instant using inbuilt functions within the software that plots a contour for a particular quantity. To obtain the free surface plots, the user requests that data be extracted for the VOF fraction=0.5 which defines the interface between the air phase (VOF=1) and the water phase (VOF=0) at each air-water interface cell.

Velocity and pressure measurements in the domain can be extracted by the definition of a “point” such that any properties of the flow along the line may be extracted for a particular time.

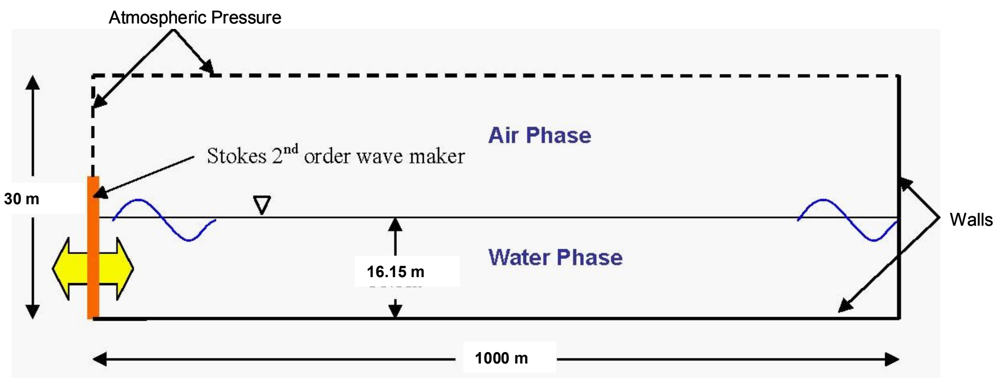

Figure 2.8 NWT Systematic Schematic

2.3.3 Mesh Generation

To discretise the Reynolds-averaged Navier Stokes equations, the domain must be covered by a computational mesh. The numerical domain and mesh were initially created using ICEM CFD geometry and mesh generation software that is a companion programme to the ANSYS CFX software. ICEM CFD can also be used to create the domain using modeling-based geometry tools or to import geometry created in standard computer aided design programs. Following creation of the geometry, the model is then meshed using a variety of different tools depending upon the problem at hand. Following creation of the geometry and mesh, the boundaries are defined and the model can then exported to a *.cfx5 file for later import directly into ANSYS CFX.

The relatively simple geometry of the NWT allows for efficient modeling of the domain using hexahedral cells. Preliminary analytical runs did identify that the resolution of the mesh at the air-water interface region was insufficient to satisfactorily model the wave shape. The model mesh was adapted in these locations by halving the cell dimensions i.e. incorporating a finer mesh near the free surface area. The mesh number: wave water tank 1.8×10^6 node, water chamber 5.2×10^5 node, cylindrical shape 8.8×10^5 node. The total mesh number consists of 3.1×10^6 node.

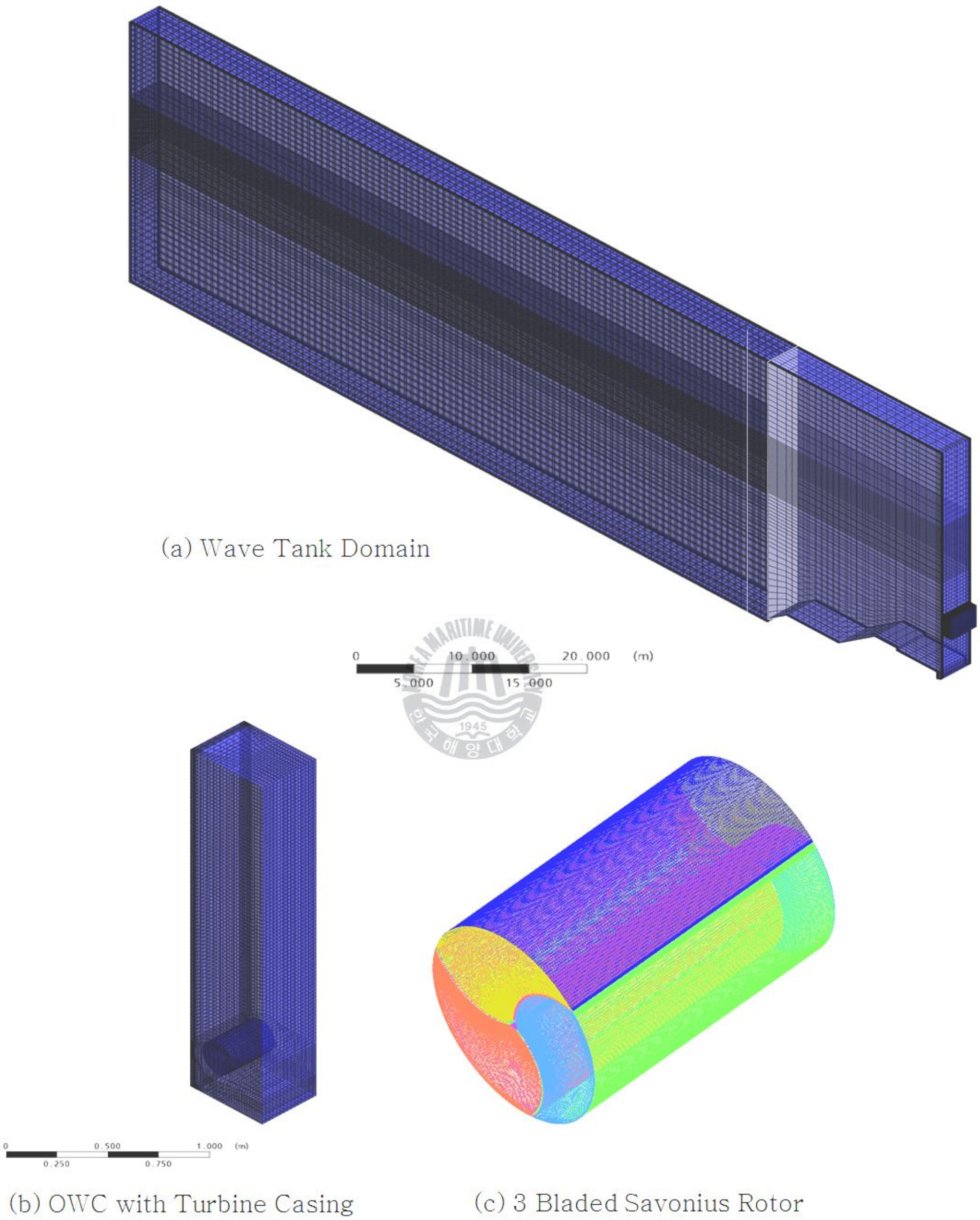

Figure 2.9 Typical Mesh for the Domains (Refined mesh near the free surface in Wave Tank Domain)

2.3.4 Boundary Conditions

To define a problem that results in a unique solution it is necessary to specify the information on the flow variables at the domain boundaries. It is important to define these correctly as they can have a significant impact on the numerical solution. The base of the tank and right hand wall are set as wall boundaries in order to bound the domain with no-slip boundary conditions. The no-slip condition ensured that the fluid moving over a solid surface does not have velocity relative to the surface at the point of contact. Tangential and normal fluid velocities are set to zero for the cells adjacent to the wall boundaries.

The NWT top is set as atmospheric pressure in order to mimic a "free" boundary such that air flows can occur, if required, either into or out of the domain. The fluid conditions used in the simulation is tabulated in Table 2.1.

Table 2.1 Fluid Conditions

Material	Phase Type	Density (kg/m^3)	Dynamic Viscosity ($kgm^{-1}s^{-1}$)	Temperature (°C)
Air	Primary	1.225	1.7894×10^{-5}	25
Water (fresh)	Secondary	998.2	0.001003	25

2.3.5 Wave Generation

To provide accurate NWT simulations of OWCs, the generation of realistic waves is crucial. A number of techniques are available to generate waves in ANSYS CFX. Firstly, waves can be generated by a moving flap that can move horizontally mimicking the wave generation techniques commonly used in experimental wave tanks.

In this study a wave is generated by dynamically linking a User Defined Function (UDF) to the inlet wall boundary. The inlet wall boundary condition allows the user to define the reciprocating movement of the plate to generate required wave height and wave length. Motion of the flap was implement through mesh motion giving specified displacement using CFX Expression Language (CEL) according to the equation below:

$$Ydis = a \sin wt \tag{2-1}$$

For a particular water depth, wave height, wave period and wavelength a UDF is created by modifying the problem parameter as shown in Fig. 2.10.

For most wave tanks, the opposite end of the wave maker is a typical beach which absorbs the waves that are generated in order to prevent their reflection back into the solution domain. This means either non-reflecting boundaries have to be used or a damping/dissipation zone is added to the solution domain for damping the waves. The non-reflecting boundary option was not feasible in the current work and it was thought that adding a damping zone would increase computational demands. Therefore, in this simulation, the far field boundary was located far enough and simulation time was chosen in such a way that such reflections were avoided. Also, the cell volumes towards the boundaries were made larger to provide some damping to avoid wave reflections.

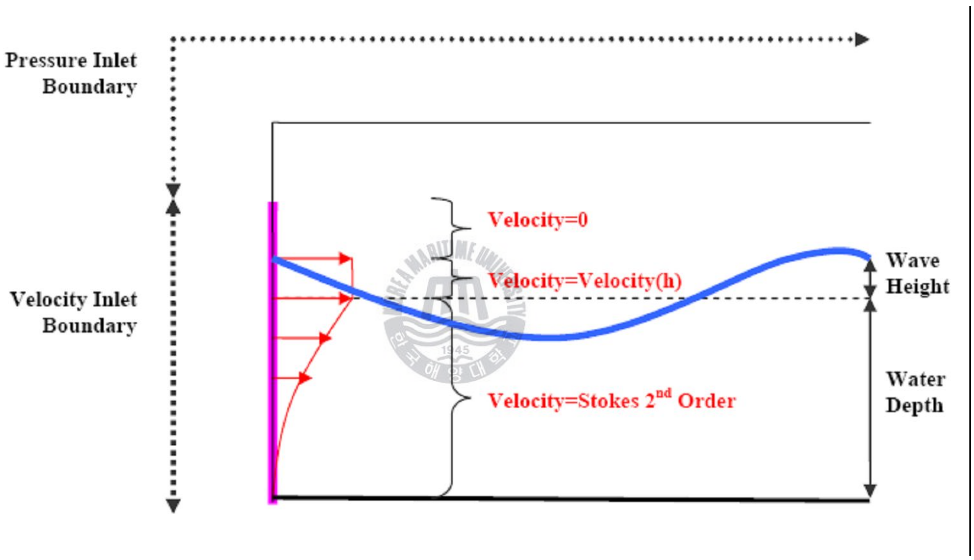

Figure 2.10 Numerical Wave-Maker Set-up

2.3.6 Multiphase

The numerical wave tank problem involves multiple phases – that is, air and water. The definition and monitoring of this interface is of primary importance to the analysis of OWCs as air/water interface within the OWC creates the 'piston' that compresses the air that drives the turbine to ultimately convert the wave energy into electricity.

ANSYS CFX has a number of techniques to cater for multi-phase flows. The Volume of Fluid (VOF) method chosen for this study has been shown to be the most applicable and sufficiently accurate to capture the essential flow features around free surface wave flows.

2.3.7 Solver Controls

Once the various physical models have been specified and the boundary conditions defined, it is the job of the solver to 'organise' all of this information and solve the governing flow equations to find values for all of the variables in each cell of the user-defined mesh such that the physical models and boundary conditions are simultaneously satisfied. In solving the equations it is necessary to reduce them to a numerical form that can be understood by a computer. This technique is called discretisation. There are three main methods for doing this: the Finite Difference Method (FDM); the Finite Element Method (FEM); and the Finite Volume Method (FVM).

The FDM uses Taylor series expansions to express first and second order derivatives in terms of differences in the dependent variables at spatial positions only a small distance apart. The FEM has its origins in stress and strain analysis of solid structures. In brief, the domain of interest is divided into small elements and a certain variation for the dependent variable assumed. Various numerical analysis techniques are then employed to determine expressions for first and second order derivatives of the dependent variable. This is carried out for every element of the domain after which all of the equations are collated and solved. Since each element is considered individually, additional computation is necessary in generating a ‘look-up’ table containing the connectivity information of the elements.

The most popular technique for discretising the governing CFD equations is the FVM. This method represents a more physical approach to transforming the differential equations. The flow domain is divided into control volumes (defined using the cells of the mesh) and the governing conservation equations are integrated over each one. In doing this, physical processes such as convection, diffusion and sources/sinks are dealt with explicitly. Inherent in its method, the FVM draws on features taken from both the finite element and finite difference methods. The FVM is the most favored discretisation technique for CFD code developers and was the method sought when selecting CFD software.

Two mesh types can be used in CFD programs -structured and unstructured. A structured mesh comprises six-sided cells arranged in a regular topology to form a cuboid. A structured mesh is necessary for implementation of the FDM. In an unstructured mesh, cells do not have to be six-sided and are often tetrahedral in shape. Since the FEM uses a unique variation of the dependent variables for every cell, the method lends itself well to unstructured meshes. The FVM is used mainly with structured meshes, although algorithms are now available that use the FVM with an unstructured mesh. In this selection process, a code employing the FVM with a structured mesh was deemed appropriate. When using the FVM, values for pressure are calculated at the cell centres. Velocity components are then calculated either at cell faces (a staggered grid) or, along with pressure, at the cell centres (a co-located grid). ANSYS CFX is based on the Finite Volume Method (FVM), and each node in the mesh is at the centre of a finite control volume, Fig. 2.11.

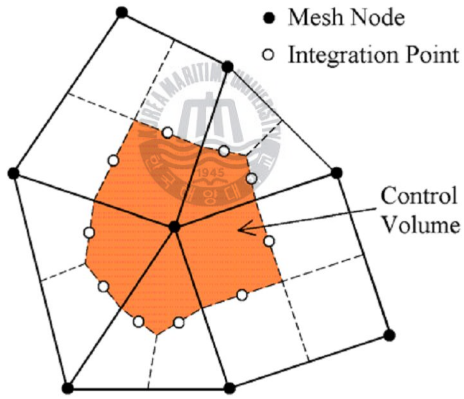

Figure 2.11 Representation of the Control Volume Associated with Each Mesh Node

2.4 Turbulence Modeling

Turbulent flow is a highly complex phenomenon. This phenomenon has been studied for many years; however it is not yet possible to characterize turbulence from a purely theoretical standpoint. Notwithstanding many important characteristics of turbulence are well-known, including the following:

- Turbulence is time-dependent, three-dimensional, and highly non-linear.
- Fully-developed turbulent motion is characterized by entangled eddies of various sizes. The largest eddies arise from hydrodynamic instabilities in the mean flow field for example, shearing between a flowing stream and a solid boundary.
- The largest eddies break down into smaller eddies which, in turn, break down into even smaller eddies. This process of eddy break-down transfers kinetic energy from the mean flow to progressively smaller scales of motion. At the smallest scales of turbulent motion, the kinetic energy is converted to heat by means of viscous dissipation.
- The dynamic and geometrical properties of the largest eddies are closely related to the corresponding properties of the mean flow field. For example, large, unstable vortices that form on the perimeter of a turbulent jet tend to possess well-defined toroidal structures.
- The time and length scales of the smallest turbulent eddy are many orders of magnitude greater than the time scales and free paths of molecular motion. As a result, the processes of viscous dissipation are statistically independent of molecular motion.

- Turbulent motion is not a random phenomenon. As a consequence, turbulent fields possess definite spatial and temporal structures.

A turbulence model is an approximation based on one or several assumptions that allows the Reynolds stresses to be solved. The relations used by a turbulence model are generally valid only for a very specific set of flow conditions; there is no universally successful turbulence model.

2.4.1 k-ε model

The k-ε model is the most commonly used of all the turbulence models. It is classified as a two equation model. This denotes the fact that the transport equation is solved for two turbulent quantities k and ε. Within the model the properties k and ε are defined through two differential transport equations (2.2) & (2-3) of both factors.

$$\frac{\partial(\rho k)}{\partial t}+\nabla.(\rho U k)=\nabla.\left[\left(\mu+\frac{\mu_t}{\sigma_k}\right)\nabla k\right]+P_K-\rho\varepsilon \tag{2-2}$$

$$\frac{\partial(\rho \varepsilon)}{\partial t}+\nabla.(\rho U \varepsilon)=\nabla.\left[\left(\mu+\frac{\mu_t}{\sigma_\varepsilon}\right)\nabla \varepsilon\right]+\frac{\varepsilon}{k}(C_{\varepsilon 1}P_k-C_{\varepsilon 2}P_\varepsilon) \tag{2-3}$$

The standard k-ε model is used in the prediction of most turbulent flow calculations because of its robustness, economy and reasonable accuracy for a wide range of flows. However, the model performs poorly when faced with non-equilibrium boundary layers. It tends to predict the onset of separation too late as well as to under predict the amount of separation. Separation influences the overall performance of many devices, such as diffusers, turbine blades and aerodynamic bodies. Separation also has a strong influence on other effects, such as wall heat transfer and multi-phase phenomena. Predicting reduced separation usually results in an optimistic prediction of machine performance. Initially all the models were solved with the turbulence model k-ε.

2.4.2 The Shear Stress Transport Model

One of the most effective is the shear stress transport (SST) model of Menter [49]. The SST k-ω turbulence model is a two-equation eddy-viscosity model which has become very popular. The SST formulation combines the best of two worlds. The use of a k-ω formulation in the inner parts of the boundary layer makes the model directly usable all the way down to the wall through the viscous sub-layer, hence the SST k-ω model can be used as a Low-Re turbulence model without any extra damping functions. The SST formulation also switches to a k-ε behaviour in the free-stream and thereby avoids the common k-ω problem that the model is too sensitive to the inlet free-stream turbulence properties. To avoid excessive shear stress value in adverse pressure gradient conditions, the turbulent shear stress in the boundary layer is limited based on the Bradshaw assumption of direct proportionality with the kinetic energy ($\tau = \rho a1k$).

$$\mu_t = \rho \frac{a_1 k}{\max(a_1 \omega; SF_2)} \tag{2-4}$$

The SST model performance has been studied in a large number of cases. In a NASA Technical Memorandum, [50], SST was rated the most accurate model for aerodynamic applications. Lastly, the best domain was solved with the SST model and results were compared.

CHAPTER 3 RESULTS AND DISCUSSION

3.1 General

The graphs generated by CFD programs are almost always pretty, however one need not be deceived by their appeal but rather be mindful of their implications and limitations. This section is in 8 parts. The stages of the research effort can be described as follows and discussed under following topics

- Numerical Tank
- Numerical wave tank with OWC
- Reflector in the rear bottom of the OWC
- Rotor angle and helical blade analysis
- 3 bladed savonius rotor angle analysis
- 3 bladed helical savonius rotor angle analysis
- OWC inlet section
- 5 bladed savonius rotor

With continual advances in computing power, the simulation of fluid dynamics using the numerical methods that iteratively solve the Navier Stokes equations and using Volume-of-Fluid techniques the free surface is now seen as a practical alternative to model testing. Desired wave was generated in the NWT and further in OWC was incorporated to study the flow for turbine integration. The research main focus is to increase the total efficiency of the system by design alteration of the

OWC and the savonius turbine. The first approach to increase the efficiency of the system was to alternate the design of the OWC by including a reflector plate at the rear bottom of the OWC to direct the flow more towards the turbine. The results did not turn out as anticipated, as the reflector plate decreases the total efficiency. Alternatively, changing the design of rotor to some extent increases the total efficiency. 3 bladed savonius rotor was simulated with various rotor angles and helical rotors respectively and the performance evaluated. Higher primary energy has to be extracted from the wave in order to increase the secondary energy, energy extracted by the turbine hence optimization of the chamber inlet design assures the increase the turbine efficiency. From the optimization, the best model was chosen and simulated with various 5 bladed savonius rotor.

3.2 Numerical Wave Tank

The numerical tank consists of a fluid domain with two phases (water and air) bounded by a layer of air on top, a bottom surface in water and four vertical boundaries. All boundaries can be physical ones if the fluid is really bounded, but otherwise they are imaginary ones. At one vertical boundary, the movement of a flap type wave maker was simulated by moving grid. Numerical beaches are incorporated near other imaginary boundaries so that no waves are reflected in most of the other cases. At solid walls, no slip conditions are applied. Regular waves are generated by imposing appropriate inlet velocities at the wave maker boundary. For the present numerical tank, average wave condition of Jeju Island was used with an amplitude 1.5 m, period 6.4s, have been generated.

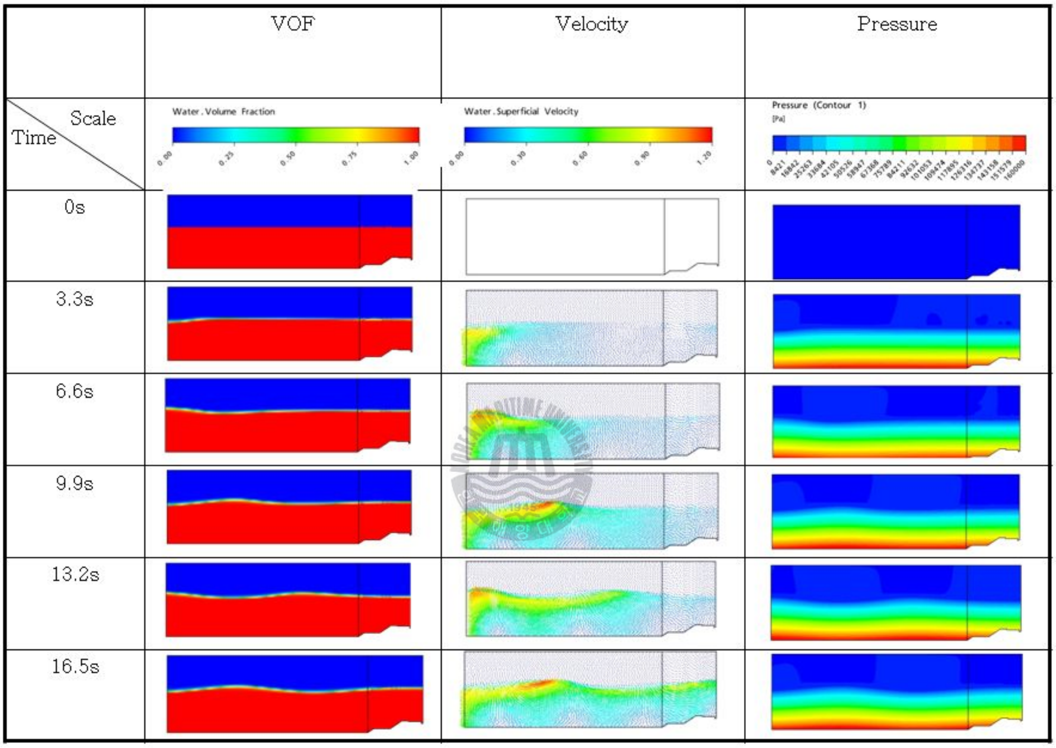

Figure 3.1 Development of the Wave Profile in the Numerical Wave Tank.

Formation of waves in the NWT is shown with the help of volume fraction. In Fig. 3.1, red shows the water and blue represents air. The air/water free surface is shown in yellowish colour. This is a multi-phase simulation where there is two phase present namely water and air. Let VW be the volume fraction of water and VA be the volume fraction of air. For any given computational cell, the volume fraction of water and air sum should be equal to 1. If we take VW, then there is 3 possible conditions; (VW = 1), the cell is full of water, (VW = 0), cell is empty of water and (0 < VW < 1), the cell contains the interface that is, the free surface interface having both water and air. From velocity vectors it can be inferred that the kinetic energy is concentrated at the surface and the velocity decreases with increasing depth. The Pressure in the NWT is shown by means of pressure contour and as predicted the pressure increases with water depth. In numerical analysis, density of element plays an important role. Physical parameters of a wave in wave tank depends on three factors namely water height, flap displacement and period of stroke displacement and period of stroke displacement. Fine hexahedral grids are employed to ensure relatively high accuracy of calculated results. Finer mesh was adopted near the free surface level, to capture more accurate movement of free surface. The water depth and the wave length in the NWT resolute that the criteria in which wave propagates was in intermediate water depths, ($0.05\lambda < d < 0.5\lambda$) and the power in the incoming waves was calculated respectively using the intermediate water wave equations.

$$c_p = \sqrt{\frac{g\lambda}{2\pi}\tanh\left(\frac{2\pi d}{\lambda}\right)} \quad [m/s] \tag{3-1}$$

$$c_g = \frac{1}{2} c_p \left(1 + \frac{4\pi d}{\lambda} \frac{1}{\sinh\left(\frac{4\pi d}{\lambda}\right)} \right) \quad [m/s] \tag{3-2}$$

$$E = \frac{1}{16} \rho g H^2 \qquad [J/m^2] \tag{3-3}$$

$$P_{Wave} = E c_g \qquad [W/m] \tag{3-4}$$

where C_p is the phase velocity, C_g is the group velocity, g is acceleration due to gravity, ρ is the water density, E is the energy density per unit area and P_{Wave} is the wave energy flux or wave power. Making appropriate substitutions in the equations, the power in the incoming waves was , P_{Wave} 22.03W/m.

Wave was also simulated with different turbulence model such as k-epsilon and SST turbulence model. It is noted that the difference is not remarkable in the results between different turbulence models.

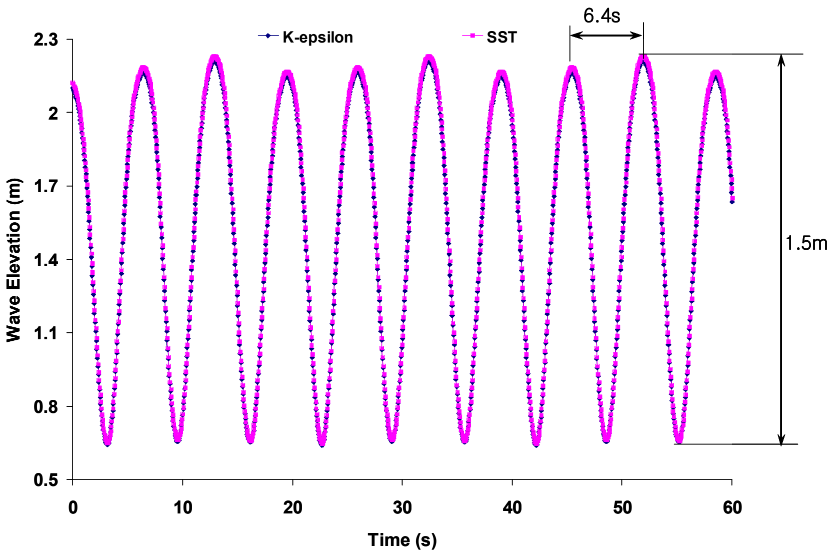

Figure 3.2 Time History of Wave Elevation for Different Turbulence for t=60s

Figure 3.2 illustrates the computation for the distribution of wave profile along the tank at point P1 for fully developed wave. The results obtained by the present method show fairly good agreement with the linear wave solutions. It also can be found that the wave elevations in the numerical prediction are slightly uneven in magnitude than the analytical solutions as the wave propagates in the tank. The results obtained by the present method show fairly good agreement with the linear wave solutions. As wave power is a function of the wave height squared, errors in wave height can have a significant effect on the wave energy conversion efficiency calculation. Upon reflection, it was identified that the standard grid and time step size, did in fact vary sufficiently from the earlier NWT validation case to cause issue.

3.2.1 Numerical Wave Tank with OWC

Subsequent to the NWT analysis, the numerical work was extended to include an OWC under the same wave condition. The numerical wave tank was incorporated with OWC once the waves were simulated as shown in Fig. 3.3. Standing wave was monitored at the end wall and analyzed with the OWC water height shown in Fig. 3.4.

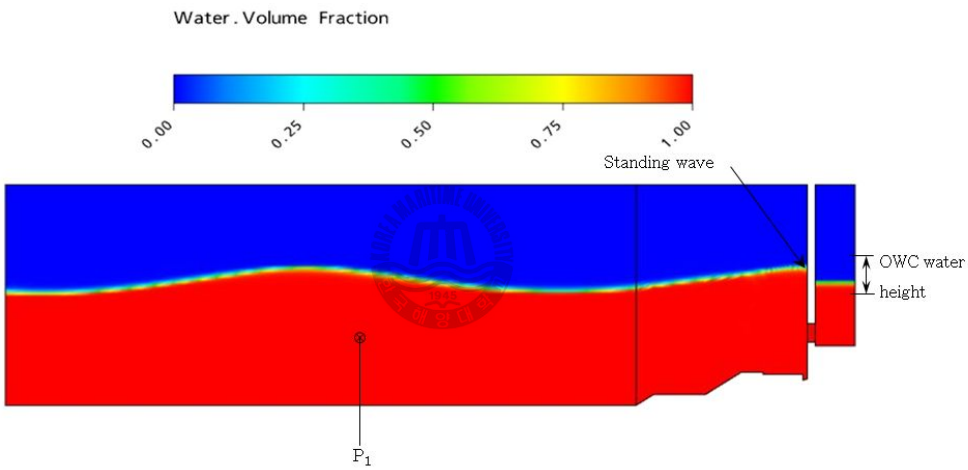

Figure 3.3 Monitor Point Locations for Pressure Prediction

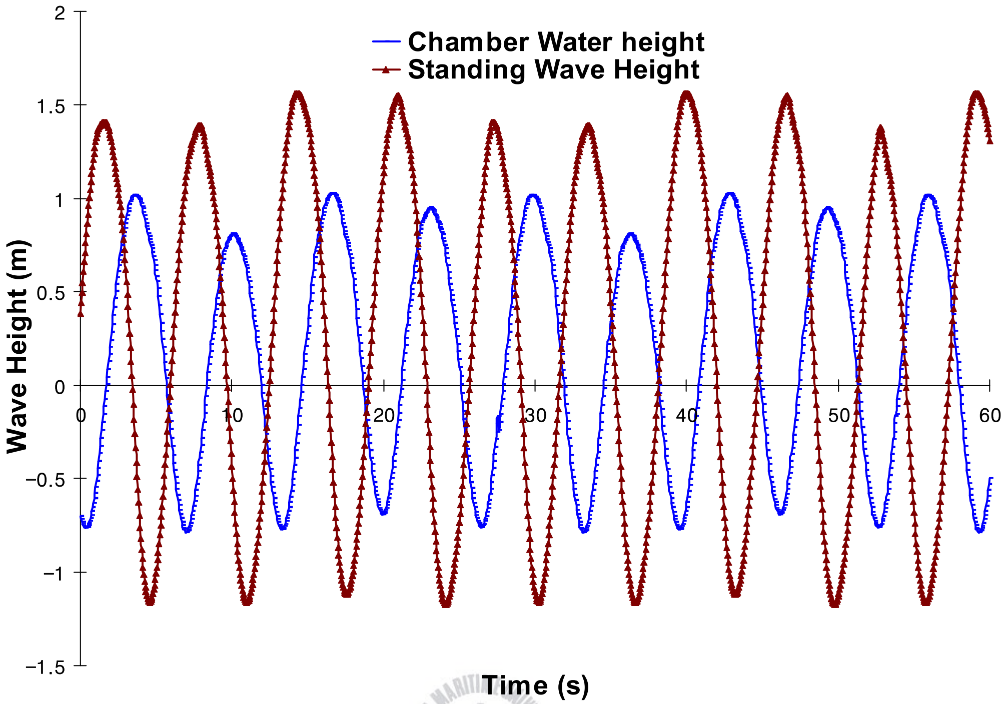

Figure 3.4 Predicted Wave Heights at the Desired Locations

It has been observed that there is a lag difference of 1.95s. The average height of the standing wave is about 2.8m and the average height of change of water level in the chamber is 1.6m. One of the reasons for a high standing wave at wall is that for most wave tanks, the opposite end of the wave maker is a typical beach which absorbs the waves that are generated in order to prevent their reflection back into the solution domain. This means either non-reflecting boundaries have to be used or a damping/dissipation zone is added to the solution domain for damping the waves. The non-reflecting boundary option was not feasible in the current work and it was thought that adding a damping zone would increase computational demands. Therefore, in this simulation, the far field boundary was located far enough and simulation time was chosen in such a way that such reflections were avoided. Also, the cell volumes towards the boundaries were made larger to provide some damping to avoid wave reflections.

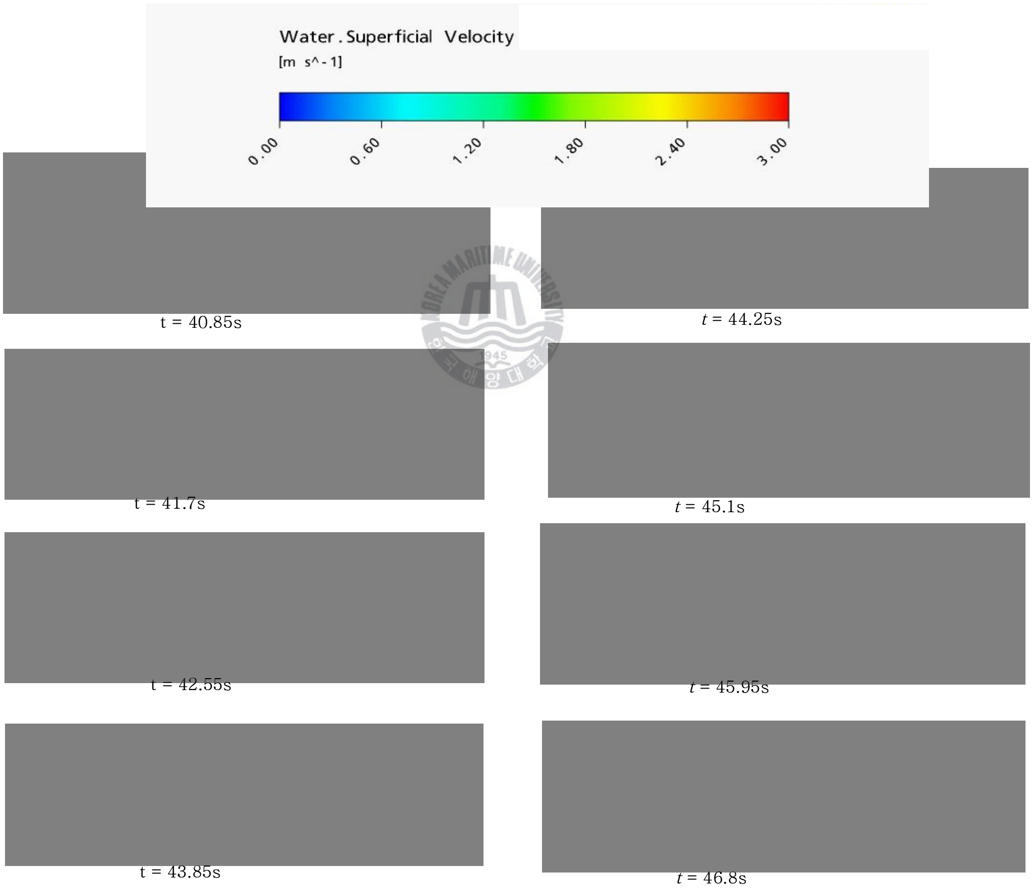

Figure 3.5 Superficial Velocity Contours in the Numerical Wave Tank

The objective of this simulation was to observe the flow at the inlet of the OWC. In Fig. 3.5 the superficial velocity contour in the numerical wave tank is shown for the time instants of fully developed wave, when the water is entering the OWC chamber and exiting the chamber for a full cycle.

3.3 Reflector in the Rear Bottom of the OWC

The purpose of the simulation was to investigate and compare the hydrodynamic performance of the system, with reflector plates. The Oscillating Water Column (OWC) has been selected as the primary object of this research. More over, the experimental is a serial research for studying the performance of the system with 3 bladed savonius rotor. Different models of the OWC have been tested in the previous research. The research reported in this section tried to apply the reflector in the rear bottom of the OWC to improve the efficiency in the previous models test as shown in Fig. 3.6. The reflector position was incremented with respect to the slope angle to obtain the best position for the maximum efficiency. The rotor configuration used in this simulation from previous research.

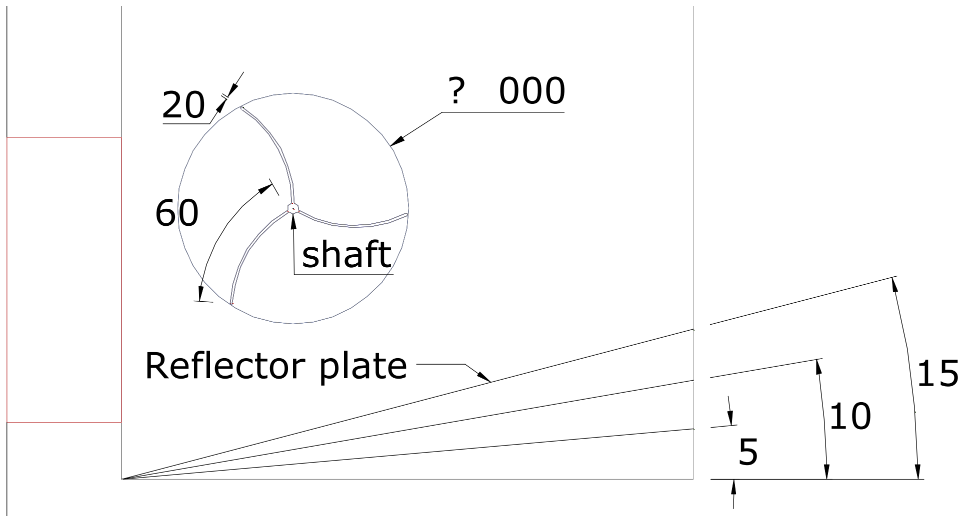

Figure 3.6 Schematic of the reflector plate at the rear bottom of OWC

The reflector plate inclusion did not increase the efficiency as expected. The net positive torque tends to decrease with the increasing slope angle. Three angles in an increment of 5 degrees were simulated and the results indicate a reflector plate does not increase the efficiency in this system.

The optimization of the turbine depends on whether the turbine rotational speed N can be controlled to match the individual sea states, or is kept constant all the time. The first preference, obviously, is to achieve a constant rpm of the turbine. The main advantage of constant rotational speed is that it allows cheaper electrical equipment to be employed. However, power electronics and variable rotational speed generators are now relatively inexpensive and have been adopted in most of the recent OWC prototypes. An additional advantage of variable rotational speed is to allow energy to be stored as kinetic energy in, and released from, the rotating parts (flywheel effect), thus producing a smoothing effect on the electrical energy delivered to the grid; this is especially important in small grids. Here, even when variable rotational speed is simulated, N is assumed to remain unchanged over each individual sea state. This is obviously not a very suitable control strategy, unless a very large set of sea states is considered. If this is the case, and if the inertia of the rotating parts is large enough, then it is reasonable to assume that the oscillations in N are relatively small over the duration of each individual sea state (say a few wave periods), and that N varies smoothly over a longer time scale. For practical reasons of numerical simulation and since the rotational speed control is not the primary objective of the present work, the Savonius turbine rotational speed was 20 rpm from previous study.

The efficiency of a Savonius type turbine wave energy converter can be calculated by the following equation [52].

$$\eta = \frac{P_{\mathrm{Tave}}}{P_{\mathrm{Wave}}}, \tag{3-5}$$

where P_{wave} and P_{Tave} are wave power and average torque power generated by the Savonius type turbine, respectively. P_{wave} and P_{Tave} are given by the following equations:

$$P_{\text{Wave}} = \frac{1}{16}\rho g H_i^2 \frac{\lambda}{T} b \left[1 + \frac{\frac{4\pi d}{\lambda}}{\sinh \frac{4\pi d}{\lambda}} \right], \tag{3-6}$$

$$\begin{aligned} P_{\text{Wave}} &= \tau\omega \\ &= \tau \left[\frac{2\pi N}{60} \right], \end{aligned} \tag{3-7}$$

where d is the water depth, b is width of the chamber opening, λ the wave length, H_i the incoming wave height, ρ the water density (998 kg/m^3), g the gravitational acceleration (9.81 m/s^2), T the wave time period, τ the average torque, and N the RPM of the turbine.

Table 3.1 Reflector Plate Performance Analysis

	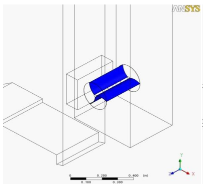	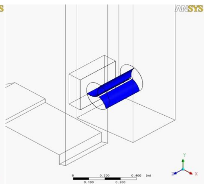	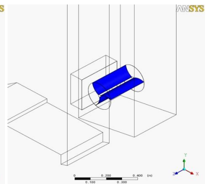	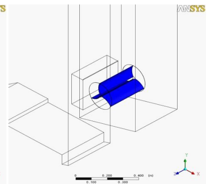
Reflector plate angle (Degree)	0	5	10	15
Wave period (s)	6.4	6.4	6.4	6.4
Water Level (m)	16.15	16.15	16.15	16.15
Average Torque (kN.m)	2.73	2.68	2.54	2.41
$P_{\tau ave}$(kW)	5.72	5.61	5.32	5.05
Total Efficiency (%)	13.18	12.94	12.26	11.63

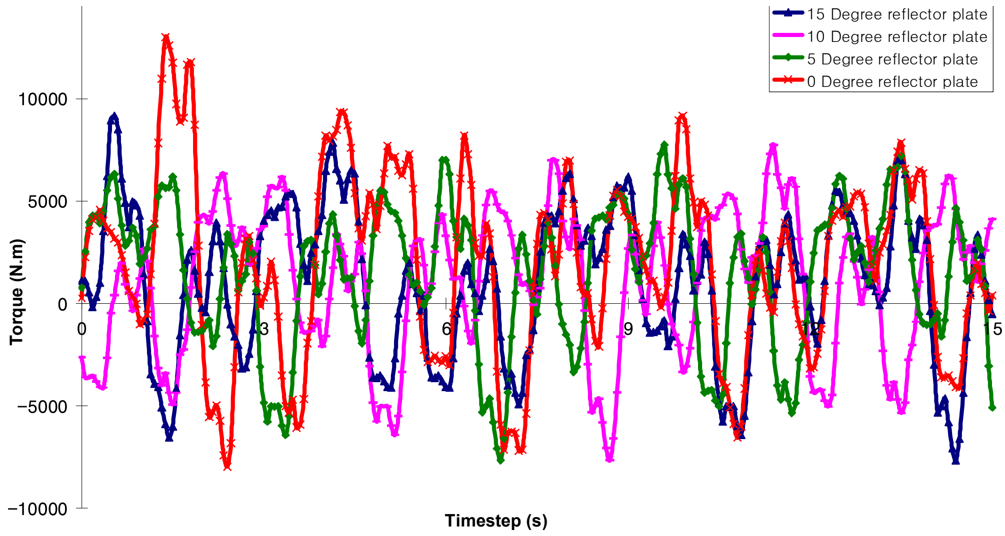

Figure 3.7 Average Torque Graph of 3 Bladed Savonius Rotor with the Respective Reflector Plate Angles

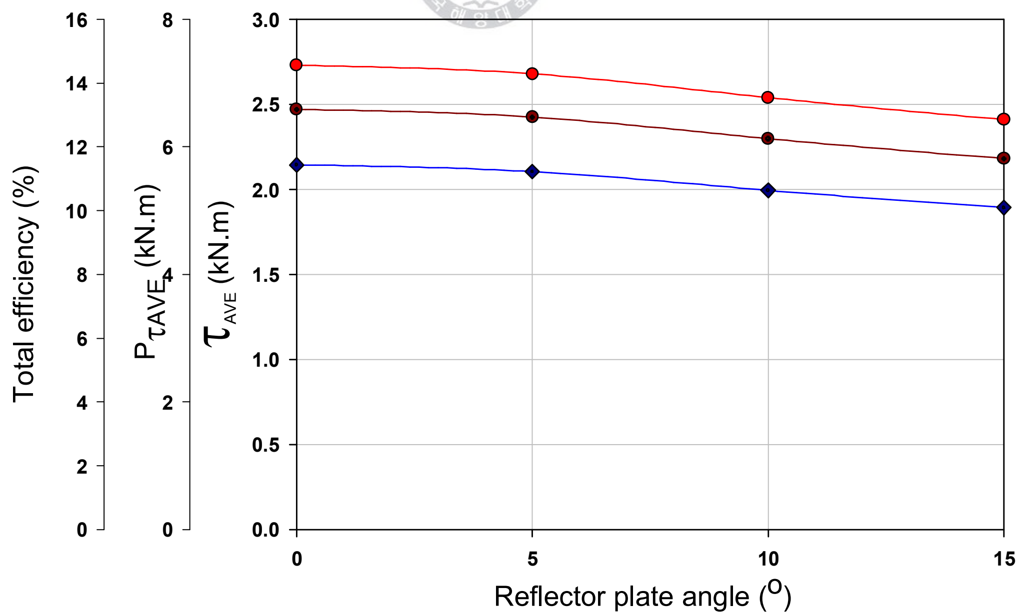

Figure 3.8 Graphical representation of reflector plate performance

The analysis has indicated that the reflector plate does not increase the performance but decreases it. Previous research indicated that a 3 bladed Savonius rotor had a total efficiency of 13.18% which had an average torque power of 5.72kW generated by the turbine. Subsequently the total efficiency decreased: 0°-5°: 0.24%, 5°-10°: 0.68%, 10°-15°: 0.63%. As can it can be seen from the graphs there is a continuous decrement of the torque with the increment of the reflector plate angle. It is also evident from the torque graph that the average positive torque decreases with the increasing reflector plate angle.

The rotor is well aligned to receive the energy of the wave and the direction of rotation is matching the wave force. The direction of rotation of the rotor is always anti clock-wise when the wave motion is in x-direction. The velocity vectors at a frequency of 0.16Hz, wave height of 1.4m and period of 6.4s for the case when the superficial velocity is the maximum is shown in the Fig. 3.9. It is observed in the 15° reflector plate that the velocity tend to decrease at the rear of the turbine for both in flow and outflow. This was the main cause of the decrease in the average net positive torque hence decreasing the total efficiency.

Model	Base Model (Previous Research)	15º Reflector Plate
Scale / Time (s)	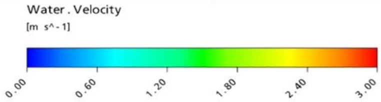	
42.5s	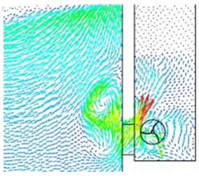	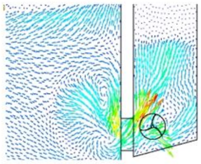
43.6s	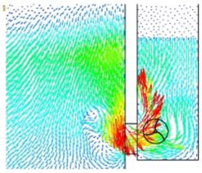	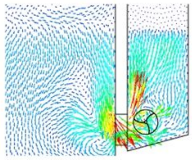
44.6s	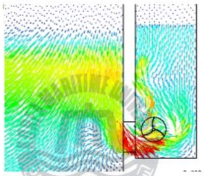	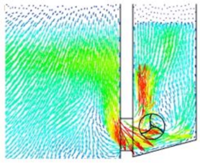
45.7s	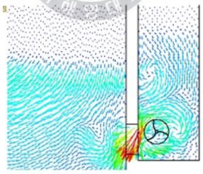	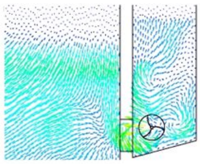
46.8s	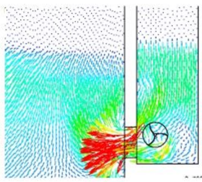	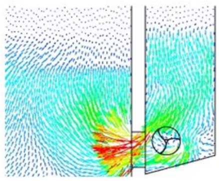
47.8s	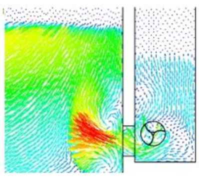	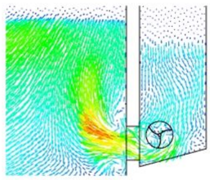

Figure 3.9 Superficial Velocity of Vector Diagram at Maximum Torque

3.4 Rotor Angle and Helical Blade Analysis

Optimizing the design of the runner to increase turbine efficiency was another imitative taken in this research; that is the secondary energy conversion. Two different cases were simulated simultaneous, Savonius rotor angle and Savonius helical blade angle. Both the studies showed an increase in the total efficiency. The rotor angle simulation had indicated that with a higher curvature blade, there is an increase in the total efficiency of about 5.4%. Also, with a helical Savonius rotor an increase of 2.94% was seen when compared to the base model. The internal flow field of the turbine changes with the blade configuration which plays an important role in generating the average net positive torque.

3.4.1 3 Bladed Savonius Rotor Angle Analysis

5 Different rotor angle cases were tested and compared with the base model for the performance analysis shown in Fig. 3.10.

Savonius Rotor Angle	Schematic	End view (fluid model)	Isometric View
Case 1	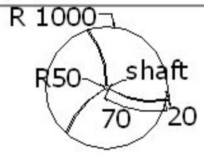		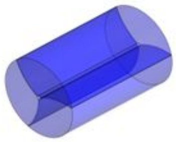
Base model	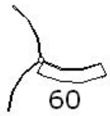		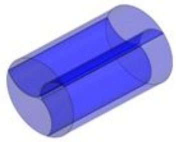
Case 2	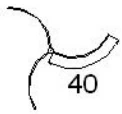		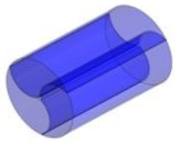
Case 3	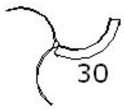		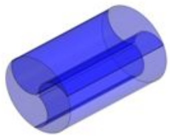
Case 4			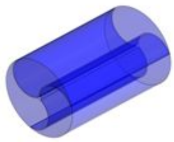
Case 5			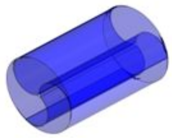

Figure 3.10 Schematics Showing Savonius Rotor with Various Rotor Angles

The obtained results shows a fairly good increase in the average net positive torque for 20° savonius rotor angle. The average net positive torque was tabulated in Table 3.2 and performance analyzed.

Table 3.2 Performance Analyses of the Savonius Rotor Angle

Savonius Rotor Angle (°)	0	10	20	30	40	60	70
Wave Height (m)	1.5						
Wave Period (s)	6.5						
Water Level (m)	16.15						
Average Torque (kN.m)	3.29	3.59	3.85	3.62	3.25	2.73	2.4
Pτave(kW)	6.89	7.52	8.06	7.58	6.81	5.72	5.03
Pwave(kW)	43.39	43.39	43.39	43.39	43.39	43.39	43.39
Total Efficiency (%)	15.88	17.33	18.58	17.47	15.69	13.18	11.58

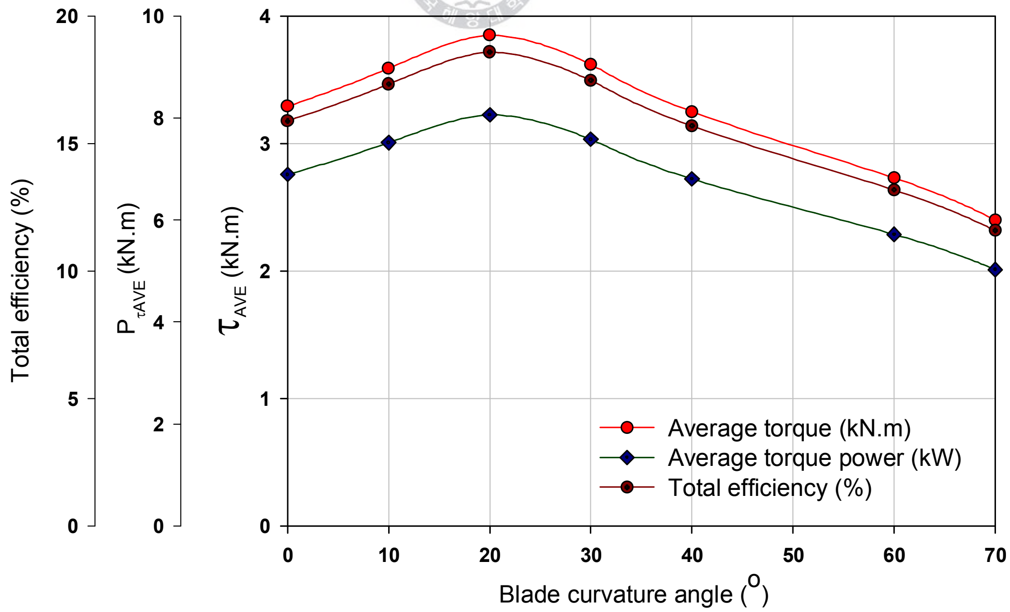

Figure 3.11 Graphical Representation of the Performance Analysis of the Savonius Rotor Angle

The aerodynamic characteristic of the rotating savonius rotor is much improved by the curved rotor blade which results in a higher rotating torque. Simulation results show smooth running, higher efficiency and self starting torque capability of the 20° rotor compared to that of the other rotor shown in Fig. 3.11. It can also be seen from the table that the difference in average torque between the highest and the lowest is 1.45kN.m. Thus, at given wave conditions, rotor angle of 20° is preferable for its highest efficiency of 18.58%.

The rotor is well aligned to receive the energy of the wave and the direction of rotation is matching the wave force. The direction of rotation of the rotor is always anti clock-wise when the wave motion is in x-direction. The velocity vectors at a frequency of 0.15Hz, wave height of 1.5m and period of 6.5s for the case when the water velocity is the maximum is shown in the figure below.

Rotor Angle (Inflow)	70°	20°
Scale / Time (s)	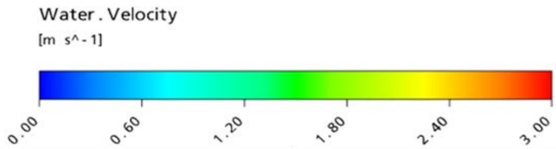	
0s	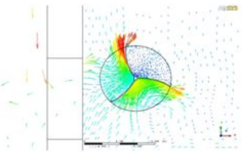	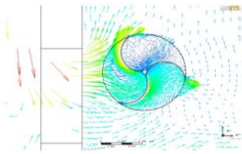
0.53s	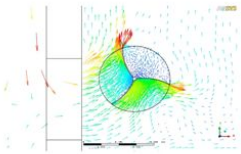	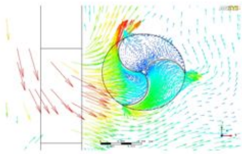
1.07s	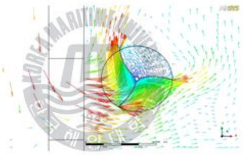	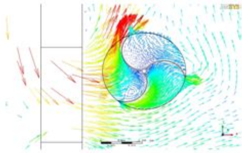
1.6s	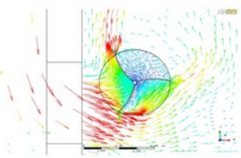	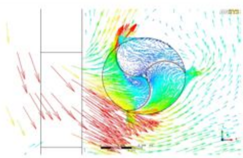
2.13s	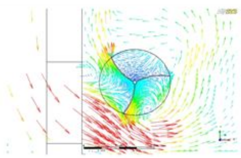	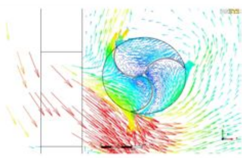
2.67s	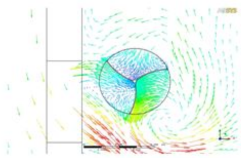	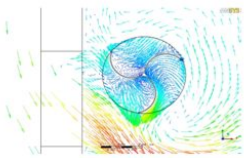

Figure 3.12 Velocity Vector Around the Savonius Rotor During Inflow in Time Increment of 0.53s

The Figures above shows respectively, the phase vector velocity distributions in and around the rotating savonius rotor at two rotor blade angles 70° and 20° for the increment of 0.53s. A dramatic change in the field is observed in the 20° figure in comparison to 70°. It is observed that the internal velocity on the advancing side is accelerated and that on the returning side, by the presence of circulation produced by the curved rotating rotor, which is not observed for the 70° rotor. The recirculation flow together with the clockwise rotation of the advancing blade generates the vortex like structure in the downstream of the advancing blade, which circulates in clockwise and grows in size in the downstream.

Rotor Angle (Outflow)	60°	20°
Scale / Time (s)	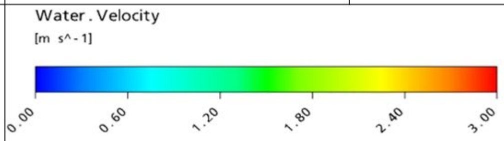	
0s	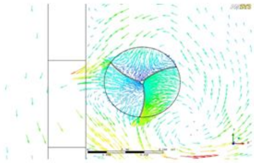	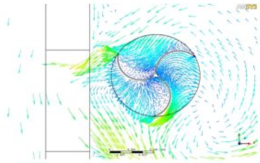
0.53s	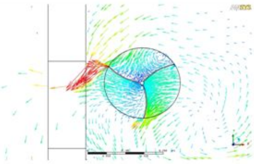	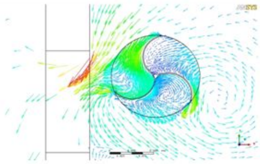
1.07s	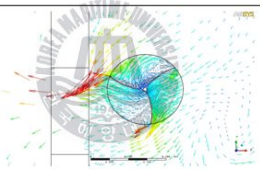	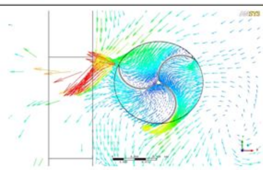
1.6s	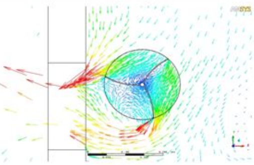	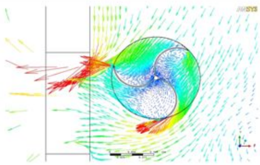
2.13s	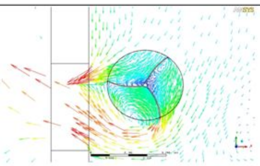	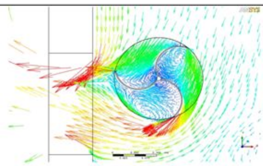
2.67s	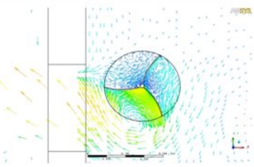	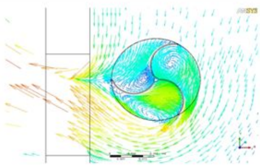

Figure 3.13 Velocity Vector Around the Savonius Rotor During Outflow in Time Increment of 0.53s

The flow in side the rotor moves form the advancing side of the blade to the returning side of the rotor, thus producing a pressure recovery effect on the concave side of the returning blade shown in Fig 3.14. This phenomenon is closely related to the appearance of favorable positive torque on the concave side of the rotor as seen in the torque graph which contributes largely to the production of positive torque.

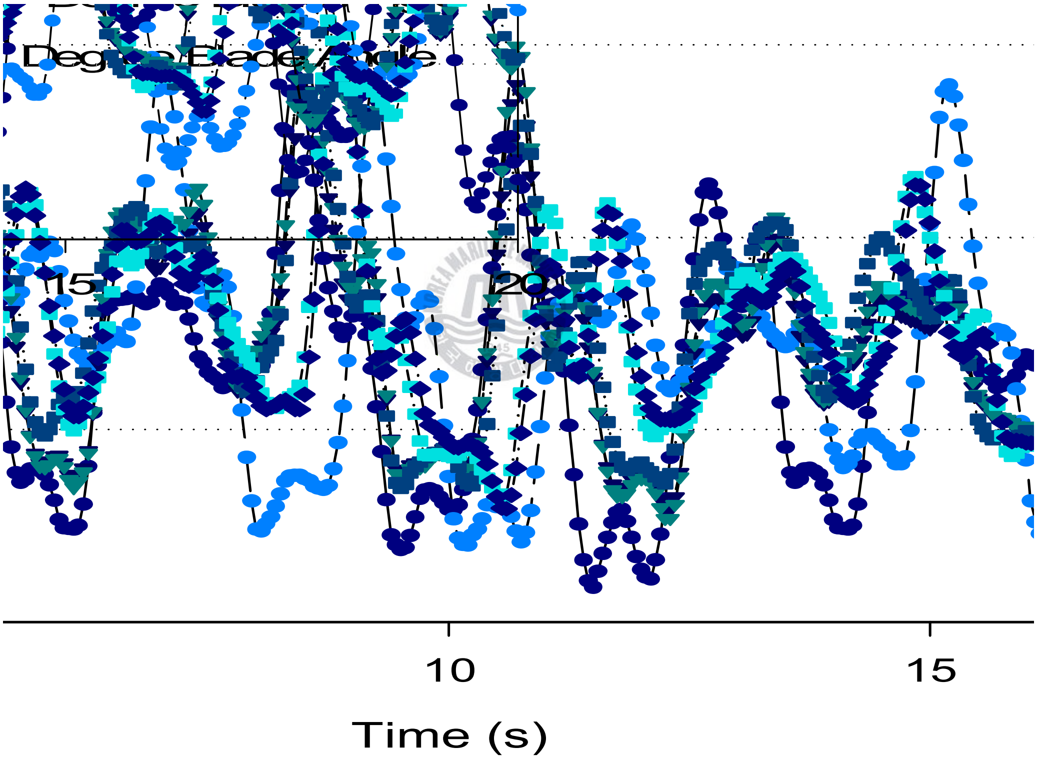

Figure 3.14. Instantaneous Torque of Savonius Rotors with Numerical Time Integration for 20seconds.

The above graph shows the variation of torque for different rotor angle for a time span of 20 s. The base model had a rotor angle of 60°. The results indicate that there is no increase in the torque so therefore, the blade angle was reduced. As the blade angle was reduced from 60°; the torque increases. The increase is in the sense that the graph shifts slightly towards 0, meaning a decrease in the negative torque. The maximum torque is obtained at blade angle of 20° which is 3.85kNm when compared to 2.73kNm. This increase is due to the fact that the blade is able to capture or extract the energy more effectively from the returning flow when water flows out of the rear chamber. This in turn increases the average net positive torque and hence the performance of the turbine. Decreasing the blade angle further has an unfavorable impact on the output power and also by increasing the blade curvature. The simulated wave energy flux is 13.77kW/m. The highest total efficiency is 18.58%. Therefore the 20° rotor angle savonius turbine converts 2.22 kW/m of the total energy flux.

3.4.2 3 Bladed Helical Savonius Rotor Angle Analysis

Helical Savonius rotors could provide positive coefficient of static torque. Helix can be defined as a curve generated by a marker moving vertically at a constant velocity on a rotating cylinder (at a constant angular velocity). Fig. 3.15 shows helical savonius rotor blades evaluated in this section. The inner edge remains vertical whereas the outer edge undergoes a twist of certain degrees. The blade retains its semi-circular cross-section from the bottom to the top. Combination of such blades is called as a helical Savonius rotor in this study. In spite of its good promise on generating positive static torque coefficient, there is no information on helical savonius rotor in the open literature. Hence, the main objective of the present study is to numerically investigate the effect of blade performance at various twist angles. The numerical results are compared with the conventional savonius rotor.

Savonius Helical angle	Schematic	Front view (fluid model)	Isometric view
Base Model			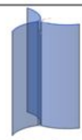
Case 6			
Case 7			
Case 8			
Case 9		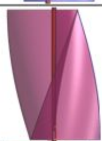	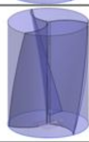
Case 10			
Case 11		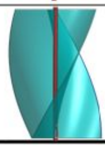	

Figure 3.15 Schematics Showing Savonius Rotor with Various Helical Rotor Angles

Table 3.2 Performance Analyses of Helical Savonius Rotor

Savonius helical Twist Angle (°)	0	15	30	45	60	75	90
Wave Height (m)	1.5						
Wave Period (s)	6.5						
Water Level (m)	16.15						
Average Torque (kN.m)	2.73	2.96	3.04	3.2	3.27	3.34	3.3
$P_{\tau ave}$(kW)	5.72	6.20	6.37	6.70	6.85	7.00	6.91
P_{wave}(kW)	43.39	43.39	43.39	43.39	43.39	43.39	43.39
Total Efficiency (%)	13.18	14.29	14.67	15.45	15.78	16.12	15.93

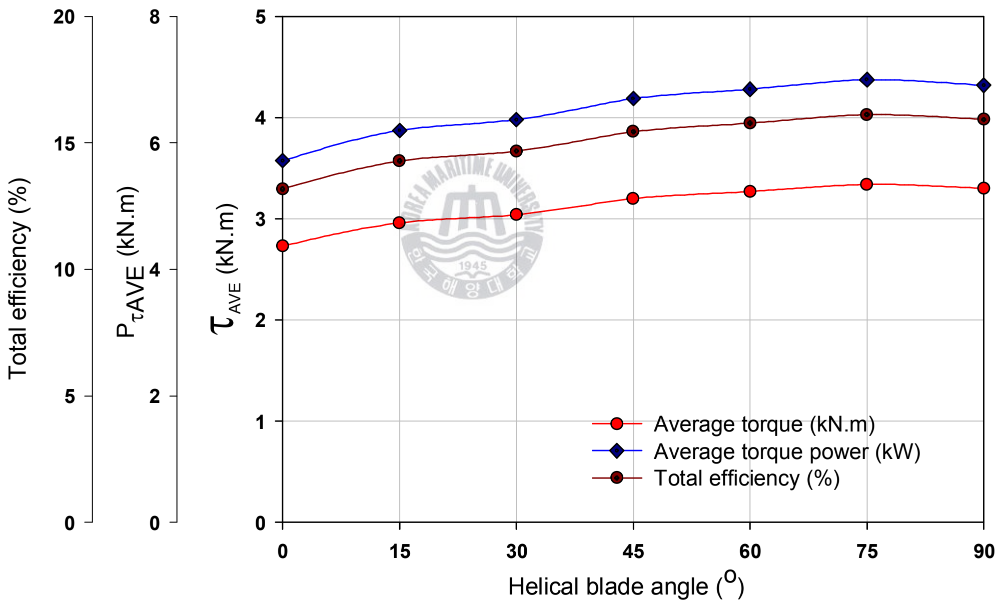

Figure 3.16 Graphical Representation of the Performance Analysis of the Helical Savonius Rotor

The performance analysis of the helical savonius rotor showed a slight increase in the total performance shown in Table 3.2 and Fig 3.16 The flow phenomenon was studied in three planes due to the twisted nature of the blades.

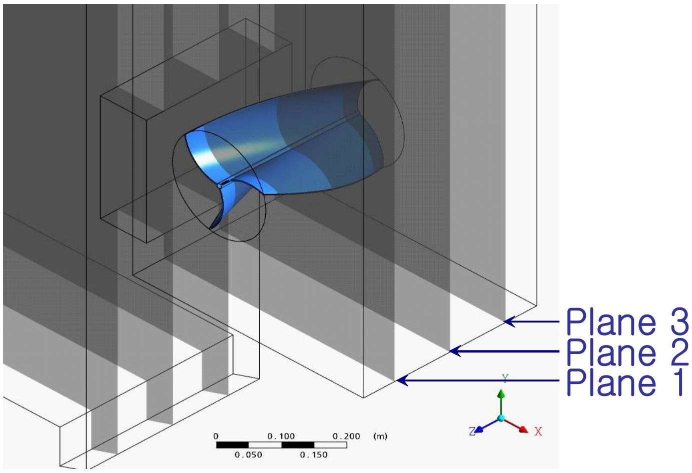

Figure 3.17 Helical Blade 2D Flow Analysis

In the conventional blade, the maximum force acts centrally (curvature center) and vertically, whereas for the helical blade, the maximum force moves towards to the tip of the blade because of the twist in the blade as can be seen in the plane velocity figure below. Due to these changes, a twisted blade gets a longer moment arm, and hence a higher value of net positive average torque.

Time (s) / 75° helical blade	Plane 1	Plane 2	Plane 3
0s	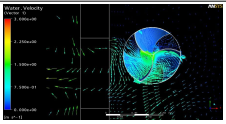	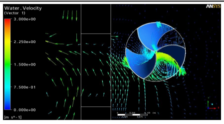	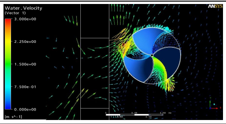
1.28s	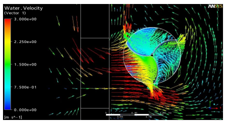	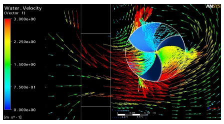	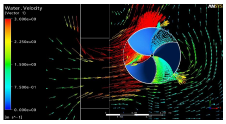
2.56s	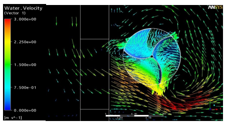	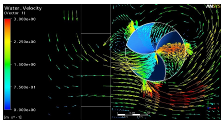	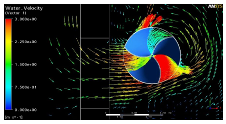
3.84s	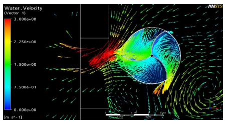	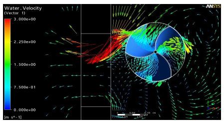	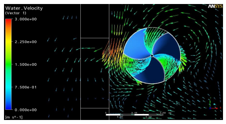
5.12s	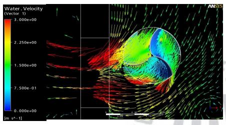	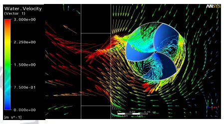	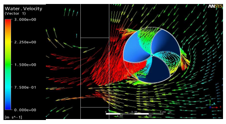
6.4s	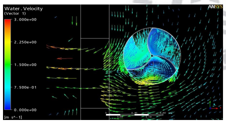	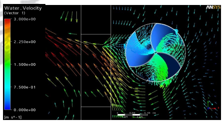	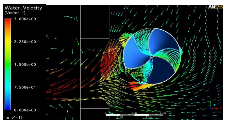

Figure 3.18 Instantaneous Velocity Vectors Around 75° Helical Savonius Rotor at the 3 Planes for a Full Cycle

The velocity vector for the 75° helical blade is shown in the Fig 3.18. The rotation of the turbine at plane 1, 2 and 3 is for a full wave cycle of 6.4s. It is shown for the same time instant. It is observed that for the particular time instant higher velocity is seen in plane 3. This is because of the longer moment arm which is available at the end purely due to the helical nature of the turbine. This design variation allows the fluid to interact with the turbine longer and hence transfers more energy to the turbine which otherwise would be lost in a conventional savonius turbine. The transfer of more energy occurs due to increase in the velocity which is preferred as this influences the torque and eventually the turbine output power. Velocity recorded in the mid plane (Plane 2) is smaller compared to that recorded in plane 3. For plane 1 the velocity at the time instant is smaller than that recorded in plane 3 but for the next cycle the flow characteristics interchanges and higher velocity is observed in plane 1. The result simply suggests is that higher velocity is always present near the tips of the turbine on both sides. The influence is due to the 2D assumption of the flow. The turbulent quantities thereby are much lower than under experimental conditions, where the radial limitations of the side walls of the channel produce more turbulence.

Finally, the design change suggests that the best geometry for the blade is with the rotor angle 20°. The overall performance with respect to the base model shows an increase of 5.4 % in the total efficiency. So under same wave conditions, using rotor angle 20° savonius rotor angle, higher power can be achieved. This increase is due to change in the flow phenomena as well as better inflow characteristics in the rotor as well as the increase net positive torque produced during outflow. The investigation shows the capability of the numerical method to simulate the flow field in a savonius turbine qualitatively. Thereby it is possible to carry out a numerical optimization process to design a more suitable savonius turbine. The savonius turbine has to be characterized by an optimal energy transfer from the fluid to mechanical power.

3.5 OWC Inlet Section Analysis

Although oscillating water column type wave energy devices are nearing the stage of commercial exploitation, there is still much to be learnt about many facets of their hydrodynamic performance. A key feature of the numerical modeling is the focus on the influence of the front wall geometry and in particular the effect of the front wall aperture shape on the hydrodynamic conversion efficiency. The effects of the front lip shape on the hydrodynamic efficiency are investigated both numerically based on pressure and velocity results. The results of the simulation have illustrated that simple changes to the front wall aperture shape can provide marked improvements in the efficiency of energy capture for OWC type devices. Tabulated below are the various OWC inlet section studied currently.

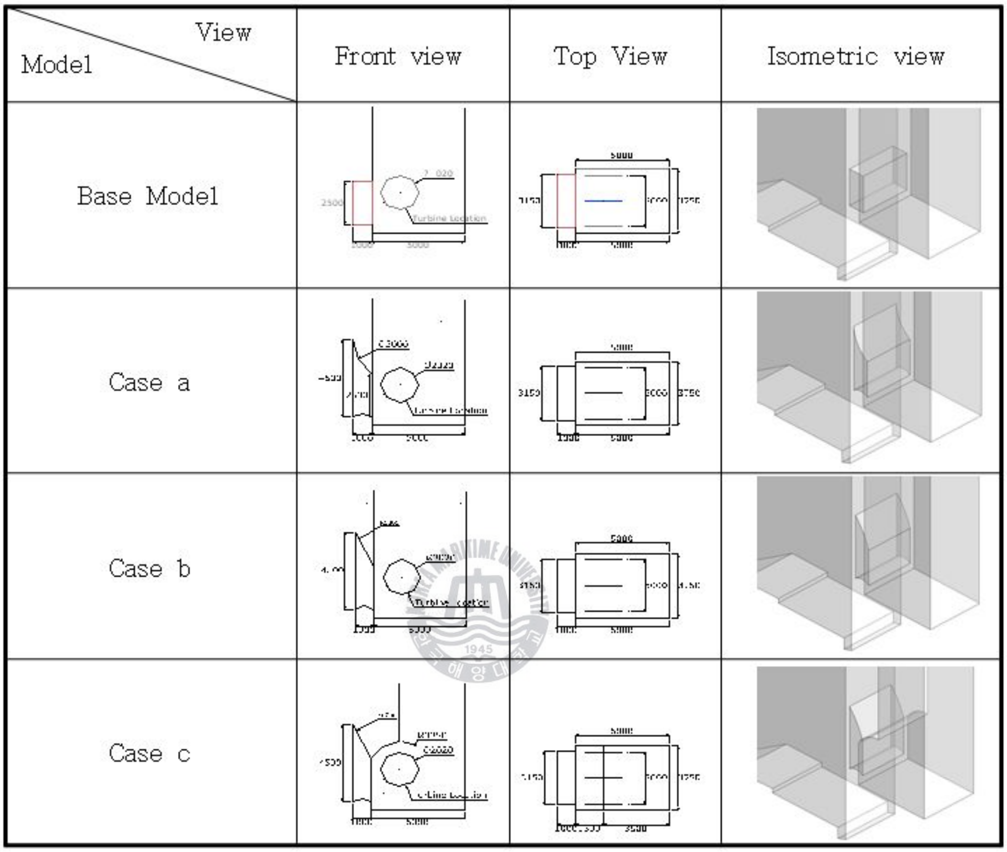

All Dimensions are in mm

Figure 3.19 Schematic of Various Front Wall Aperture Shapes

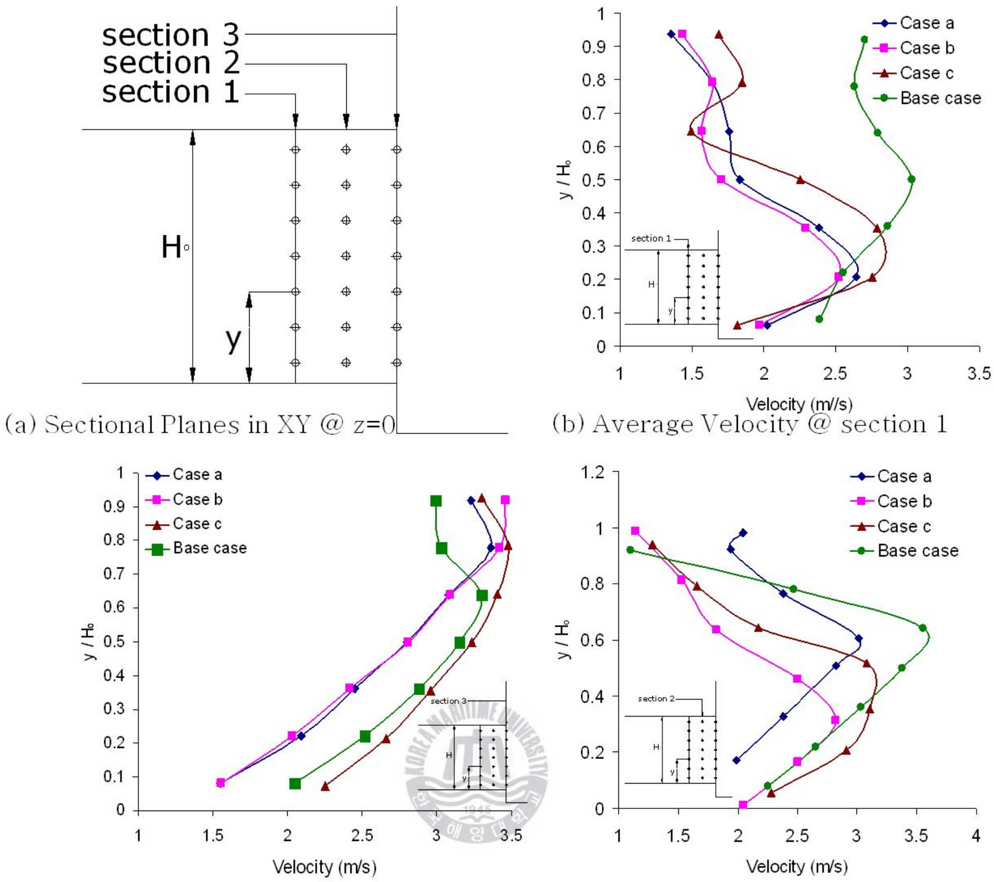

(a) Sectional Planes in XY @ z=0
(b) Average Velocity @ section 1
(c) Average Velocity @ section 3
(d) Average Velocity @ section 2

Figure 3.20 Average Velocity for Different Inlet Shapes in XY Plane at z = 0

The average velocity in the vertical plane in the middle of the various OWC inlet section is shown in the figure above. The velocity recorded at section 1 is highest for the base model. Higher velocity is recorded in the middle for all the cases than the upper and lower walls. There is a dramatic change in the velocity at y/H_o = 0.25 for cases a to c. Similar trend in the velocity profile is seen in section 2. At section 3 there is a gradual increase in velocity until y/H_o = 0.65 and then the velocity drops slightly. It is interesting to see that at this section, highest velocity is recorded for Case c and not the base model.

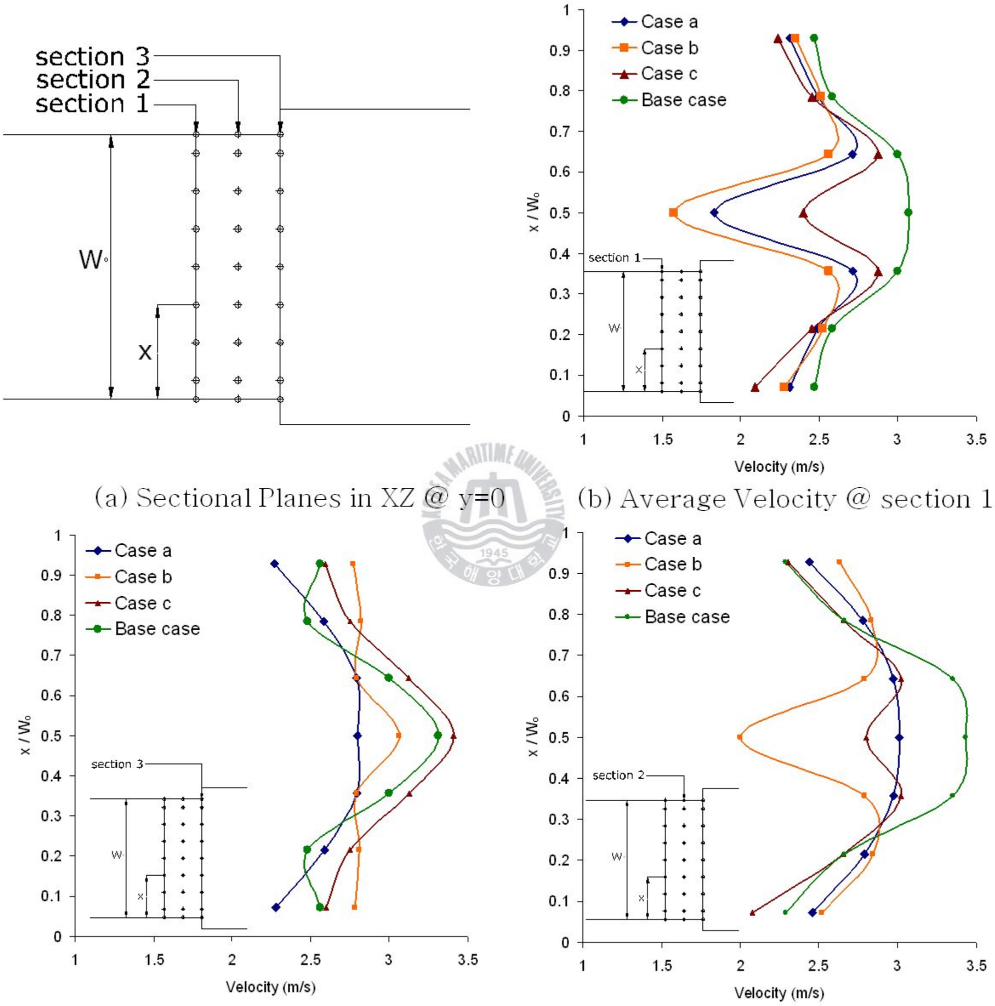

(a) Sectional Planes in XZ @ y=0 (b) Average Velocity @ section 1

(c) Average Velocity @ section 3 (d) Average Velocity @ section 2

Figure 3.21 Average Velocity for Different Inlet Shapes in XZ Plane at y = 0

The average velocity in the horizontal plane in the middle of the various OWC inlet section is shown in the figure above.

The velocity recorded at section 1 is highest for the base model. Higher velocity is recorded in the middle than the side walls. However, for case a and b the velocity right at the centre that is, x/W_o = 0.50 is the lowest than the velocity recorded near to the side walls. For case c the velocity is slightly higher than case a and b. Similar trend in the velocity profile is seen in section 2. At section 3 there is a moderate increase in velocity from the side walls towards the middle between x/W_o = 0.35 and x/W_o = 0.65. Again, the highest velocity at section 3 is recorded for Case c and not the base model.

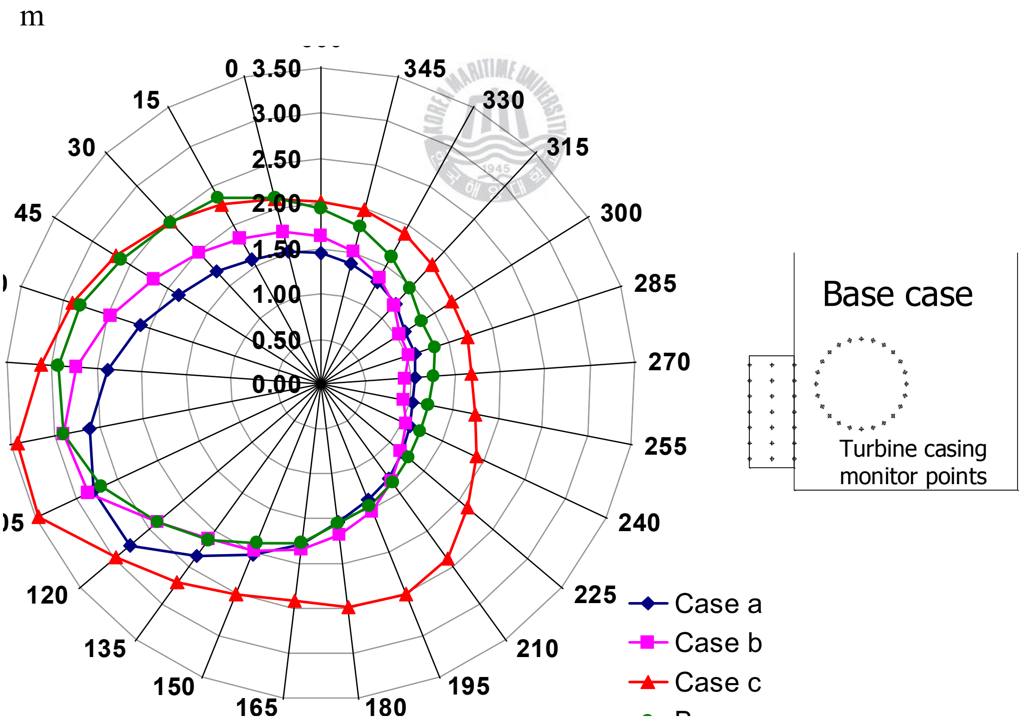

Figure 3.22 Circumferential Average Velocities at Turbine Location

The Fig. 3.20 shows the velocity recorded at the periphery where the turbine is located at 15° phase angles. Higher velocity is observed towards the OWC inlet for all the cases. The highest velocity is recorded for case c. There is also increase in the velocity recorded at the rear. This increase seen in case c is due to the returning flow having higher energy. This increase in the kinetic energy is beneficial as it will increase the power output from the turbine. The best model is then simulated with various design of 5 bladed savonius rotor.

The flow under the OWC front lip is a critical aspect of OWC design given it is the “entry” point for the energy into the OWC where the turbine is located. The flow demonstrates the development of an area of recirculation just behind the front lip as the fluid flows into the OWC chamber. The formation of these flows is a good indicator of energy loss, particularly when the counter flow extends into the domain away from a wall.

Time (s) \ Model	Base case	Case c
0 s	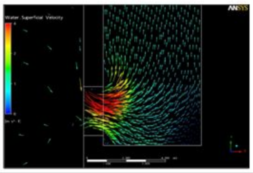	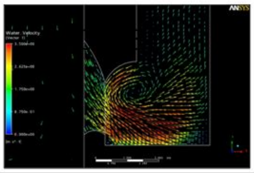
1.07 s	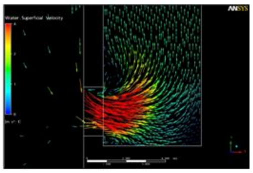	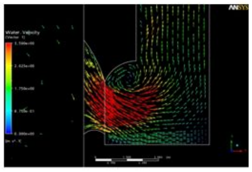
2.13 s	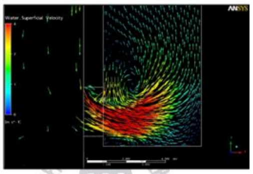	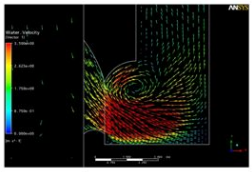
3.2 s	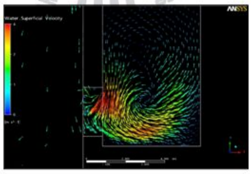	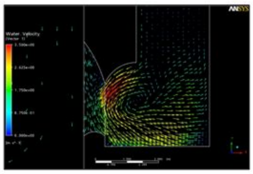
4.27 s	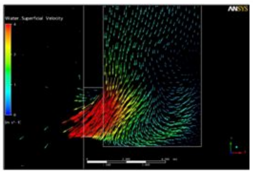	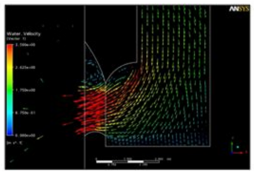
5.33 s	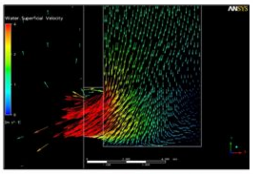	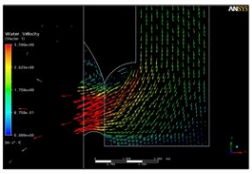
6.4 s	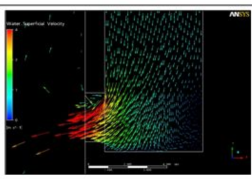	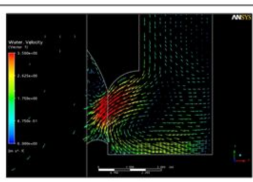

Figure 3.23 Velocity Vector at the Inlet Section for the Period t=6.4s

The flow patterns shown in Fig. 3.23 for the case 3 illustrate well formed flow patterns with smaller area of opposing flows and where there are flows they are inclined to be a good deal closer to the turbine casing. The best model i.e. Case c was further incorporated with various 5 bladed savonius rotor and the performance was analyzed.

3.6 5 Bladed Savonius Rotor Analysis

The best model from the OWC inlet section was incorporated with 5 blade savonius rotor for a higher efficiency. Previous study carried out obtained 21.47% efficiency for a 5 bladed savonius rotor. The 5 bladed savonius rotor was integrated in the best model from the previous section (Case 3) and simulated. Further to that, more simulations were carried out with a less steep angle to direct the flow more towards the inner curvature of the rotor (concave side) for a improved flow phenomena. Below is the tabulated results obtained for the different cases.

Models		Torque (k.Nm)	$P_{\tau ave}$(kW)	Total Efficiency (%)
Base case (Previous Study)	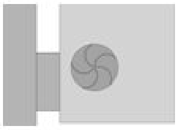	6.58	10.34	21.47
Case I (Case 3)	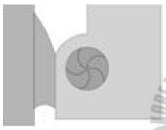	8.12	15.75	26.50
Case II	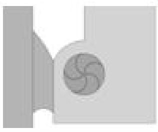	7.62	11.97	24.86
Case III	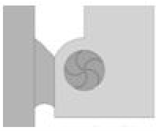	7.18	11.28	23.43

Figure 3.24 Schematics of 5 Bladed Savonius Rotor with Various Inlets Section

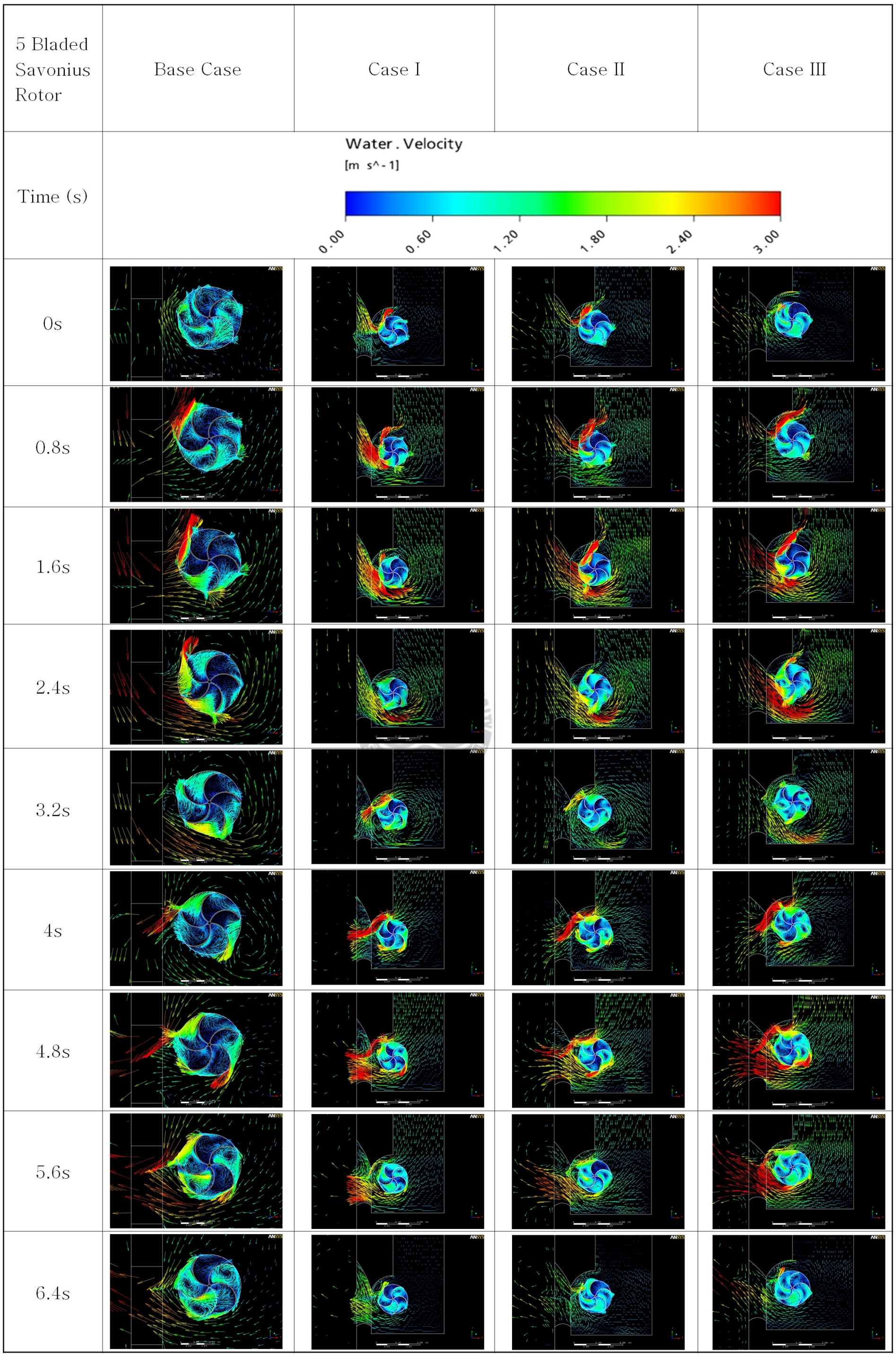

Figure 3.25 Instantaneous Velocity Vectors a 5 Bladed Savonius Rotor for a Full Cycle of 6.4s

The flow occurrence in and around the savonius rotor for all the case shows a vast dissimilarity with respect to the inlet section shown in Fig. 3.25. For a square section, flow is direction towards the center of the rotor thus generating a torque of 6.58kN.m i.e. it extracts 2.96kW/m of the total energy wave flux. The figure above shows that the flow needs to be direct towards the tip of the rotor in order to obtain a higher efficiency. Flow vector velocity of Case I (Case 3) shows that the flow enters at the angle favorable to hit the savonius rotor at the tip of the rotor. It stands to a reason that the flow needs to be directed towards the tip of the rotor in order to obtain a higher efficiency.

CHAPTER 4 CONCLUSION

The research performed on this wave energy concept aims to understand and evaluate it thoroughly from a physical, technological, point of view. With the current simulation set-up it has been shown that long term, slowly varying, power generation from ocean waves, using the presented technology is possible. In this research, a commercially available computational fluid dynamics code has been used to perform simulations of an oscillating water column with savonius turbine incorporated at the rear bottom of the chamber to determine the efficiency of energy absorption. The focus of this work has been on the simulation of the interaction of the incident wave on the OWC and in particular the effects from varying the design parameters associated with the savonius rotor and the front lip of the device such as aperture shape. Prior to numerical modeling of the entire system, wave generation within a numerical wave tank has been examined with particular attention paid to the free surface modeling and internal wave kinematics. Following this study, a systematic numerical investigation was then carried out on an OWC system to model the interaction between the incoming waves and the complex geometries affecting fluid entry into the OWC chamber including the interaction with the savonius rotor with different rotor angles and blade number.

- CFD simulation studies show the potential of the savonius rotor for wave energy conversion.

- Subsequent to the recognition that OWC modeling requires significant resolution of chamber geometry, numerical testing of different OWC chamber configurations was carried out with reflector plates. The addition of reflector plate did not increase the efficiency as expected. The total efficiency decreased respectively: 0°-5°: 0.24%, 5°-10°: 0.68%, 10°-15°: 0.63%.
- The aerodynamic characteristic of the rotating savonius rotor is much improved by the curved rotor blade and also a helical blade which results in a higher rotating torque. Aerodynamic optimization for a savonius turbine means to design a blade geometry which gives the maximum power output.
- Conventional savonius rotor is 13.18% efficient but 20° rotor angle blade is 18.58% and a 75° helical blade is 16.12% efficient. An increase of 5.4% and 2.94% respectively.
- The simulated wave energy flux is 13.77kW/m. The highest total efficiency is 18.58%. Therefore the 20° rotor angle savonius turbine converts 2.22 kW/m of the total wave energy flux.
- Due to these changes in the rotor angle, the 20° generates an enhanced recirculating flow between the rotors, thus results in a higher rotating torque. The twisted blade gets a longer moment arm, and hence a higher value of net positive torque is achieved.
- The studies show that the chamber inlet section indeed significantly affects the total efficiency. The inlet section

shapes simulated illustrated that the flow under the inlet as the fluid enters and exits the OWC chamber is particularly sensitive. The CFD flow visualization provided confirmation that the variations tested allowed for smoother flows by reducing the abrupt change in flow direction between the external and internal chamber fluid reducing turbulent back-flow.

- The highest efficiency obtained for a 5 bladed savonius rotor was 26.50% which included the best chamber inlet section. The generated torque was 8.12 kN.m i.e. it converts 3.66kW/m of the total wave energy flux

Finally, the overall results show that by making design changes to savonius rotor and inlet section of OWC increases the total efficiency hence the secondary and the primary energy conversion of the system can be improved under same wave conditions.

The research has revealed that it is possible to take an off-the-shelf numerical CFD and apply it to the complex problem of oscillating water column efficiencies with great effect. Given the global interest in ocean renewable energy, the optimal design of wave energy extraction model is a research area that requires significant attention and thus the ability to utilize commercial CFD codes to further this work should benefit both the theoretical analyst and the wave energy developer alike. This work has covered a range of topics and several areas of significance to OWC design and savonius rotor design which have only just been touched upon. Further extensions to this work could be to:

- Extended CFD modeling to a full 3-dimensional domain Perform the numerical modeling under irregular wave conditions
- Introduce real turbine characteristics such as Fluid Structure Interaction (FSI) to allow complete wave to wire efficiency modeling
- Investigate whether commercial CFD can be used investigate other key areas of interest to OWC designers such as extreme wave loading.
- Investigate the hydrodynamics modeling of the numerous chamber inlet section shapes, in particular, the effect of swirl as demonstrated in the CFD studies.
- Perform further experimental and numerical modeling to investigate venting under the front lip as function of wave height/lip submergence and the phase lag between the incident wave and OWC motion.
- Extend the analysis to investigate design parameters such as maximum and minimum chamber oscillating water static pressures for various OWC configurations and sea states.

These additional investigations may assist to the continued development of the systems such that one day they may at least partly contribute to providing power for the global energy demand.

ACKNOWLEDGEMENT

First and foremost I would like to express my deepest gratitude and appreciation to my supervisor, Prof. Dr. Young-Ho Lee for the continuous support of my Master's study and research, for his patience, motivation, enthusiasm, and immense knowledge in the field of wave power extraction and fluid dynamics. My thanks and appreciation also goes to my thesis committee members, Prof. Dr. You-Taek KIM and Prof. Dr. Kweon-Ha PARK for their guidance in completing this manuscript.

It has been a pleasure to study at the Korea Maritime University during the years. My fellow Flow Informatics Lab students are cordially thanked for their friendship. Especially, to my friend Deepak Divashkar Prasad for his good company and support.

Most importantly, none of this would have been possible without the love and patience of my family. I would like to express my heart-felt gratitude to my parents, my elder brother, sister-in-law and two younger sisters for their support, encouragement, love and concern, and strength for all these years.

I dedicate this thesis to my parents who unremittingly supported me during my years of study, without whom I would never have been able to achieve so much.

REFERENCE

[1] International Energy Agency (IEA). World Energy Outlook 2006. Head of Publications Service, IEA, Paris,France,2006.

[2] D. Mollison, O.P. Buneman, and S.H. Salter. Wave power availability in the NE Atlantic. Nature, 263:223 - 226, 1976.

[3] L. J. Duckers. Wave energy; crests and troughs. Renewable Energy, 5(2):1444 - 1452, 1994.

[4] J. Falnes and J. Løvstedt. Ocean wave energy. Energy policy, 19(8):768 - 775, 1991.

[5] H. Polinder, M.E.C. Damen, and F. Gardner. Linear PM generator system for wave energy conversion in the AWS. IEEE Trans. on Energy Conversion, 20(3):583 - 589, 2004.

[6] J.P. Kofoed, P. Frigaard, E. Friis-Madsen, and H.C. Sørensen. Prototype testing of the wave energy converter Wave Dragon. Renewable energy, 31(2):181 - 189, 2006.

[7] M.C. Carcas. The OPD PelamisWEC: Current status and onward programme. Int. Journal of Ambient Energy, 24(1):21 - 28, 2003.

[8] C.B. Boake, T.J.T. Whittaker, and M. Folley. Overview and initial operational experience of the LIMPET wave energy plant. pages 586 – 594, Kitakyushu, Japan, 2002. Proc. of the 12th International Offshore and Polar engineering Conference.

[9] R. Waters, M. Stålberg, O. Danielsson, O. Svensson, S. Gustafsson, E. Strömstedt, M. Eriksson, J. Sundberg, and M. Leijon. Experimental results from sea trials of an offshore wave energy system. Applied Physics Letters, 90:034105, 2007.

[10] A. Weinstein, G. Fredrikson, M.J. Parks, and K. Nielsen. Aquabuoy – the offshore wave energy converter, numerical modeling and optimization. Oceans '04. MTTS/IEEE Techno-Ocean '04, 4:1854 – 1859, 2004.

[11] M. Ruellan, H. Ben Ahmed, B. Multon, C. Josset, A. Babarit, and A.H. Clement. Design methodology for a SEAREV wave energy converter. Electric Machines & Drives Conference, 2007. IEMDC '07. IEEE International, 2:1384 – 1389, 2007.

[12] A. Muetze and J.G. Vining. Ocean wave energy conversion – a survey. Industry Applications Conference, 2006. 41st IAS Annual Meeting. Conference Record of the 2006 IEEE, 3:1410 – 1417, 2006.

[13] A. Clément, P. McCullen, A. Falcão, A. Fiorentino, F. Gardner, K. Hammarlund, G. Lemonis, T. Lewis, K. Nielsen, S. Petroncini, T. Pontes, P. Schild, B.- O. Sjöström, H. C.

Sørensen, and T. Thorpe. Wave energy in europe: current status and perspectives. Renewable & Sustainable Energy Review, 6(5):405 - 431, 2002.

[14] The Carbon Trust 2006, Future Marine Energy, Carbon Trust CTC-601, London, United Kingdom.

[15] International Energy Agency, 2005, Energy Statistics of Non-OECD Countries, 2003-2004, IEA, Paris,France.

[16] "Pelamis."(2007). Ocean Power Delivery Ltd. Retrieved September 25, 2005, from http://www.oceanpd.com/.

[17] Pontes, T., and Falcão, A. (2003). "Ocean Energy Recovery." Instituto Naticional de Engenharia e Tecnologia Industrial. Retrieved June 16, 2009, from http://www.poemsinc.org/papers/pontes-oeconv.pdf.

[18] McCormick, M. E. (1981). Ocean Wave Energy Conversion, Wiley, NewYork.

[19] Boyle, G., and Open University. (1996). Renewable energy: Power for a Sustainable Future, Oxford University Press in association with the Open University, Oxford;NewYork.

[20] Hagerman, G., and Bedard, R. (2003). "E2I EPRI Specification for Preliminary Estimation of Power Production by Offshore Wave Energy Conversion Devices." Electric Power

Research Institute Inc. E2I EPRI - WP - 001. Retrieved September 28, 2009, from
http://www.epri.com/attachments/297213_001_WEC_Power_Production.pdf.
.
[21] Bretschneider, C. L., and Ertekin, R. C. (1989). "Estimation of Wave Power as an Energy Resource for Hawaii." Proc. 1st Int. Conf. on Ocean Energy Recovery, Honolulu, Hawai'i, 189-201.

[22] "Wave and Tidal Energy."(2005). NaREC. Retrieved June 25, 2009, from
http://www.narec.co.uk/technologies-wave-tidal.php#.
.
[23] Graw, K.-U. (2002). "Wave Power Stations: Inexhaustible Energy Reservoir Ocean." Physics in Our Time. Retrieved June 25, 2009, from
http://216.239.39.104/translate_c?hl=en&u=http://www.unileipzig.de/~grw/lit/texte_100/114_2002/114_2001_weum.htm&prev=/search%3Fq%3D%2522Graw,%2BK.-U%2522%26hl%3Den%26lr%3D%26ie%3DUTF-8%26oe%3DUTF-8%26sa%3DG.

[24] Hagerman, G. (1992). "Wave Energy resource and Economic Assessment for the State of Hawaii." Prepared by SEASUN Power Systems for the Department of Business, Economic Development, and Tourism, Final Report. Retrieved June 18, 2009, from
http://www.hawaii.gov/dbedt/ert/wave92/wave92.pdf.

[25] Ertekin, R. C., and Xu, Y. (1994). "Preliminary Assessment of the Wave-energy Resource Using Observed Wave and Wind Data." Energy, 19(7), 729.

[26] "Options for the Development of Wave Energy in Ireland."(2002). Marine Institute and Sustainable Energy Ireland. Retrieved October 1, 2005, from http://www.irishenergy.ie/uploads/documents/upload/publications/wave.pdf.

[27] "Wave Energy."(2005b). World Energy Council. Retrieved, from http://www.worldenergy.org/wec-geis/publications/reports/ser/wave/wave.asp.

[28] "Wave Energy." China New Energy. Retrieved, from http://www.newenergy.org.cn/english/ocean/casestudy/wave/.

[29] Graw, K.-U. (1996). "About the Development of Wave Energy Breakwaters." Lacer No. 1, Leipzig Annual Civil Engineering Report, Universität Leipzig.

[30] "The Power of the Wind: Cube of Wind Speed."(2005). Danish Wind Industry Association. Retrieved October 1, 2009, from http://www.windpower.org/en/tour/wres/enrspeed.htm.

[31] Graw, K.-U. (1993a). "Shore Protection and Electricity by Submerged Plate Wave Energy Converter." European Wave Energy Symposium, Edinburgh,UK,1-6.

[32] Harris, R. E., Johanning, L., and Wolfram, J. (2004). "Mooring Systems for Wave Energy Converters: A Review of Design Issues and Choices." Heriot-Watt University, Edinburgh, UK. Retrieved September 19, 2009, from http://www.supergenmarine.org.uk/documents/papers/Public/Moorings/Marec_2004_RHLJJW.pdf.

[34] "WavePlane International A/S."(2005). WavePlane International A/S. Retrieved September 13, 2009, from http://www.waveplane.com/.

[35] Bedard, R., and Hagerman, G. (2004). "E2I EPRI Assessment Offshore Wave Energy Conversion Devices." Electricity Innovation Institute E2I EPRI WP - 004 - US - Rev 1. Retrieved September 20, 2009, from http://www.energy.ca.gov/development/oceanenergy/E2I_EPRI_REPORT_WAVE_ENERGY.PDF.

[36] "WavePlane International A/S."(2005). WavePlane International A/S. Retrieved September 13, 2005, from http://www.waveplane.com/.

[37] International Energy Agency (IEA). IEA-OES, International Energy Agency Implementing Agreement on Ocean Energy Systems, Annual report 2007. IEAOES Executive Committee, Paris, France, 2007.

[38] N. J. Baker, and M. A. Mueller, “Design and Integration of Linear Generators into Direct Drive Wave Energy Converters'', Proceedings of Marine Renewable Energy Conference, Newcastle, March 2001 ISBN 1-902536-43-6

[39] Cho, Y. J., “A study on the characteristic of a direct drive turbine for energy conversion generation using commercial ode CFD” Masters Thesis (Korean).

[40] Vantorre, M, Banasiak, R, Verhoeven, R. 2004, ‘Modelling of hydraulic performance and wave energy extraction by a point absorber in heave’, Applied Ocean Research, vol. 26, pp 61-72.

[41] Savonius S J. The S-rotor and its applications. Mech Eng, 1931, 53: 333–338

[42] Menet J L. A double step Savonius rotor for local production of electricity: A design study. Renewable Energy, 2004, 29: 1843–1862.

[43] Reupke P, Probert S D. Slatted-blade Savonius wind-rotors. Appl Energy, 1991, 40: 65–75

[44] Khan M N I, Iqbal M T, Hinchey M. Sea-floor power generation system. 8 July 2009. http://necec.engr.mun.ca/ocs2007/viewpaper.php? id¼11&print¼1

[45] Jobb G. An ocean wave energy converter. 8 July 2009. http://www. treefinder.de/Ideas/WaveConverter.pdf.

[46] Merriam M F. Wind, waves, and tides. Annu Rev Energy, 1978, 3: 29-56

[47] Faizal, M., Ahmend, M. A., and Lee, Y. H., “On utilizing the orbital motion in water waves to drive a Savonius rotor” Renewable energy, Vol. 35:164 – 169, 2010.

[48] Koo, W, Kim, MH, Lee, DH, Hong, SY 2006, ‘Nonlinear Time-domain Simulation of Pneumatic Floating Breakwater’ , Journal of ISOPE, Vol. 16, No 1, pp 25-32.

[49] Saramento, AJNA, Brito-Melo, A 1995, ‘An experimental-based time-domain mathematical model of OWC power plants’, Proceedings of the 5th ISOPE Conference. The Hague, vol. 1, pp 321-327.

[50] Menter, F.R., “Zonal Two Equation k-ω Turbulence Models for Aerodynamic Flows,” AIAA Paper 93-2906, 1993.

[51] Bardina, J.E., Huang, P.G. and Coakley, T.J., “Turbulence Modeling, Validation, Testing and Development,” NASA Technical Memorandum 110446, 1997. (See also Bardina, J.E., Huang, P.G. and Coakley, T., “Turbulence Modeling Validation,” AIAA Paper 97-2121.

[52] Orer G, Ozdamar A. An experimental study on the efficiency of the submerged plate wave energy converter. Renewable Energy, 2007, 32: 1317-1327

APPENDIX A
WAVE ENERGY CONVERSION DEVICES

This appendix gives a brief introduction to the various wave energy conversion devices. The devices are first classified as to whether they are shoreline, nearshore or offshore devices. Further they are separated into operating principles as: Oscillating Water Column (OWC), Overtopping Devices (OTD) and Wave Actuated Bodies (WAB). The WAB devices are further described by their primary motion.

A.1 Shoreline Devices

A.1.1 Oscillating Water Columns

In an oscillating water column (OWC) device, wave action causes water to rise and fall in a cylinder, forcing trapped air in the shaft out through a smaller orifice on top. Due to the reduction in volume, the pulsating air's velocity is increased. This higher velocity air is then directed towards the blades of an air turbine causing it to rotate. To get rotation in one direction, the air is rectified through one-way valves or using a self-rectifying axial flow Wells turbine. The turbine is coupled to an electric generator to produce electricity.

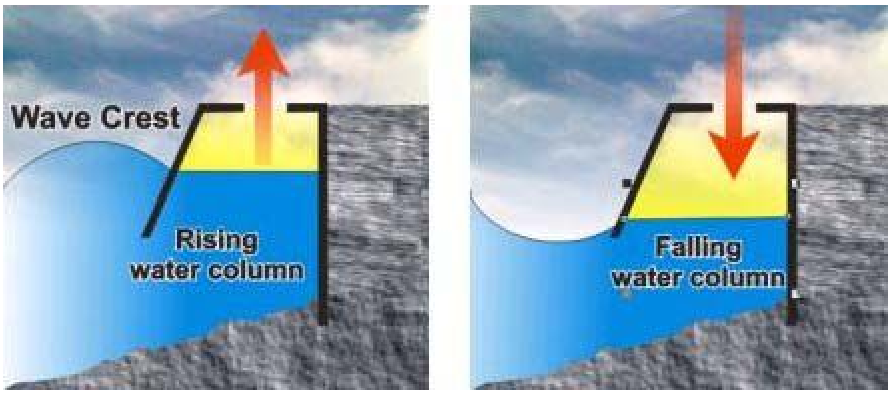

Figure A. 1 Principles of the oscillating water column [1]

Advantages of onshore OWC over other wave energy technologies:

• Structural costs are less, as the OWC is located on onshore, and thus experiences less wave loading.

• Cost distributive - OWC can be built as part of the harbor breakwater
• Less maintenance costs, as it is easily accessible.
• On shore installation mean less expense to transmit energy to the grid.
Constraints
• Deep water conditions must be present near shore
• Waves of good average energy required
• Due to the air water combination, corrosion is more significant than if a WEC is submerged.
• The efficiency of an OWC drops off when operated outside of a tuned frequency band
• Noise generated by the air turbine may be an issue depending on where the OWC is installed and whether sound baffling on the unit has been added.

A.1.1.1 LIMPET AND LIMPET 500

On the island of Islay, off the west coast of Scotland, a pilot 75KW OWC device or LIMPET (Land Installed Marine Powered Energy Transformer) was constructed. This was a joint project between Wavegen and Queens University Belfast and was the world's first commercial WEC. The unit ran for 10 years and has presently been decommissioned.

Figure A.2 Pilot shoreline wave power station, Islay [2]

Wavegen, installed the LIMPET 500 on the island of Islay in 2000. The LIMPET 500 is a commercially available 0.5 MW unit that is built on the existing shoreline using the cliff edge for support. It uses a hollow concrete or steel structure which is submerged below the water line and is open to the sea on bottom with an air column at the top. Its water depth is generally 7 m with a water plane area of 170 m2. Maximum performance is achieved with average wave intensities between 15 and 25 kW/m. To achieve the 500 kW, a pair of counter rotating Wells turbines are used which each drive a 250 KW generator. (Note: In 1992, Wavegen's co-founder and former Queen's professor of civil engineering, Alan Wells invented the Wells turbine.)

Figure A.3 LIMPET 500, Islay[3, 4]

Figure A.4 LIMPET 500, Islay(PhotoWavegen) [5]

Figure A.5 Cutaway diagram of the Islay shoreline wave energy device, UK[3]

Constraints for the LIMPET:

• The shoreline construction was built on rocky shores that experience wind and waves
• For the prototype Islay OWC system, a dam had to be built to protect the unit while being constructed.
• Noise is a concern

A.1.1.2 Parabolic - Australia

Energetech Australia Ply Ltd. founded by Dr. Tom Dennis has developed a new OWC converter that touts [6]:

• Parabolic shape reflector that concentrates wave energy. Dr. Ennis proposed this shape in 1992 and a model was developed in 1997 at the University of New South Wales Water Research Laboratory in Manly Vale. Maximum focusing occurs if:

1. Wave crest direction is parallel to the axis of symmetry of the parabola
2. Flat sea floor near the device so as not to alter the wave direction or cause waves to break
3. The focal length determined so that waves don't have time to disperse.

• The device has a Denniss-Auld turbine design that functions on an oscillating airflow. This turbine has a slower rotational speed and higher torque than traditional turbines resulting in higher efficiency, better reliability and less maintenance. Parameters of this variable-pitch turbine are controlled from a pressure sensor placed at the focal point of the parabolic shape
• Low noise level of an average reading of 73db

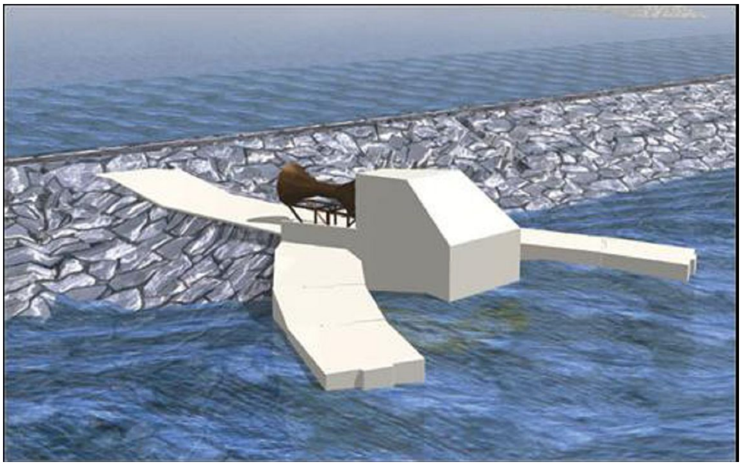

Figure A.6 Artistic impression of Energetech parabolic OWC [6]

This WEC can be used in the construction of coastal structures and harbor breakwaters. The generator is of the induction type at 415V L-L at 50 Hz. The power from the generator is coupled to the grid through converters having voltage and frequency control.

Constraints to this design:

• Requires deep water up to the coastline
• Requires 40 m of coastline Investments:
• July 2005, the Energetech WEC was installed and operated at Port Kembla, approximately 100 km south of Sydney, Australia. It is presently undergoing testing [6].
• The wave energy plant was towed to Port Kembla June 2005, after assessing the mooring and installation, minor improvements were needed and it was returned to port [6].
• Feb 2002 Energetech was chosen to work with BC Hydro to develop a 2 MW wave energy facility on Vancouver Island, hoping to produce 100 MW by 2008 [6].

A.1.1.3 Wave Energy Conversion Activator

Daedalus Informatics, Ltd. of Greece has proposed a theoretical concept, a Wave Energy Conversion Activator (WECA), where the energy of waves impacting on a breakwater is converted into compressed air. The impacting waves act as a virtual “Wedge” of kinetic energy. This hydrodynamic phenomenon is characterized as the “Critical Momentum Wedge” (C.M.W.) principle. A full scale prototype made of steel is planned for a breakwater. It can also be constructed of other materials and mounted onshore, near shore or on offshore structures.

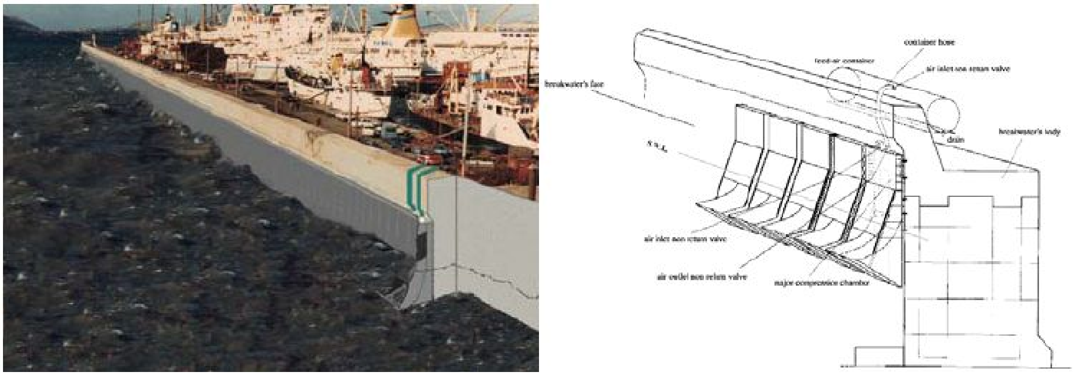

Figure A.7 Computer rendering of WECA on a breakwater runup wall (left), design details (right) [7]

The web site gives a theoretical explanation of the phenomenon and is summarized as follows: Water particle orbits become elongated as they enter shallow water and are deflected by a modified sea bed.

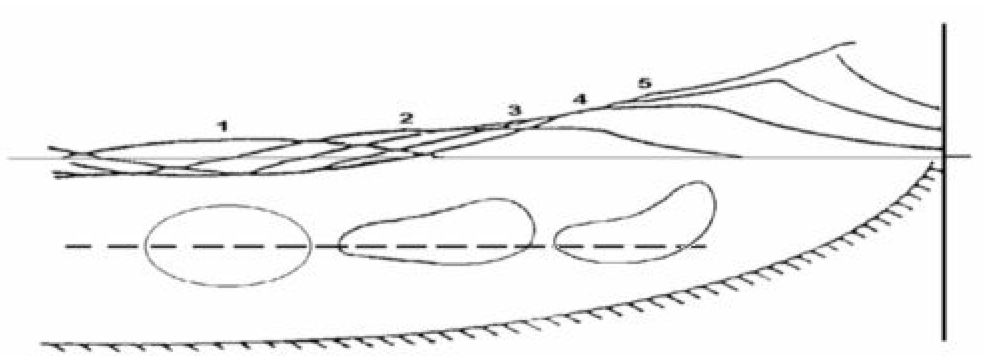

Figure A.8 Deflection of water particle orbits due to progressive wave motion over a modified sea bed [7]

Under certain conditions, the orbits will collapse, resulting in a burst of kinetic energy resembling a linear hydraulic ram. Fig. A.9 shows a wave approaching a modified sea bed, resulting in an initial peak due to the momentum of the wave form, while the second peak is theorized due to C.M.W. momentum. The separation between the first and second peak is dependent upon the wavelength of the wave.

Computer simulation was used to determine the hydrodynamic behavior of the device with progressive waves, as well as determining the energy and pressure ratios from waves of varying wavelengths.
A full scale prototype is planned - 7 m high and 6m wide designed to deliver 20 KW of power.

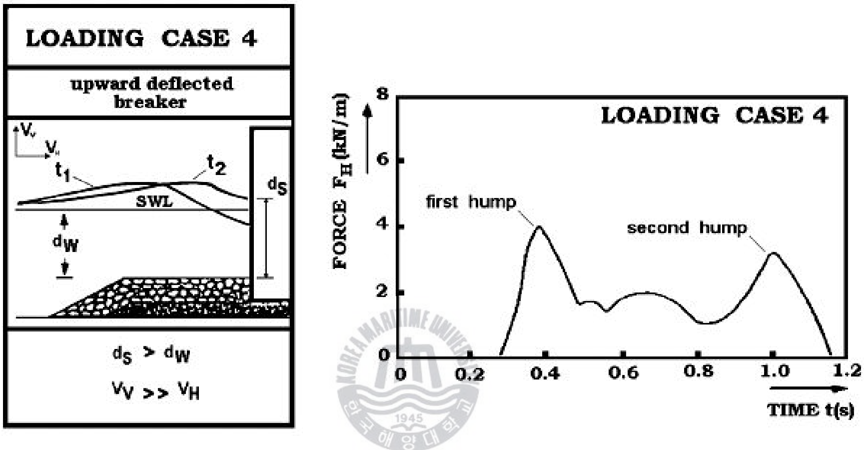

Figure A.9 Horizontal force induced on a vertical breakwater by upward deflected of the wave [7]

A.1.2 Overtopping Devices

A.1.2.1 TAPCHAN

The tapered channel or "TAPCHAN" invented by Dr. Even Mehlum of Norway, focuses wave surge to fill a reserve with sea water. It then uses the elevated water to run a low-head hydro generator. This WEC has few moving parts and relies on well-proven hydroelectric technology. The incoming waves enter a tapered channel, with the entry section being the widest. Channel walls are typically 3 to 5 meters above sea level. As the waves propagate down the narrowing channel, the wave height increases to several meters above sea level until reaching an elevation where the wave crests spill over the walls into a reservoir. Thus the wave's kinetic energy has been converted into stored potential energy of the reservoir. The stored water is used to turn a Kaplan turbine, which produces electricity. The water that exits the turbine returns to the sea.

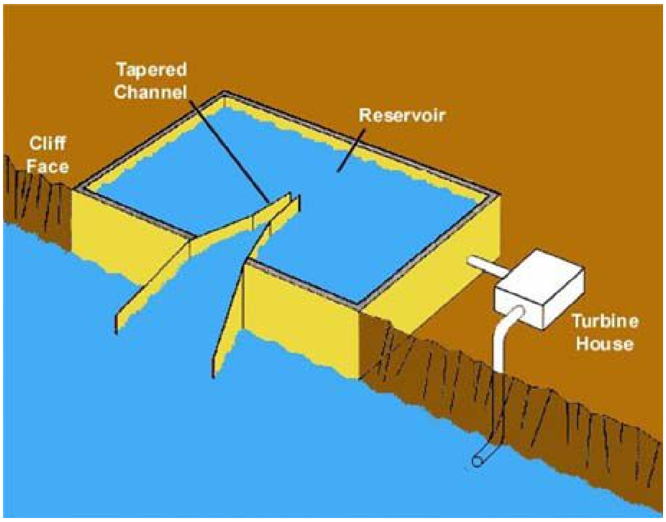

Figure A.10 TAPCHAN wave energy device - Copyright Boyle, 1996 [8]

Constraints for the tapered channel are:

• Not all coasts are suitable for this wave energy device. Deep-water conditions should be resent near the shore and a suitable reservoir location should be available. Installation costs will be largely dependent on whether extensive blasting or dam building is required.
• Waves of good average energy are required.
• The tidal range must be less than one meter.

Tapered channel installations:

• Indonesia -“In 1998, following experience gained from Norway's demonstration plant near Bergen and a feasibility study, a Norwegian team coordinated by Indonor AS and including Norwave AS, Groener AS and Oceanor ASA won a contract to deliver a TAPCHAN wave power plant. The site, at Baron on the south coast of Java, utilizes a bay with its own natural basin. The 1.1 MW wedge-groove plant will harness power from waves entering the 7-metre wide mouth, flowing down a narrowing channel, being forced over the walls of the basin (reservoir) and being returned to the sea via a conventional low-head turbine” [2].

• “A demonstration device with rated output of 350 kW began operating in 1985 at Toftesfallen, in Norway. The device functioned successfully until the early 1990s, when work on modifying the device destroyed the tapered channel” [9, 10, 11].

A.1.2.2 Seawave Slot-Cone Generator

Egil Andersen of Norway patented a concept utilizing wave overtopping to store water in multiple chambers above sea level, to drive a hydro turbine. Bakke and Leif Inge Slethei of WAVEenergy AS of Norway purchased the patent rights in 2003 and are presently developing the Seawave Slot-Cone Generator (SSG) concept [12]. The SSG is also planned for offshore applications that are fixed or floating installations.

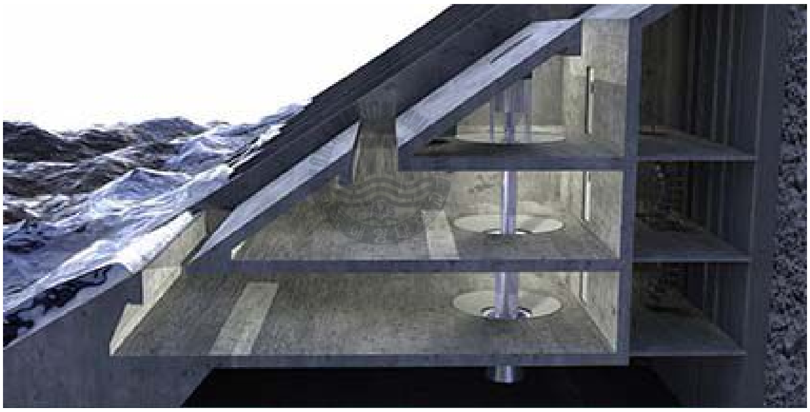

Figure A.11 Onshore Seawave Slot-Cone Generator (SSG) of WAVEenergyAS [12]

Figure A.12 Offshore Seawave Slot-Cone Generator (SSG) of WAVEenergyAS[12]

A.1.3 Wave Activated Bodies - Hydraulic Platform

Shmuel Ovadia of S.D.E. Energy and Desalination Ltd. has patented a WEC device that uses hydraulic platforms to convert wave energy into hydraulic pressure, to generate electricity. The device can also be used to desalinate sea water. (US Patent #5,461,862 and PCT#IL98/00118) [12]. The device produces about 40 kWh per meter of shoreline, with 1 meter wave height per hour [13].

Figure A.13 S.D.E. Ltd Hydraulic Platform [12]

Constraints:

• Requires deep water conditions to shoreline. Investments:
• Produces electricity at 1 cent/KW at a cost of $600K/MW [13]
• Shmuel Ovadia received a "20-year contract to sell 4 mega-watts of power to the Israel Electricity Corporation from a plant he plans to build in the seacoast city of Ashdod".
• A prototype was built in the port of Jaffa verifying that this WEC can generate 40 kilowatts of electricity per meter of shore line

A.2 Near Shore Devices

A.2.1 Oscillating Water Columns

A.2.1.1 Osprey 2000

The Osprey 2000 short for “Ocean Swell Powered Renewable Energy” is a Wavegen OWC for nearshore use. It rests on the seabed and can generate up to 2 MW of power. Like the LIMPET 500, it uses self rectifying Wells turbines. The turbines run induction generators that are connected to the grid through sub sea cables. Wavegen describes the following of this device [14]:

• Modular design constructed of low cost steel/ concrete. It can be incorporated into caisson breakwater structures and floated to site.
• Minimal environmental impact
• 60 Year structural design life with 20 year M & E plant upgrades

Figure A.14 Artistic Impression of Wavegen's Osprey 2000 [15]

Background Osprey I: The 2 MW Osprey I, launched in August 1995, was destroyed due to bad weather (structure but not equipment) while being towed to Dounreay, Scotland. This was during the tail end of hurricane Felix (Duckers, 2000). The unit shown in Fig. A.14 is the replacement.

Constraints:

• Must be placed in 15 m of water and within 1 km of the shore.
• The maximum power output occurs from an ocean swell generated by a fetch of over 400 km. Under storm conditions, the power output is capped.

A.2.1.2 Pneumatically Stabilized Platform or PSP

The pneumatically stabilized platform is a platform of concrete that obtains its primary buoyancy by resting on trapped air acting on the underside of the deck. The platform is composed of cylindrical shaped elements that are placed together in rectangular shaped modules. The air in the cylinder, which is slightly above atmospheric pressure, is sealed on top but open to the sea on the bottom. Between the cylinders, buoyant material can be placed such as air, foam or other materials.

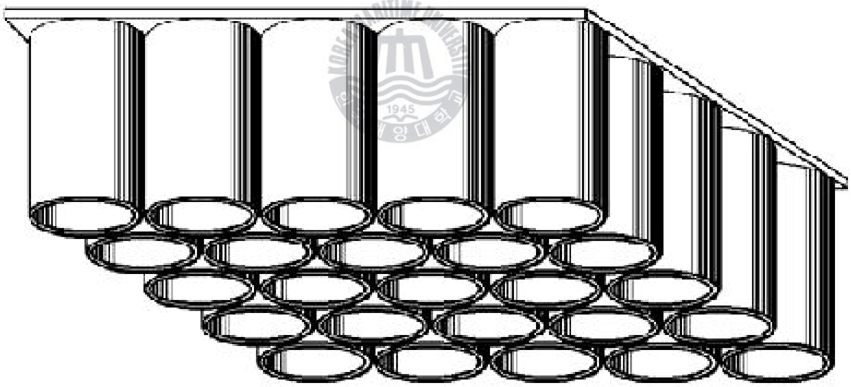

Figure A.15 Float Inc. pneumatically stabilized platform [16]

By allowing air to flow between cylinders through a manifold or connecting orifice, pressure peaks beneath the structure can be reduced and overall stability improved. Directing this air through an air turbine to generate electricity is being considered, and depending on the sea condition the oscillation of water columns could be tuned to reduce overall hydrodynamic loading.

Constraints:
• At this time are performance of the air pocket and cost of construction.

A.2.2 Wave Activated Bodies

A.2.2.1 Pivoting Flap - Pendulor Device

The Pendulor device is a rectangular shaped pendulor box, open at one end. A hinged pendulum flap covers this opening, which is aligned to face incident ocean waves. A standing wave is created by incident waves interacting with reflected waves from the back of the device. The Pendulor is placed at the node of the standing wave, to maximize the forces on the flap. Movement of the flap drives a hydraulic cylinder to pump hydraulic fluid to turn a hydraulic motor. The motor is coupled to a generator to produce electricity. To provide a more constant speed and torque on the generator shaft, a double-acting hydraulic cylinder is used with one hydraulic motor driven on the compression stroke and the other driven on the expansion stroke.

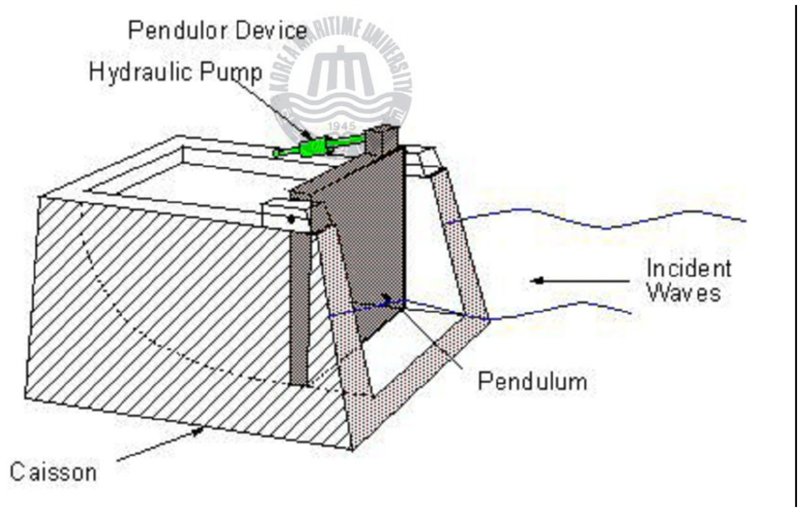

Figure A.16 Pendulor device[27]

Constraints:

• Needs to be tuned to the incident wavelength

A.2.2.2 Wave Mill

"Alan Vowles and his brother Gerald have been developing the Wavemill, a desalination unit powered by the ocean's waves" [17]. The Wavemill is a WEC device that can be mounted either at the shoreline or nearshore. The wave energy from the heave motion of rising wave force is captured using a buoyant float and the falling wave gravitational force is harnessed by a lower suction chamber. Wave surging forces are captured by a surge wall. Under low wave conditions, the device's surge wall changes shape to maximize wave energy capture. One of the features being touted by this company is that the units are modular in format and parts are available off-the-shelf.

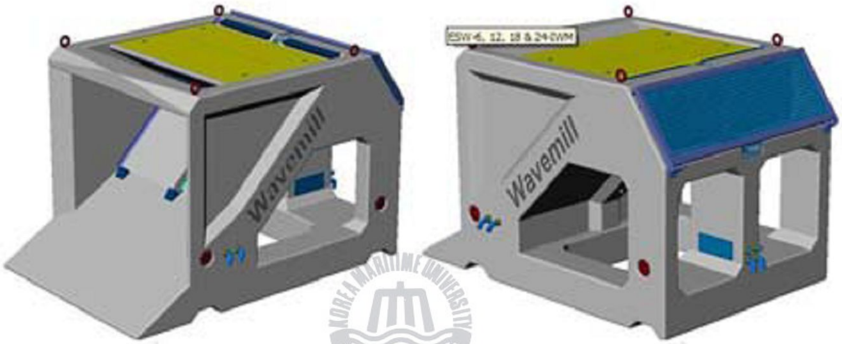

Figure A.17 One unit of Wavemill [17]

• Pumping Unit – "The Hydraulic Pumping Unit is the most basic Wavemill in this series. It provides the platform on which other systems in the series are built. These units provide pressurized seawater for a variety of applications outlined below. The HPU unit can be upgraded with WEC's unique Watermaker, Hydraulic Power, or Electric Power add-on modules at a later date" [17]. • Watermaker – "Designed to produce freshwater ranging from 800 GPD in ½ meter waves to 460,000 GPD in 3 meter waves. Where higher volumes are required, these modular units may be installed in multi-unit arrays" [17]. • Electric Power –"Designed to produce electricity ranging from 10 kWH/day in ½ meter waves to 5,600 kWH/day in 3 meter waves. Where higher volumes are required, these modular units may be installed in multi-unit arrays" [17]. In the question and answer section at the company's web site the following was found: "Q: What about electrical generation? Electrical generation units are now in the planning stage and expected to become available early on" [17].

The Wavemill does not have site specific parts and thus is adaptable to different locations. A caisson of lightweight marine concrete is used to provide rigidity while having the mass to support wave forces without requiring extensive mooring devices. On installation, the concrete unit is floated to site and then ballasted accordingly.

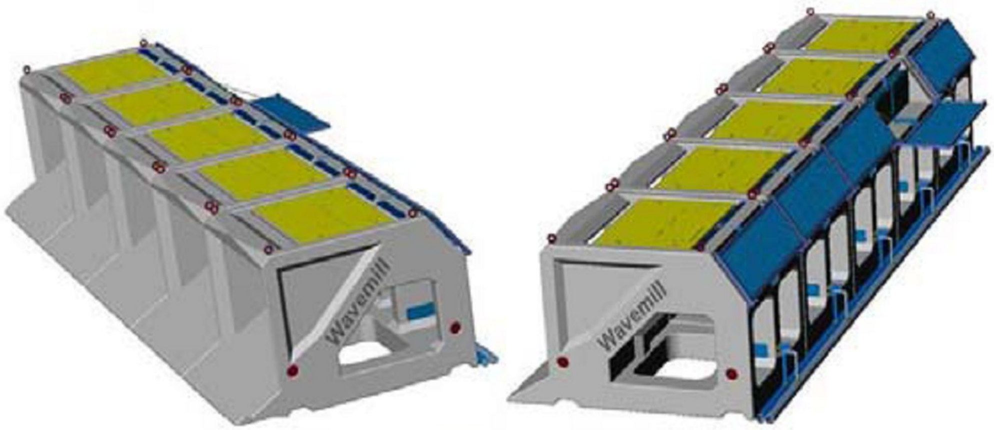

Figure A.18 Five units Wavemill [17]

Constraints:

- As the Wavemill ESW Series is modular, the model chosen depends on the application:
- ESW-24 is a utility-scale 26-foot cube
- ESW-12 is a commercial module roughly 14-foot cube
- ESW-6 half size version of the ESW12 - For eco-tourism resort, small village, research sites, military applications etc.
- The unit can be towed to shore or the wave follower unit can be separated from the concrete caisson and reinstalled at a later date when weather conditions improve [17].

A.3 Offshore Devices

A.3.1 Oscillating Water Columns

Commander Yoshio Masuda of Japan developed the initial concept of using an OWC to generate power for navigation light buoys [18]. These buoys have been in operation for more than 20 years. Employing the OWC concept, they have a long vertical column that extends below the wave action so that the column is not affected by local wave action. It is the bobbing up and down action of the buoy, which causes air in the column to be compressed and decompressed to drive an air turbine.

A.3.1.1 Mighty Whale

In 1940, Yoshio Masuda conducted early wave energy conversion experiments. A largescale floating prototype name Kaimei in 1970 was developed and tested by JAMSTEC off the sea of Japan. In the 80's JAMSTEC ran tests on an onshore device near Sanze, also located in Yamagat Prefecture. In 1987, another large floating device called the Mighty Whale was developed. It was completed in 1998 and towed to GOKASHO Byai in Mie Prefecture where testing began in 1998. This off shore unit contains multiple OWC devices. The Mighty Whale is a floating structure that looks like a floating whale. On its windward side are 3 air chambers that absorb wave energy. The structure also has buoyancy tanks and a stabilizer to reduce wave-pitching action. "In Japan, a 50m-long, 30m-wide Mighty Whale prototype, with three air-chambers with 10KW, 50KW and two 30 KW turbo-generators, was tested from 1998 to 2000 at Gokasho Bay, Mie Perfecture." [17].

Research test goals are:

- Validate theory - energy absorption, mooring system, hydrodynamic loading
- Obtain response and operation data to real sea conditions
- Study the effects the device has on the environment

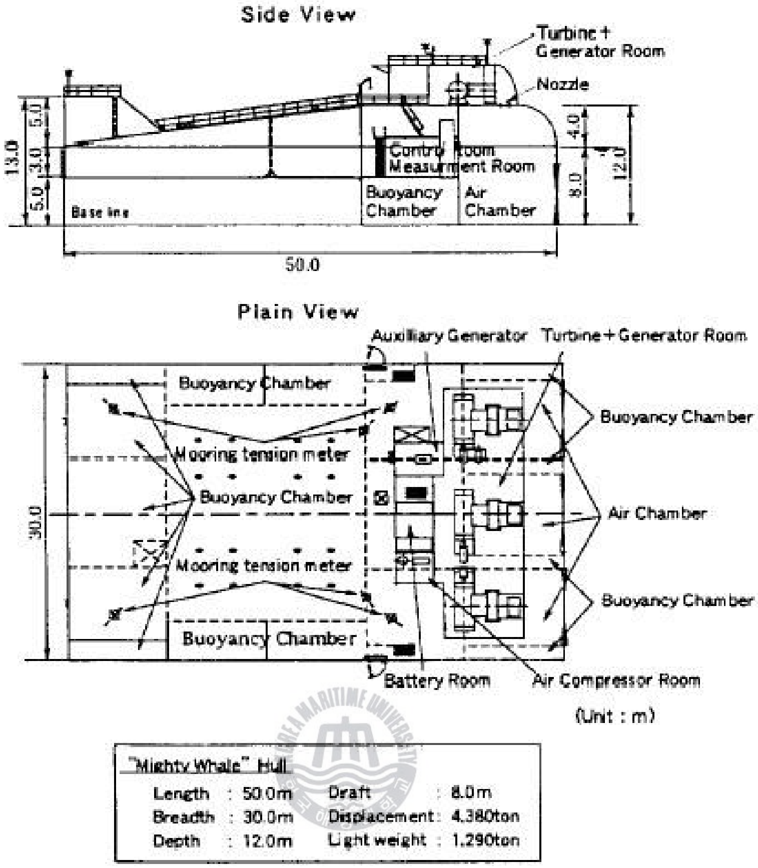

Figure A.19 Side view of Mighty Whale [19]

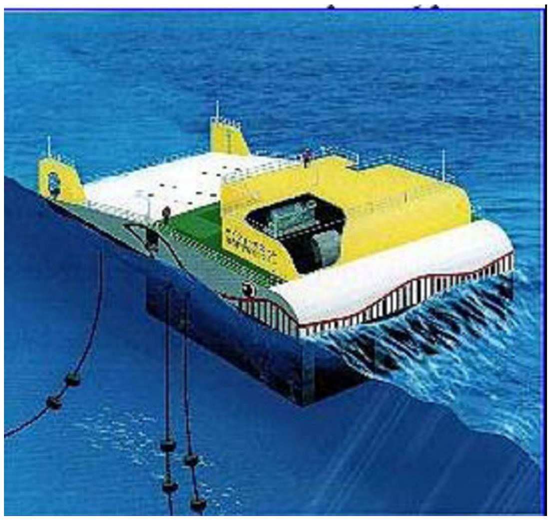

Figure A.20 Moored Mighty Whale [20]

Constraints:

• The slow drift oscillation effects observed need to be considered in a mooring system design
• The average wave power density at the Mighty Whale site is 4 kW/m

A.3.1.2 Multiple Oscillating Water Column

From sea trials of the SPERBOY prototype design, a simpler device, the multiple oscillating column (MOWC) wave energy conversion device was created by the Orecon Company (The Orecon company, is an offshoot of the University of Plymouth). This WEC contains six oscillating water columns that operate similarly to other OWCs discussed in previous sections except that each column is “tuned” to a different wave frequency. In so doing, the device can resonate at multiple frequencies broadening the bandwidth of energy capture, thus increasing the WEC’s overall efficiency. (Note: A single OWC has the disadvantage that the efficiency drops off significantly outside of a small frequency bandwidth.) The output of the device’s six columns is fed into one self-rectifying air driven turbine, which is coupled to an electric generator. To achieve lower cost and better reliability, the equipment was designed using technology from the off-shore gas and oil industry.

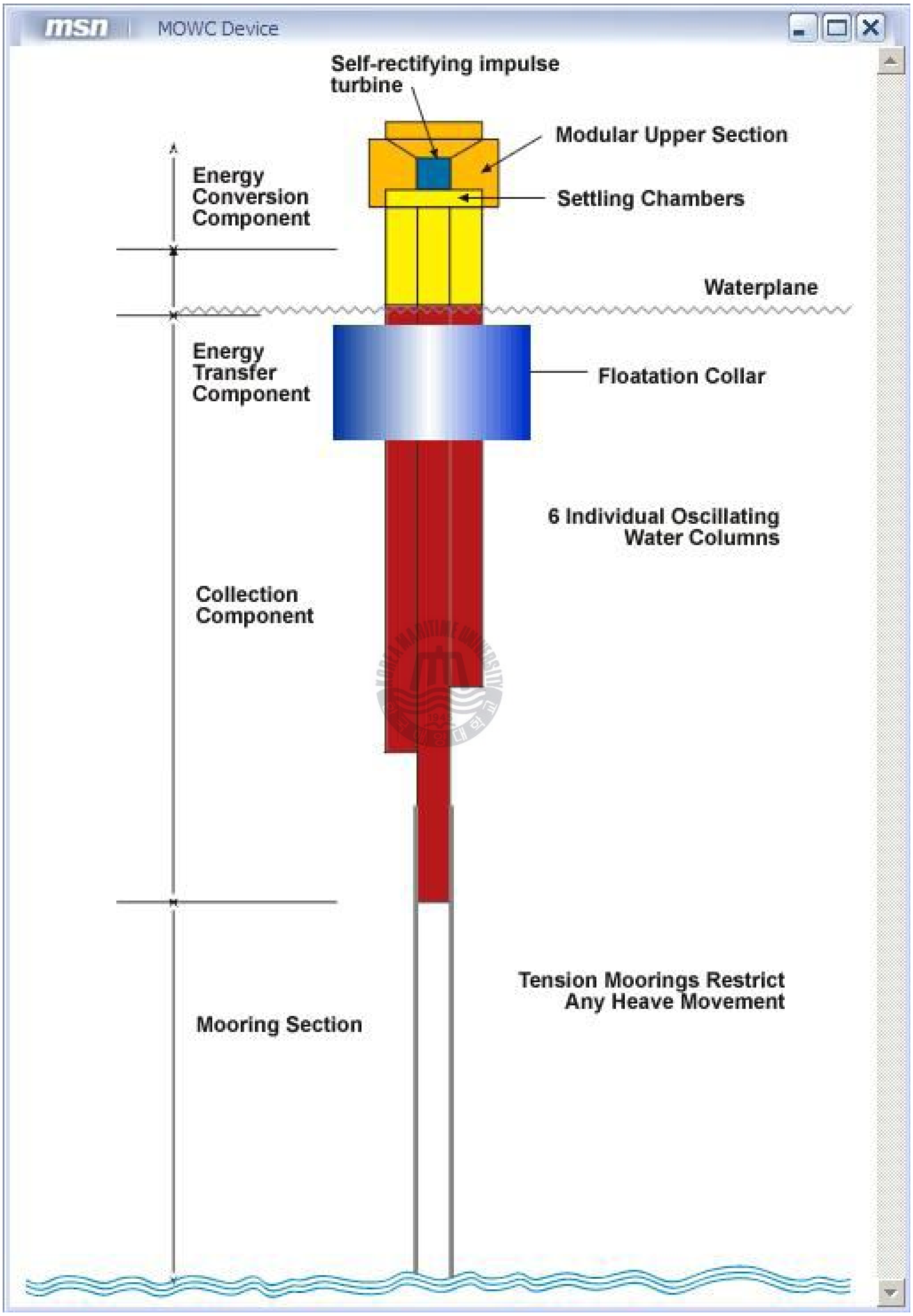

Figure A.21 Multiple Oscillating water column - Side view [21]

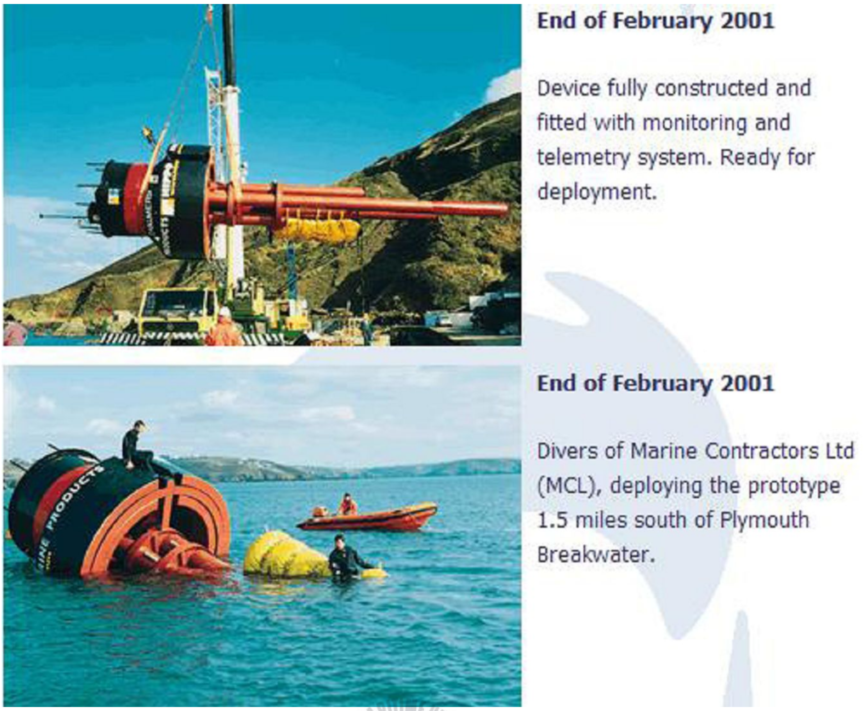

Figure A.22 Multiple Oscillating water column - Installation [21]

Figure A.23 Multiple Oscillating water column - Operational [21]

Constraints:

• It was found that reducing heave motion by altering the mooring system improved efficiency levels. “Refined calculations followed that eliminated the motion of the device. This secondary analysis showed that by constraining the device against heave via a mooring system, a 20-25% increase in power was possible” [21].

A.3.1.3 Backward Bent Duct Buoy

The backward bent duct buoy (BBDB), was an improvement on Masuda’s earlier OWC designs, with an improvement of 2 to 3 times over the navigation buoy and 10 times better than the barge KAIMEI [22]. This WEC utilizes a long horizontal water-filled duct held up by a float on the water surface with the opening of the duct facing away from the incident waves. The duct is connected to a vertical chamber and like other OWCS discussed previously, the oscillation of the air/water interface drives an air turbine. Energy is absorbed through wave heave and pitch action. The horizontal length of the duct is chosen to be 20-30% of the wavelength at the peak wave period of the installation site. From model tests, 59% of the wave power is converted to pneumatic power and 60% of the air power results in electricity generation or a “capture width” of 59% x 60% = 35% [22]. Light-buoys that must operate in shallow waters use the BBDB design as it can function without using the customary long vertical pipe. These lightships have been used for some time in China.

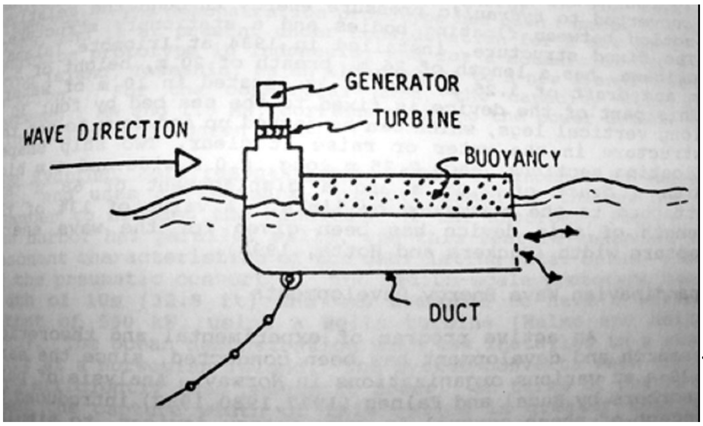

Figure A.24 Backward bent duct buoy drawing from [22]

Figure A.25 Scale Model Indian Backward Bent Buoy [23]

A.3.2 Overtopping Devices

A.3.2.1 Floating Power Vessel

The Floating Power Vessel (FPV) operates like a tapered channel device. "The floating wave power vessel is a steel platform containing a sloping ramp, which gathers incoming waves into a raised internal basin. The water flows from this basin back into the sea through low-head turbines. In these respects, it is similar to an offshore TAPCHAN, but the device is not sensitive to tidal range" [27].

Figure A.26 Floating Power Vessel [24]

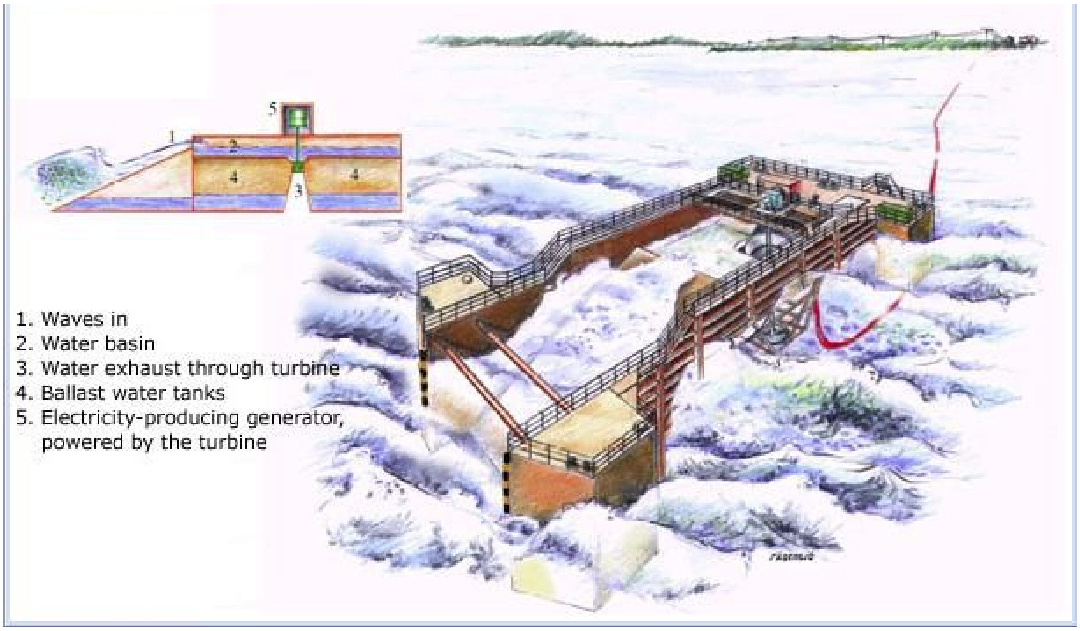

Figure A.27 Floating Wave Power Vessel operations [24]

The FPV will adjust to storm conditions. “The platform computer is programmed to register extreme wave heights and pressure changes that occur in conjunction with the build-up of a small storm or hurricane. Should that happen the computer will ballast the platform so that only a small area is exposed. Subsequently, should the platform encounter very large waves during a hurricane, such extreme waves will simply wash over the platform. Even so, the anchoring is dimensioned to handle a "hundred-year wave", i.e., an extreme wave that statistically occurs once every hundred years. Off the south coast of England, such a wave would for instance reach a height of about 20 meters and a length of up to 500 meters” [24].

A.3.2.2 Wave Dragon

The Wave Dragon is a floating, slack-moored, prototype WEC. Curved reflectors (patented) focus the incident waves to a ramp where the waves spill over (overtopping) and are captured in a reservoir. Hydro generators produce power from the difference in water level. (This concept is similar to the TAPCHAN but now it is floating offshore.) The units can be combined in arrays of 2 to 200. In extreme wave conditions, the waves pass over the rig. For high wave conditions, the Wave Dragon can be lowered so that the surface is just above sea level.

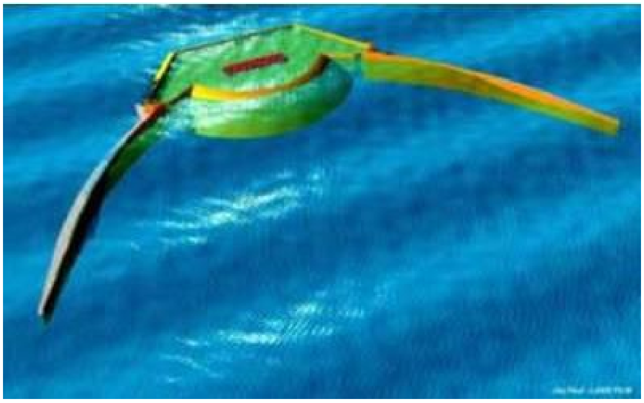

Figure A.30 Wave Dragon shape [25]

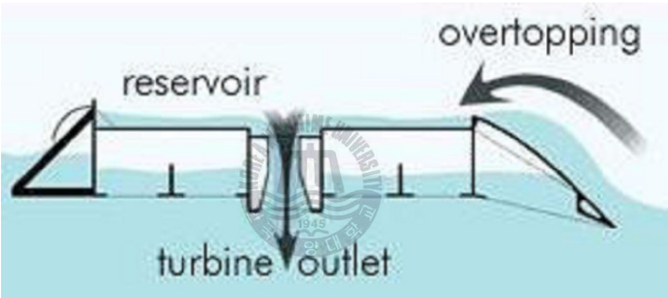

Figure A.31 Wave Dragon operation [26]

Table A.1 Wave Dragon specifications [26]

Wave Dragon key figures:	Nissum Bredning prototype 0.4 kW/m	24 kW/m	36 kW/m	48 kW/m
Weight, a combination of re-enforced concrete, ballast and steel	237 t	22,000 t	33,000 t	54,000 t
Total width and length	58 x 33 m	260 x 150 m	300 x 170 m	390 x 220 m
Wave reflector length	28 m	126 m	145 m	190 m
Height	3.6 m	16 m	17.5 m	19 m
Reservoir	55 m3	5,000 m	8,000 m3	14,000 m3
Number of low-head Kaplan turbines	7	16	16 - 20	16 - 24
Permanent Magnet Generators	7 x 2.3 kW	16 x 250 kW	16 - 20 x 350 - 440 kW	16 - 24 x 460 - 700 kW
Rated power/unit	20 kW	4 MW	7 MW	11 MW
Annual power production/unit	-	12 GWh/y	20 GWh/y	35 GWh/y
Water depth	6 m	> 20 m	> 25 m	> 30 m

A.3.2.3 WavePlane

The WavePlane converts potential and kinetic energy of the incoming wave into a whirling vortex which either runs a hydroelectric converter or oxygenates the water. WavePlane Solutions Ltd is a newly formed company with the merger of WavePlane International A/S and Caley Ocean Systems Ltd. It was founded in 1994 by Dansk Bølgeenergi Udvikling A/S (DBU) (Danish Wave Energy Development Ltd.). The first official testing of the unit occurred in 1996, at the University College at Cork Ireland and is ongoing. The triangular shaped WavePlane prototype floats on foam-filled tanks, which automatically adjust pitch. Beneath the unit is a large damping-plate or plates. The device is anchored between two inlet ducts and aligns itself to incoming waves.

Figure A.32 Oxygen-WavePlane in the sea [34]

The incident wave enters the device at just above the still water level, where it encounters an artificial beach, which slows the lower portion of the wave while throwing the upper part of the wave into a series of reservoirs. Water from the lower reservoirs enters a narrowing channel, increasing the water velocity before heading directly into a whirling flywheel type tube of water. The WavePlane got its name from the multiple plates of the upper reservoir, which plane or cut the incoming wave into a number of horizontal slices. The reservoirs store the water, i.e., potential energy of the passing crest of the wave. The irregular pulsed wave is converted into an even flowing vortex stream, which continues to rotate even if two or three waves are missing in the wave train. Under extreme weather conditions, the WavePlane is submerged below the surface. WavePlane Solutions Ltd. describes the WavePlane as having:

- Few moving parts
- A higher wave energy conversion per unit weight than other WECS
- Multiple generators
- Flexgrid (patented) which creates a multi-plane of multiple units.

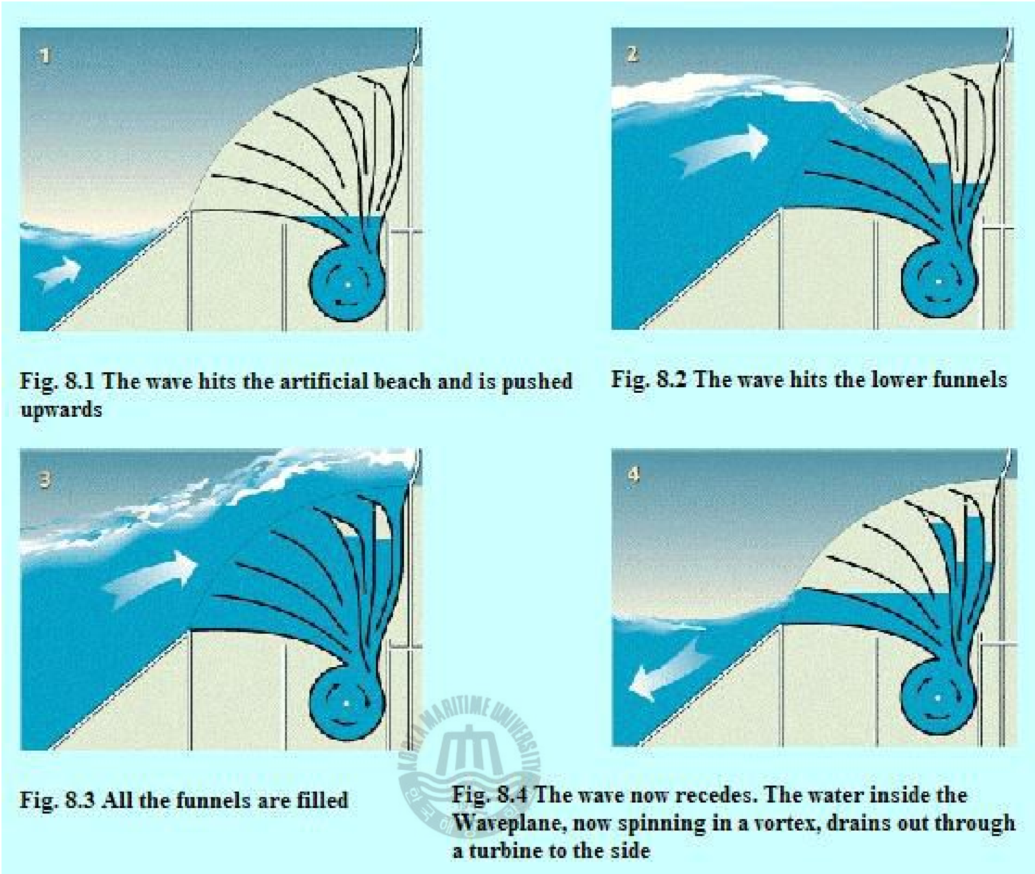

Figure A.33 Diagram of WavePlane operation [28]

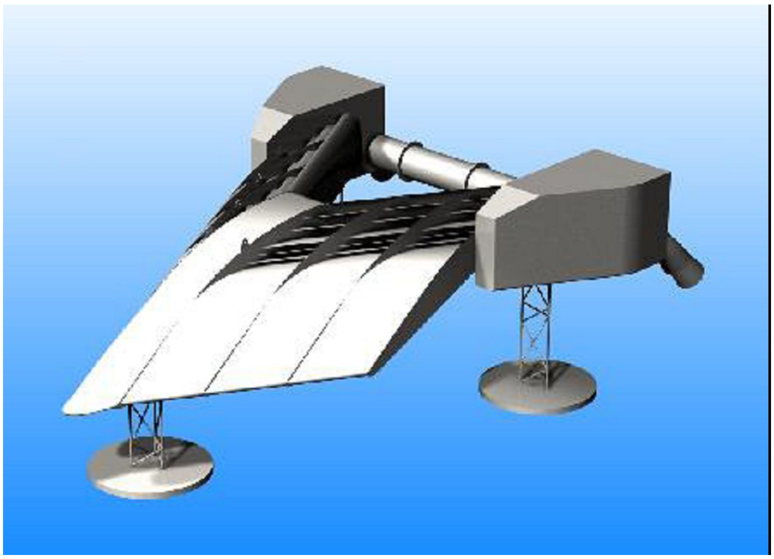

Figure A.34 Artistic impression of WavePlane, for generating electricity [34]

The Oxygen-WavePlane is capable of raising the oxygen level of a moderately polluted area of one hectare (2.5 acres). It does this by generating two downward eddies with opposite spins which whirls colder water from the bottom. The resulting difference in water temperature and induced kinetic energy ensures maximum oxygenation of the water. The Oxygen-WavePlane located at a site with an average of 20 cm waves and 12 mg O2 / liter, produces a minimum of 60 tons of oxygen per year - sufficient to break down:

- 60 tons algae or
- 15 tons nitrogen or
- 30 tons fish feed

Figure A.35 Shipping and installation of a WavePlane [34]

A.3.3 Wave Activated Bodies

A.3.3.1 Pitch - Salter's Duck

A.3.3.1.1 Salter's Duck

Professor Stephen Salter developed the "Duck" at the University of Edinburgh in 1983 under the UK Wave Energy Program (ETSU, 1985). It is one of the earliest WECS of high efficiency. Several of these cam shaped devices are connected together on a spine that spans the crest of multiple waves. Each device works independently. The 2 GW duck consists of 8 strings, with each string having 54 floating concrete cylinders or spines. On each spine, 2 ducks are mounted with a retaining strap allowing the duck to freely rotate around the spine or nod with wave action. Inside of each of the ducks are two completely sealed power canisters which contain gyroscopes. These provided an independent reference for power generation relative to the nodding motion of the Duck and also to reduce torque on the spine. Each Duck drives a hydraulic pump; the fluid is used to drive a generator. Hydraulic rams are mounted between spines to allow flexibility of the spine in extreme wave conditions while being less compliant under normal wave conditions to maximize the amount of power captured [11]. Figure A.36 shows the Solo Duck, which operates without a spine but whose mechanical support penetrates through the cam's casing. It is a quite efficient device. The tension leg system was designed for extreme wave loading but had the undesired effect of unloading when a wave trough occurs while the Duck has a significant amount of kinetic energy; this condition is called "the snatch load" by Professor Salter [18].

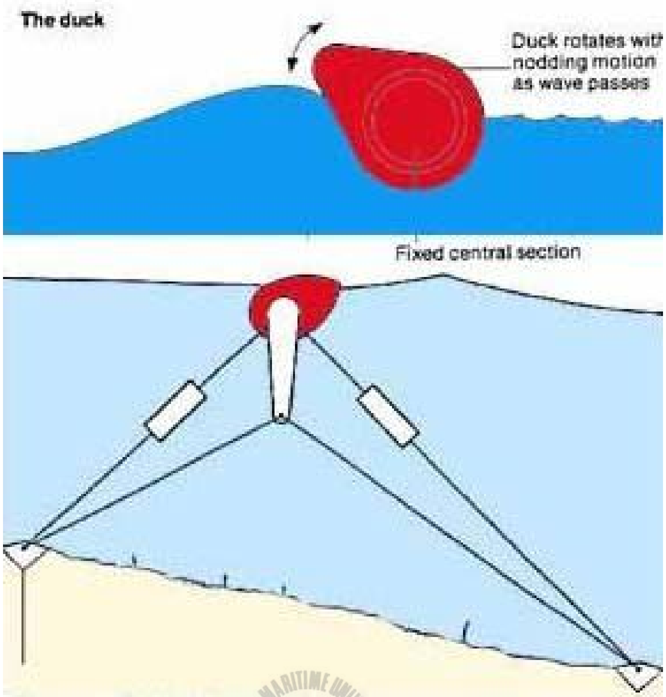

Figure A.36 The Salter Duck wave energy conversion device [27]

"The Salter Duck is able to produce energy extremely efficiently, however its development was stalled during the 1980s due to a miscalculation in the cost of energy production by a factor of 10 and it has only been in recent years when the technology was reassessed and the error identified" [27].

A.3.3.2 Pitch and Heave

A.3.3.2.1 Cockerell Raft

Sir Christopher Cockerell, the inventor of the Hovercraft, designed the Cockerell raft. It is constructed from a series of floating rafts or pontoons, linked by hinges that allows the rafts to follow the wave contour. The rafts are placed at right angles to the wave front. Wave energy is extracted as each raft is phased differently to the wave. Across the top of each hinge are two hydraulic jacks that pump hydraulic fluid with movement of the raft. The hydraulic fluid turns a hydraulic motor coupled to an electric generator.

Figure A.37 Cockerell Raft [29]

Advantages:

- Straightforward design that could easily be manufactured
- Robust design with possible long life
- In extreme wave conditions, large waves will pass over the top of the rafts
- The floating structure is better able to withstand storms than a fixed OWC design

Constraints:

- For longer waves, the efficiency will decrease but the power output remains the same. Very long waves would cause two or three sections to move as one unit resulting in no wave energy being extracted. Maximum efficiency is achieved, when the wavelength is the length of one raft. (It was planned to have the rafts built in groups of three) [18]
- Maintenance in high seas is a concern. The model had all working parts on top of the raft.

A.3.3.2.2 Pelamis

"The Pelamis (named after a sea-snake), under development by Ocean Power Delivery Ltd in Scotland, is a series of cylindrical segments connected by hinged joints. As waves run down the length of the device and actuate the joints, hydraulic cylinders incorporated in the joints pump oil to drive a hydraulic motor via an energy-smoothing system. Electricity generated in each joint is transmitted to shore by a common sub-sea cable. The slack-moored device will be around 130m long and 3.5m in diameter. The Pelamis is intended for general deployment offshore and is designed to use technology already available in the offshore industry. The fullscale version has a continuously rated power output of 0.75MW [27].

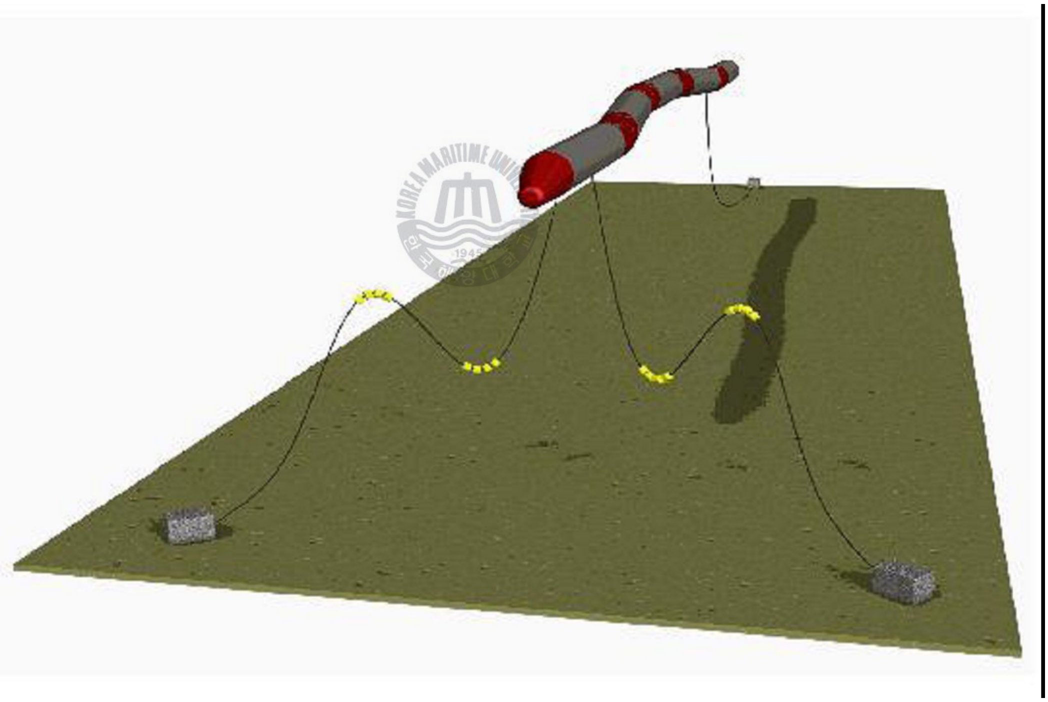

Figure A.38 The Pelamis wave energy converter (Ocean Power Delivery Ltd.) [30]

Constraints:

• Maintenance of a complex hydraulic system
• A secure mooring system that keeps Pelamis into the waves

A.3.3.2.3 McCabe Wave Pump

Dr. Peter McCabe of Ireland developed the McCabe Wave Pump under Hydam Technology Ltd. This wave pump consists of three steel pontoons which are hinged together, the center pontoon is stabilized with a damper plate, and the two outer pontoons undergo a pitching action by wave interaction. The hydraulic takeoff is located on the center pontoon and is driven by the movement of two outer pontoons. The pump was developed to deliver potable water by reverse osmosis but can also generate electric power through a hydraulic motor / generator combination.

Figure A.39 McCabe Wave Pump [31]

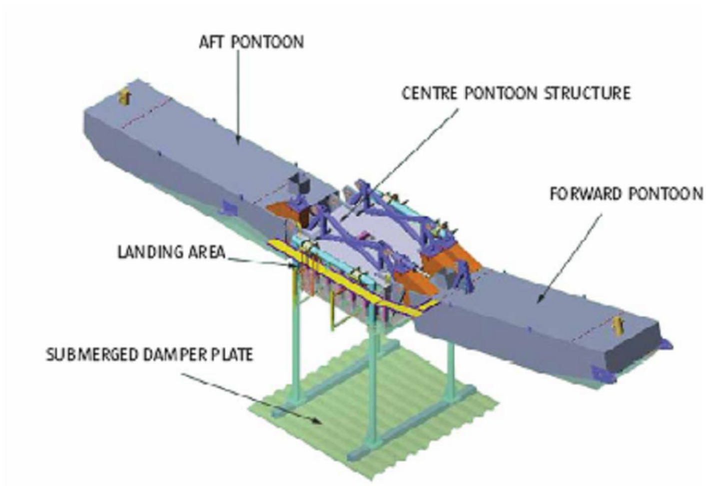

Figure A.40 McCabe Wave Pump side view [31]

The Waveberg wave energy converter design was conceived by John Berg of Waveberg Development Limited New York, NY USA. Wave action moves the device's three outer pontoons relative to a center pontoon driving a water pump. The pressurized water is pumped to shore to turn a Pelton impulse turbine/generator to produce electricity. The turbine/generator combination can also be mounted on a platform near to the Waveberg device and electricity can then be transmitted to shore by way of undersea cable.

On the web site, pictures of the Waveberg are shown as far back as 1979. The device has 3 patents, the latest being US 6,045,339. Maintenance is reduced by making all part accessible on the ocean surface and providing the electrical generation equipment mounted on shore.

FIG. 1

Figure A.41 Waveberg 15' prototype 2004, Cape Canaveral, Florida (left), patent diagram (right) [32]

A.3.3.2.5 Lilypad

The Ecovision Lilypad is a modification of the Swedish hosepump. Developed by consultants Ove Arup UK, it uses multiple hosepumps mounted between a flexible membrane on the ocean surface and a lower membrane anchored to the ocean seabed.

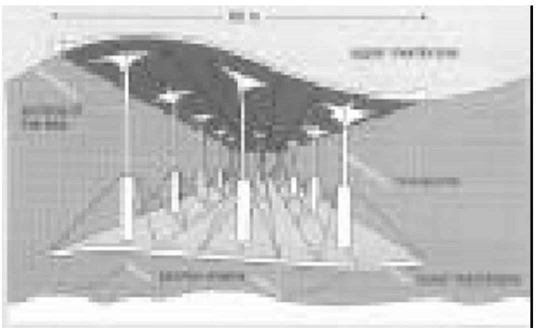

Figure A.42 Ecovision Lilypad.[29]

A.3.3.2.6 Wave Energy Module

The Wave Energy Module (WEM) was developed in 1976 and tested at the University of Rhode Island's Ocean Engineering Department. It operates on the relative motion between a circular raft and a circular reaction plate beneath, pumping hydraulic fluid to a hydraulic motor which in turn rotates a generator. The 1/30-scale model was tested with irregular waves. In figure A.43 is a 1/10-scale model of a 1kW WEM, which was operational on Lake Champlain, South Hero VT, USA in 1978. A computer program was developed to simulate the WEM operation.

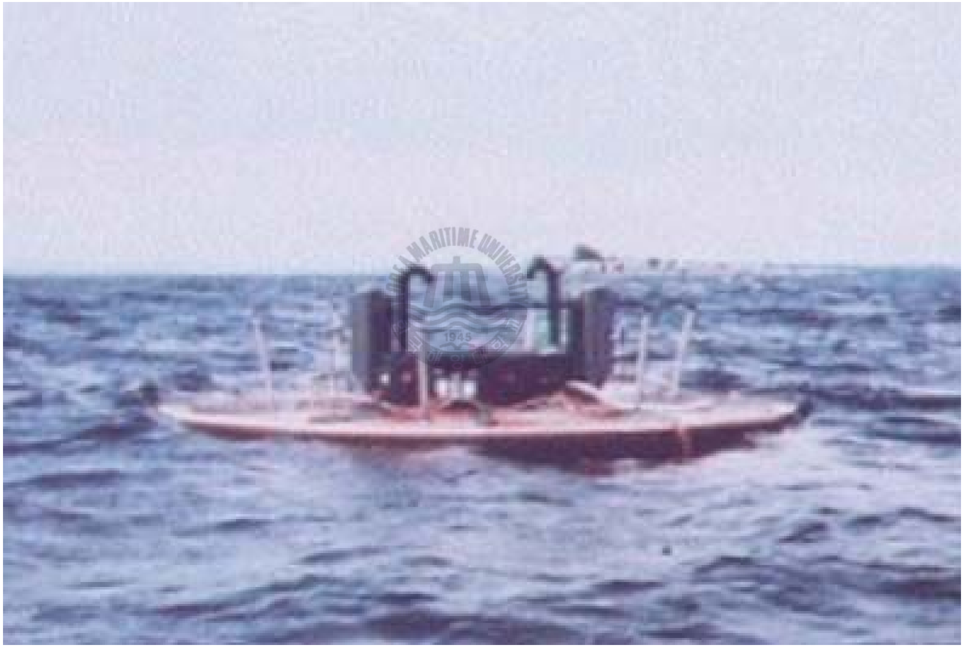

Figure A.43 1 kW x 3.6 m WEM on LakeChamplain [33]

Table A.2 Simulation results of the 1 MW Wave Energy Module [27]

Country	Site	Mean WEM Output (KW)
Cook Islands	Ngatangia Harbor	324
Fiji Islands	Muani, Kadavu	296
Samoa	Lotofaga, Upolu	253
Tonga	Tongatapu	276

A.3.3.2.7 Ocean Wave Energy Converter

The Ocean Wave Energy Co. in Rhode Island, USA has developed the Ocean Wave Energy Converter. Three floats on each module are driven by wave action. The floats are interconnected to linear generators to produce electricity. The linear generators are mounted within tubes of the converter assembly that are constructed in a tetrahedron configuration. The converter assembly is provided with an added buoyancy chamber to get the correct submergence depth. The tubes are restrained by damping plates, and ballast, as needed, is placed on top of the plates. The damping plates are located at a depth where wave action is a minimum. Multiple modules are interconnected to generate the desired power level.

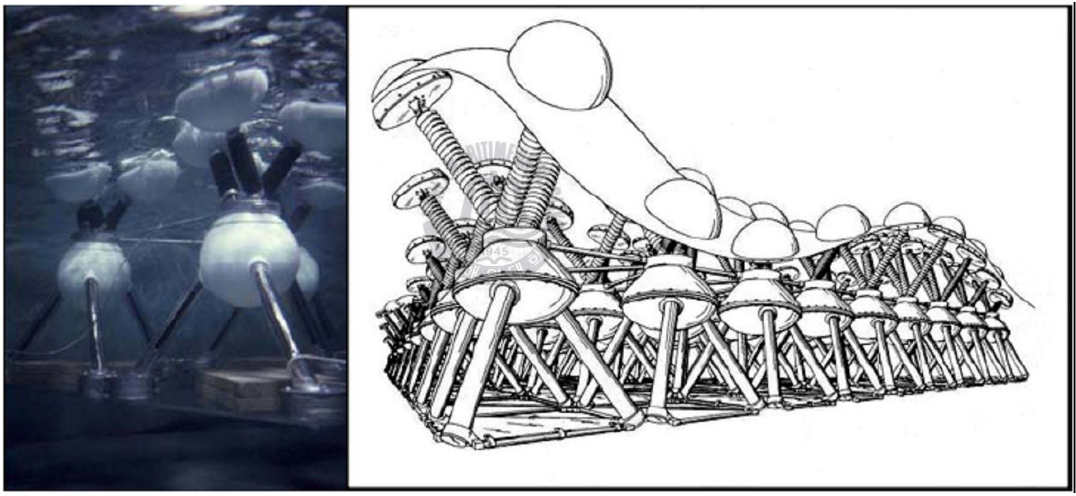

Figure A.44 Ocean Wave Energy Converter undergoing tank tests (left), and drawing of array of converters (Right) [34]

Constraints:

• The U.S. Patent 4,232,230 was issued November 4, 1980 and U.S. Patent 4,672,222 was issued June 9, 1987. Dates of further activity with the OWEC are not given on the web site. When the web site was updated is also not provided [34]:

• Maintenance may be an issue as the device seems quite complex with many moving parts.

A.3.3.2.8 Piezoelectric Polymer

Dr. George W. Taylor of Ocean Power Technologies (OPT) of New Jersey has developed an innovative piezoelectric polymer strip that generates electricity when deflected mechanically. If this strip is then attached between a float on the ocean surface and an anchor on the ocean floor, this material will generate electricity though wave action. OPT and Japan's Penta-Ocean Construction Company Ltd plan to jointly develop a prototype. In exchange, Penta-Ocean will have exclusive rights to market this product in Japan [35].

Constraints:

- Efficiency per plate area
- Flex lifetime and durability of the sheet

A.3.3.3 Heave

A.3.3.3.1 Float-Pump

The Danish Wave Power float-pump device uses a float which is attached to a seabed mounted piston pump; the rise and fall motion of the float causes the pump to operate driving a turbine and generator mounted on the pump. The flow of water through the turbine is maintained as unidirectional through the incorporation of a non-return valve [27].

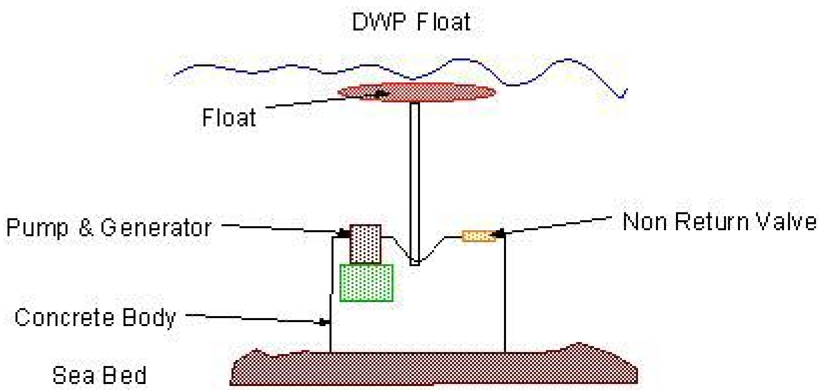

Figure A.45 Danish Wave Power float-pump device [27]

Constraints:

• Depth limited to which the float and unit can be submerged
• Maintenance of pump and generator as submerged
• Clogging of valves may be an issue

A.3.3.3.2 Archimedes Wave Swing

This wave energy conversion device was invented by Fred Gardner who holds a world patent on this device. The project is directed by Teamwork Tech. BV, a Dutch company.. The Archimedes Wave Swing (AWS) works on the principal that a wave passing over a submerged gas vessel will cause the vessel to contract and expand. The AWS pilot plant has an upper moveable floater (diameter 9.5 m, height 21 m) which is pressurized with air and a fixed lower structure. The floater moves down under a wave crest (gas contracts) and moves up under a wave trough (gas expands); thus it resonates at wave frequency.

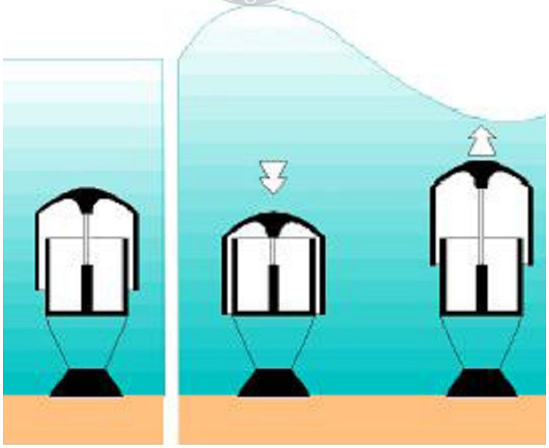

Figure A.46 Motion of the Archimedes Wave Swing [36]

A 2 MW prototype mounted on the sea bed near the coast of Portugal is placed 10 m below sea level and is mounted on a pontoon so that the structure can be raised or lowered from the sea floor at will. Having this unit below sea level, shelters it from storms.

Figure A.47 Archimedes Wave Swing construction [37]

As the AWS pilot plant is designed to operate in waves of significant wave height less than 5 meters, the unit has wave dampers that operate along with the generator to absorb power levels up to 25 MW. In the center of the AWS is a power take off (PTO) system consisting of two generators, a gas spring and the AWS structure. Mechanical energy of the floater is converted to electrical energy through the up and down movement of a permanent magnet within a coil. The University of Delft developed this linear rectangular shaped generator, and the stator constructed by Alstom. A 6 km long cable brings the power to shore.

Figure A.48 Archimedes Wave Swing linear generator [37]

The alternating current generated by the WEC varies in both voltage and frequency. To connect this varying WEC generated power with the constant voltage and frequency of the grid, a power conversion unit is first used to rectify the alternating current into direct current. Then with an inverter, reconverts it into an AC current at grid frequency and with a transformer at the grid voltage.

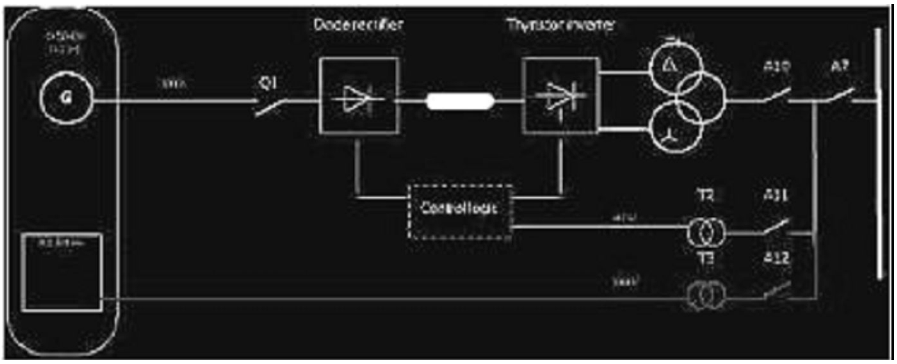

Figure A.49 Archimedes Wave Swing one-line diagram [37]

Constraints:

• The AWS requires ocean swells of long wavelength and therefore is only suitable in areas with oceans of large open expanses[36].
• Operates in waves less than HS of 5 m [90].

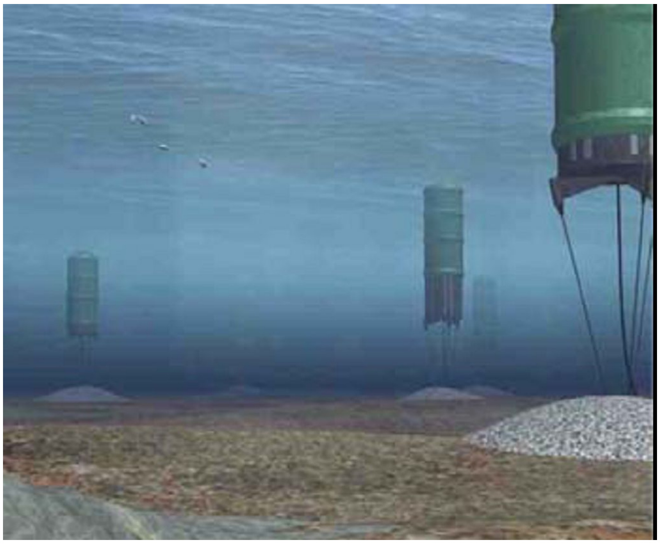
Figure A.50 AWS with single mooring point [37]

Table A.3 Technical specification for AWS Pilot Plant and commercial operation [38]

	AWS PILOTPLANT	COMMERCIAL SYSTEM
Purpose	To test all equipment at full scale	To produce electricity at market price via learning curve
Location	Lexious (offshore North Portugal)	Not decided yet (Portugal, UK, Spain)
Anchor	Pontoon for flexible submergence	Tension leg with gravity anchor
Energy Collector Diameter	Vertical motion off floater 9.5 m	Vertical motion of floater 12 m
Stroke	7 m (nominal) 9 m (maximum)	11 m (nominal) 12 m (maximum)
Power take off	Linear permanent magnet generator	Linear permanent magnet generator
Voltage	3.3 kV at 2.2 m/s (10s cycle)	3.3 kV at 3.5 m/s
Max. power	2 MW at 2.2 m/s(10 s cycle	9.5 MW at 3.5 m/s
Rated power	1 MW (average over 1 cycle)	4.75MW at 3.5 m/s (average over 1 cycle)
Converter	Thyristor (Cycloconverter)	IGBT (to be specified)
Grid connection	15 kV 4.8 MVA	Depending on location.
Tuning	from 9 to 20 second	9 to 12 second
Operating wave heights	Hs 0.75 m - Hs 4 m	Hs 0.75 m - Hs 5 m
Survival conditions	To be measured	Hs 20 m (in secure mode)

• "A 2 MW demonstration plant was launched outside the coast of Portugal in 2000 and there are plans of installing a larger facility with several 5-6 MW plants in the autumn of 2003." Portugal was chosen at the prototype site as it has suitable wave conditions, the grid is close to shore, the seaports Viana do Castelo can assemble and repair the unit and AWS partners IST and INETI are knowledgeable about wave energy. The Portuguese will be studying how this unit affects the local fish population (it may act as an artificial reef) and its relative noise level (low). Note: The joint venture AWS B.V. is a European cooperative involving five companies, three universities and two research institutes.

A.3.3.3.3 PowerBuoy

The Ocean Power Technologies, Inc. (OPT) of New Jersey was co-founded by Dr. George W. Taylor. OPT makes the PowerBuoy, which is placed more than a meter below the water surface (not visible from shore) and heaves up and down with wave action to generate electric power. OPT has experience both in the U.S.A. and Australia. The buoy's up and down motion drives a hydraulic cylinder located inside the buoy, which pumps hydraulic fluid to turn a hydraulic motor connected to an generator mounted on the ocean floor. The power is transmitted by underwater power cable to the shore. The "smart" buoy uses sensors and computerized systems to maximize the conversion of random broadband wave energy. The control will automatically disconnect the unit in very large waves and reconnect when conditions are favorable for generating electricity.

Figure A.51 OPT PowerBuoy in the process of deployment off the coast of NewJersey.TheOPTPowerBuoyisinvisiblefromtheshoreline. [39]

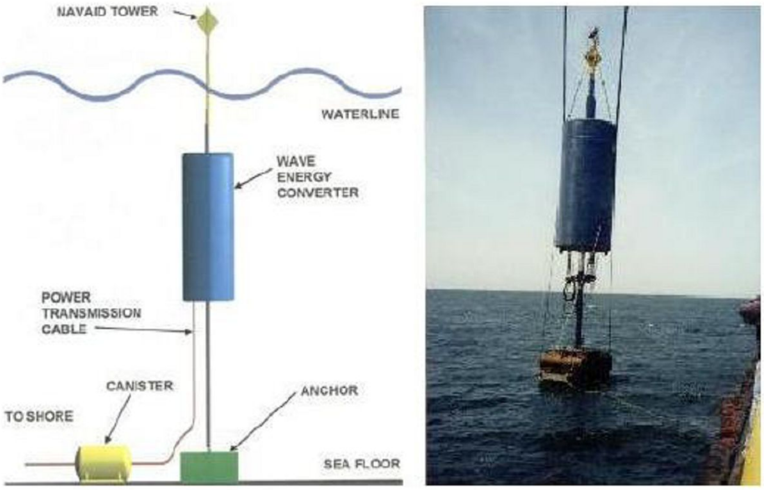

Figure A.52 Diagram of PowerBuoy components and being lowered by a crane [40]

Multiple identical PowerBuoys can be placed together in an array to create a power plant. (Note: As shown in Table A.4 as the power level increases, the individual power units do not remain the same but increase from 50 kW to 100 kW and then to 500 kW.)

Table A.4 PowerBuoy's power parameters [40]

OPT POWER WAVE STATION PHYSICAL PARAMETERS

Based on Nominal 2m Wave Height					
Station Capacity Megawatts	Quantity OPT Units Deployed	Average Power/Unit (kW)	Surface Area (Acres)	Min./Max. Ocean Depth (Feet**)	Offshore Distance (Miles)
1	20	50	5	100-300	0.5-5.0
10	100	100	50	100-300	0.5-5.0
100	200	500	480	100-300	0.5-5.0

Note: 640 acres equals 1 square mile

**Power output is reduced in ocean depths of less than 35m. Mooring costs increase significantly for depths greater than 100m.

Constraints for PowerBuoy [39]:

• Placed 0.5 to 5 miles from shore
• Installed in approx. 100 feet (30 meters) of water.
• Generator mounted on the sea floor
• "As dictated by local marine regulations, the PowerBuoy has a mast that rises above the surface of the water, with navigational aids attached, such as a radar reflector, day
mark, and warning light to help aid mariners in the vicinity."
• Power output is reduced in ocean depths of less than 35m. Mooring costs increase significantly for depths greater than 100m (Listed in the chart above).

A.3.3.3.4 AquaBuOY

AquaBuOY, is a wave energy conversion device marketed by AquaEnergy Group Ltd. that outputs high pressure seawater, which turns a pump to generate electricity. “AquaEnergy is the intellectual property successor to Interproject Service AB of Sweden” ("Wave Power the Energy Source of Tomorrow," 2005). Two Swedish companies Interproject Service ABS (IPS) and Technocean (TO) have worked to together to market the IPSOWEC Buoy ("A Large Offshore Wave Energy Converter,"). The AquaBuOY combines the IPS buoy technology with that of the Technocean hose pump. Standard undersea cables are used to bring the power to shore. The buoy operates in water depths of between 150 to 250 feet deep. It has blowout protection and uses 2 opposing, full-cycle and 2-stroke hose pumps. Patents are present in US, Europe, Japan and Australia. IPS OWC web site describes the buoy further: 6-8 meter buoy hull, 20 meter acceleration piston, Units are available in 10kW-150 kW and generated system of 50-100 MW.

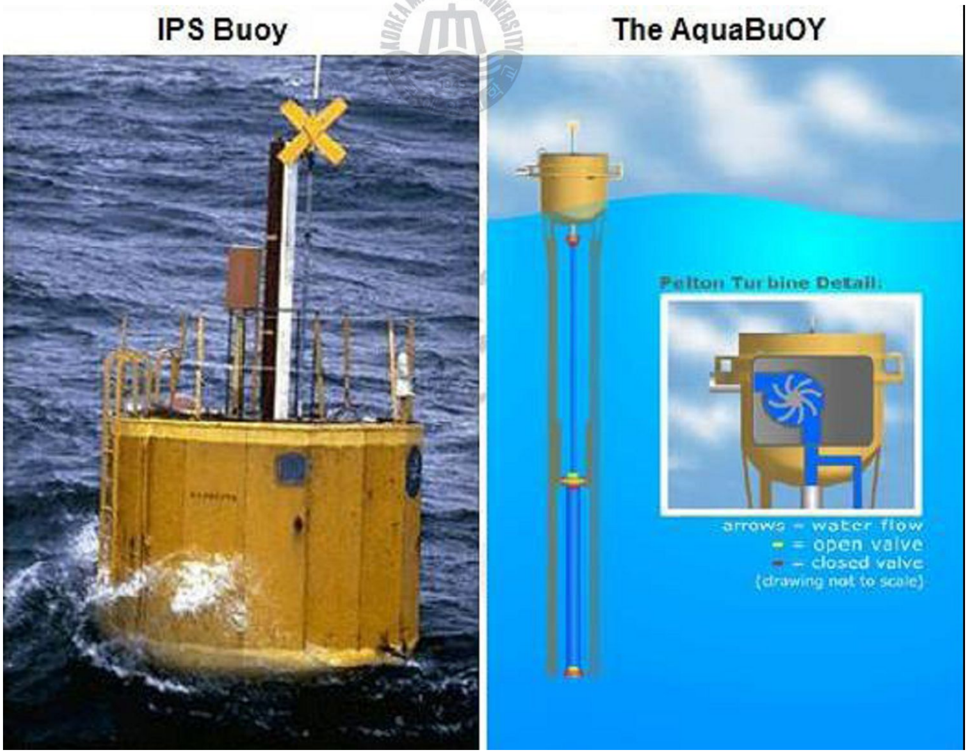

Figure A.54 IPS Buoy and AquaBuOY [41]

The AquaBuOY web site provides an animated diagram showing the device operation. It does not provide a technical description of how it operates. Interproject Service briefly describes the operation under the name of IPSOWEC Buoy. Upon reviewing both web sites together, and also considering the operation of the hose pump, a general idea can be gleaned on how the AquaBuOY operates. As the AquaBuOY buoy moves up due to wave action, the water column “traps” water in the water piston causing it to lag behind the buoy movement. (The water piston movement is smaller that the buoy movement). This results in stretching of the upper hose that connects the water piston to the buoy. (Note: Phase shift between buoy action and water piston action.) The stretching action causes the inner diameter of the hose to contract and with the upper valve open and lower closed, water is pumped to a Pelton turbine inside the bell of the buoy. During this action, the lower hose pump fills with water as it returns to its normal shape. The process reverses as the buoy moves downward, with the lower hose doing the pumping action and the upper hose returning to normal by filling with water.

A.3.3.3.5 Hose-Pump

“The Swedish hose-pump has been under development since 1980. It consists of a specially reinforced elastomer hose (whose internal volume decreases as it stretches), connected to a float which rides the waves. The rise and fall of the float stretches and relaxes the hose thereby pressurizing sea water, which is fed (along with the output from other hose-pumps) through a non-return valve to a central turbine and generator unit” [27].

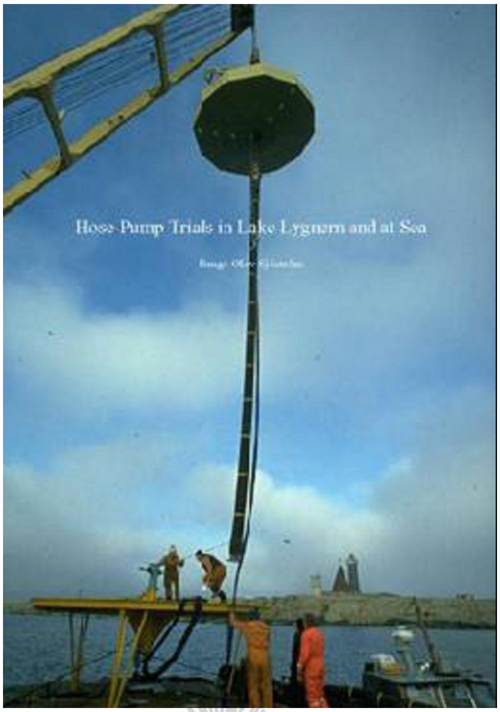

Figure A.55 Technocean hose-pump [41]

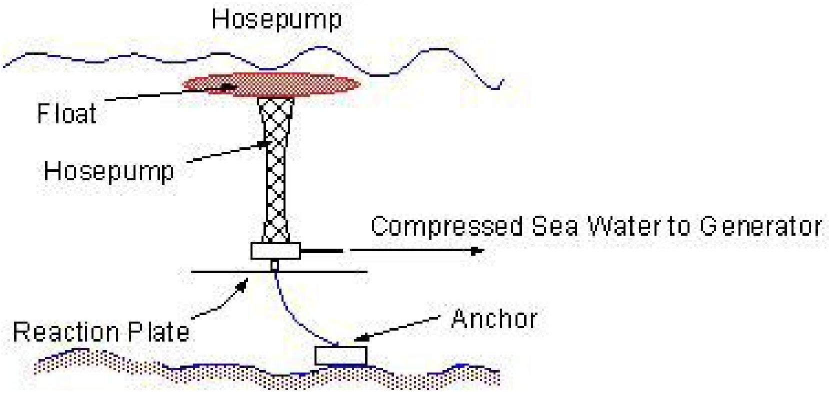

Figure A.56 The Swedish hose-pump [27]

"The hose-pump wave energy converter, developed over 15 years by Technocean in Sweden, is intended to pump sea water from an array of hose-pumps fixed to the sea bed .A Pelton wheel extracts energy from the water as it is released from an upper reservoir back to sea. A hose-pump light buoy is undergoing pre-production tests, and an evaluation of such wave power plants for Ireland, Spain, Sweden and the USA has been carried out. Despite the low cost/kWh predicted for such schemes, the Swedish Government has halted research funding because it does not envisage wave energy as a major contributor to Sweden's energy system. The potential along the Swedish coast is about 5-10TWh/year (about 0.6-1.1 GW average or 3-7% of demand) but the potential along the Norwegian coast is put at around 3.0-3.5 GW, which could contribute 12-15% of Sweden's electricity demand via the Nordic grid" [28]. A hose-pump is shown hanging from a crane in Fig. A.55

A.3.3.3.6 Wavebob

Wavebob limited, is an independent private limited company registered in Dublin which got start in 1997 . The Wavebob wave energy conversion device moves up and down like an offshore heaving buoy, floating mainly below the ocean surface. It generates power by pulling against a tethered cable mounted to the ocean floor or a large plate. Power generation is obtained through pumping hydraulic fluid to turn a generator. Its sensors tune the device to varying wave frequencies and can detune itself in storm conditions. "Clearpower Technology's Wavebob is a self-reacting point absorber that exploits the relative movement of two floating bodies that have different heave frequency responses. This gives it greater bandwidth and scope for tuning over a range of sea conditions than is possible with a conventional single buoy point absorber. The Wavebob has innovative features that allow it to respond to high energy long period waves while maintaining small displacements" [42].

Figure A.57 Wavebob [27]

A.3.3.3.7 Point Absorber

The Point Absorber wave energy converter developed by Rambøll in Denmark, consists of a float connected with a polyester rope to a suction cup anchored on the ocean floor. The float, activated by wave action, drives a piston pump between the float and the rope. Hydraulic fluid is pumped to a hydraulic motor which is coupled to a generator. A 1:10 scale mode was tested at the Danish Maritime Institute “Nisum Bredning”. A 1:4 scale model 2.5 m in diameter is being developed [44].

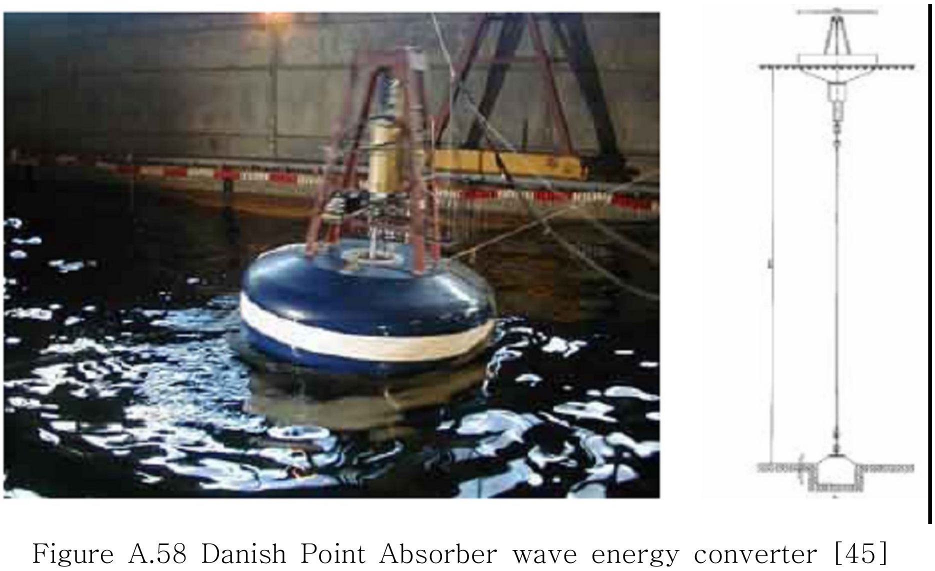

Figure A.58 Danish Point Absorber wave energy converter [45]

A.3.3.3.8 Combined Energy System

Ocean Motion International (OMI) provides a Combined Energy System (CES). Multiple buoys supported by a platform are activated by wave action, their up and down motion drives simple sleeve pumps. These patented ("Modular Pumping Unit" Patent #5,411,377) positive displacement OMI WavePumps in turn pressurize water, which drives a hydro-turbine generator to generate electricity, produces potable water using Reverse Osmosis (RO) filters and through electrolysis generates hydrogen.

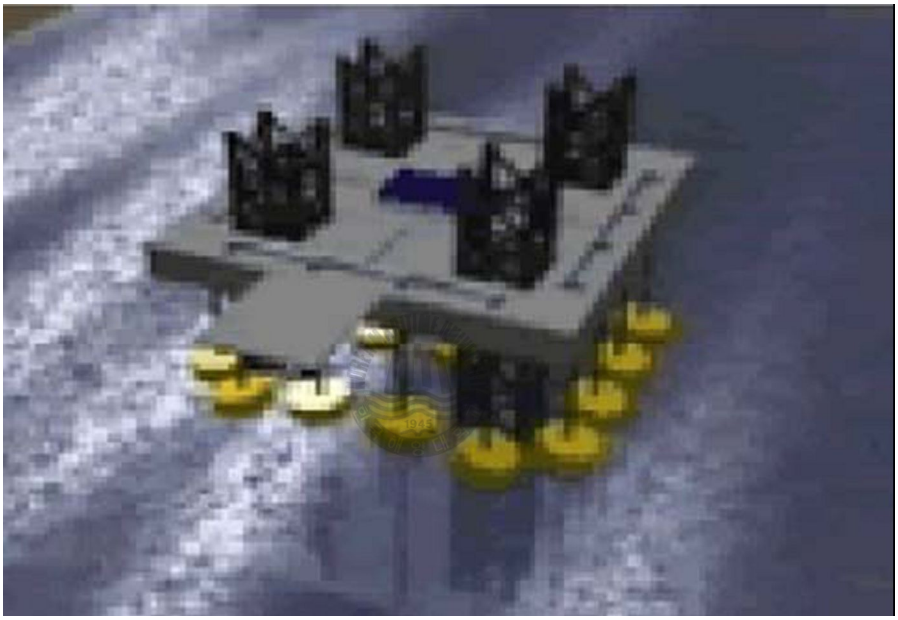

Figure A.59 Ocean Motion International floating platform - Combined Energy System[46]

Table A.5 OMI CES Performance / Output Summary[46]

Production	Pump – 26 inch diameter, 1900 GPM ea & 11,000,000 GPD for 4 pumps Wave Action – 9 ft swell with 10 s intervals RO Filtration - 40% efficiency	Output
Water (RO)	4 pumps	4.4 million gallons per day or 13 acre ft per day
Water (RO)	35 pumps	29 million gallons per day or 90 acre ft per day
Electricity	Based on production size	5 to 50 megawatts
Hydrogen	Based on production size	~573 gallons/hr liquid hydrogen

A.3.3.3.9 SEADOG Pump System

Independent Natural Resources, Inc. (INRI) markets a SEADOG Pump System for converting wave energy into mechanical energy for multiple purposes. Through wave action, a float contained within a structure is driven up and down. The float forces a piston within a cylinder to pump air or water for generating electricity, providing potable water or pressurized air for other applications. The 1/32-scale prototype was tested at Texas A&M University.

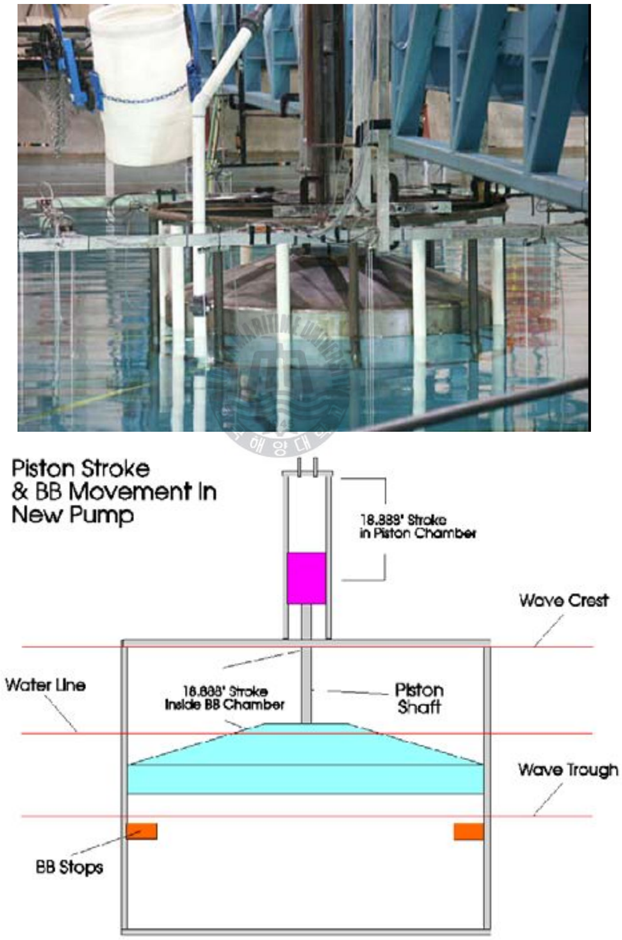

Figure A.60 SEADOG at Texas A&M (Top), one slide of an animated schematic diagram (Bottom) [47]

Constraints:

The SEADOG has not been tried in an ocean environment.

A.3.3.3.10 Ocean Wave Energy Conversion

SARA Inc. (Scientific Applications & Research Associates) has developed an Ocean Wave Energy Conversion system using a magnetohydrodynamics (MHD) generator that converts local fluid motion into electricity. The MHD eliminates intermediary mechanical stages and rotary generators used with WECs. SARA is sponsored by the Office of Naval Research via NSWCCD-SSES [48].

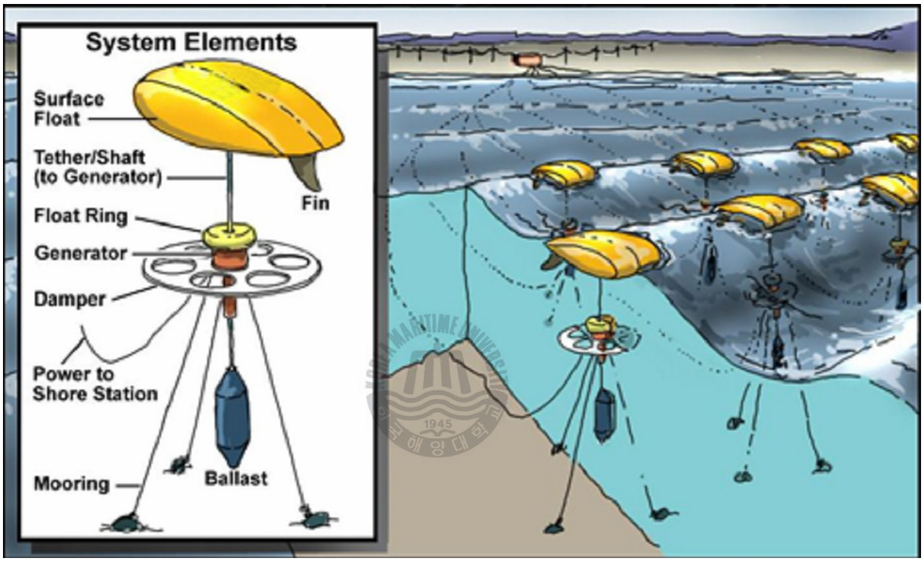

Figure A.61 Ocean Wave Energy Conversion System [48]

A.3.3.4 Heave and Surge

A.3.3.4.1 Bristol Cylinder

Invented by Dr. David Evans of the University of Bristol, U.K., the Bristol Cylinder is a large concrete mass that floats below the surface and moves in a circular motion by following the orbital water paths of the waves. The device is constrained to the ocean floor through mooring legs whose internal pressure can be varied to tune the device to the incident wave frequencies. The original design used a number of elastomer hose-pumps to pump pressurized sea water to a Pelton turbine to generate electricity. This was improved on by using hydraulic rams instead of hose-pumps to pump high pressure oil to turn an electric generator. From 1974 to 1982, the

British Government provided extensive support for wave energy development with the intention to produce a 2 GW power station in the Outer Hebrides Islands. Shown in Fig. A.63 is a 1982 reference drawing of the Bristol Cylinder having hollow pre-cast concrete cylinders, 100 m x 16m and submerged 6 m below the sea surface at a depth of 42 m. Each cylinder had six mooring legs, with each leg connected with two double-acting pumps. The hydraulic output of the 46 cylinders is sent by undersea pipes to a fixed platform containing three 120 MW Pelton turbine/generators and then transmitted to shore by 270 kV submarine cables. Six of these platforms cylinder groups would generate 2 GW.

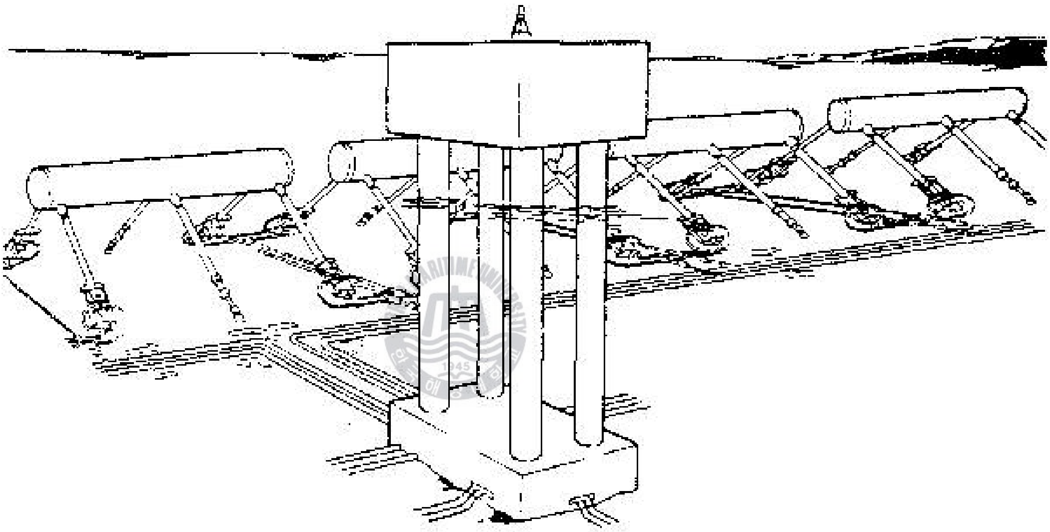

Figure A.62 Bristol Cylinder - Platform and turbine generator arrangement [24].

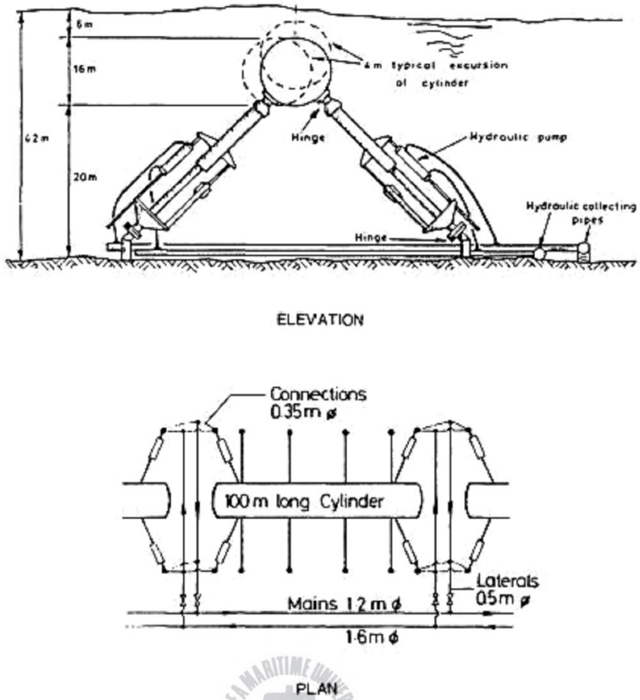

Figure A.63 BristolCylinder[24]

Constraints:

• Maintenance can be an issue as the Bristol Cylinder is submerged
• Depth of submergence will affect wave capture

A.3.3.4.2 Sloped IPS Buoy

The sloped IPS buoy, evolved from a Swedish design, the “IPS buoy” of Inter-Project Services (IPS). The sloped IPS buoy is a replacement for the Solo Duck and is under development by the Edinburgh University in the UK. By designing a buoy to move at a sloped angle (35 to 45 degrees) between heave and surge motion, the natural frequency was reduced and a greater wave energy capture bandwidth was achieved relative to device size.

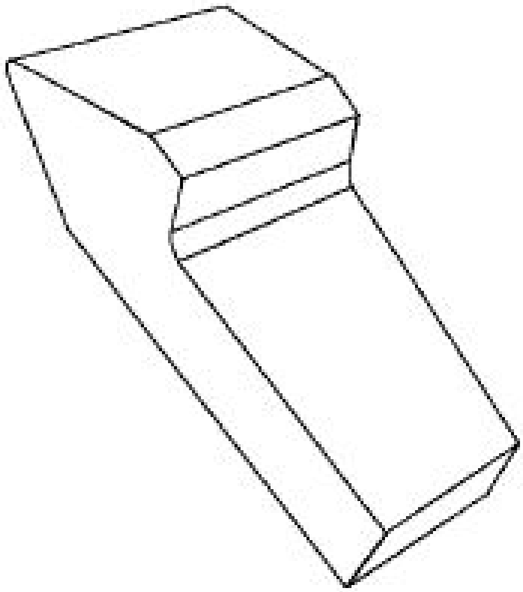

Figure A.64 Sloped IPS Buoy [11]

The slope IPS buoy is a free floating structure with an inclined flat plate held just under the water surface with a curved asymmetrical float head. (Approx. 30 m wide and 6m long) The tail is made up of two or more inertia tubes, open on either end to the sea and long enough to reach down to calm water. The function of the tail is to create a large inertia in all directions, except for the back and forth action in the direction of the slope angle.

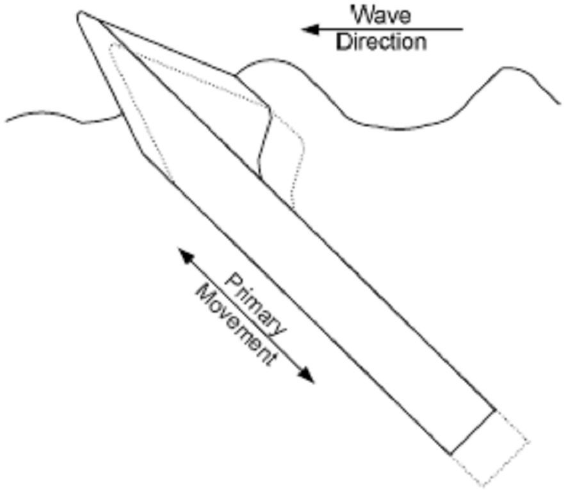

Figure A.65 Movement of the sloped IPS buoy [11]

Double acting hydraulic rams within the device move with the slope structure against a lagging large diameter water piston, centrally located in each of the inertia tubes. Movement of the hydraulic ramps pumps high pressure fluid to turn an electric generator.

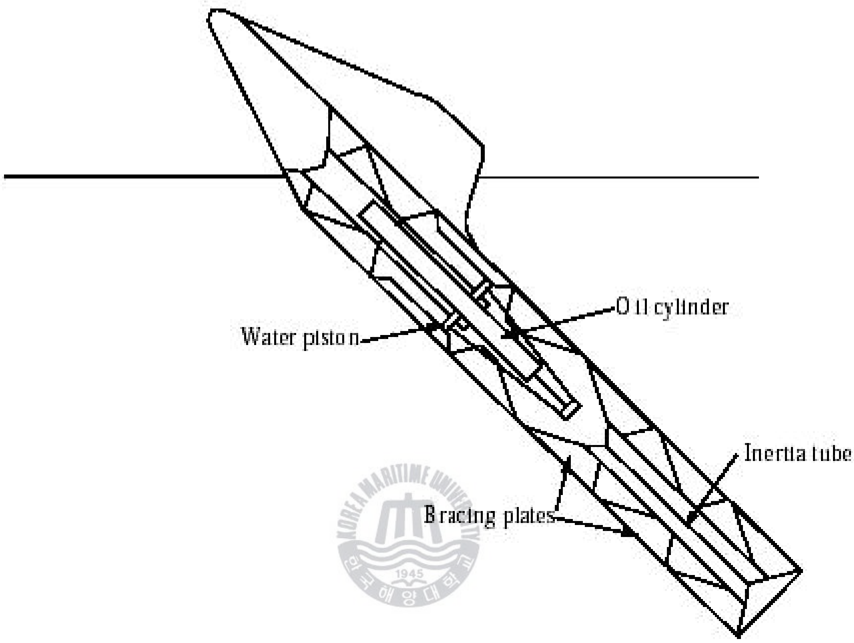

Figure A.66 Details of sloped IPS buoy [11]

A Swedish end-stop solution was used to prevent shock loading in extreme wave conditions. The water piston tube is flared at either end, to allow water to freely bypass the water piston at extreme travel, unloading the piston and hydraulic ramps at either end-stop. Tank tests were conducted by Chia-Po Lin on a constrained half-cylindrical float wave energy device. Placing the device at various fixed angles, he observed its operation relative to incoming waves with a wide range of periods. From the tests, he was able to determine the “hydrodynamic coefficients” of the sloped wave energy device and demonstrated the benefits of slope on bandwidth efficiency [49].

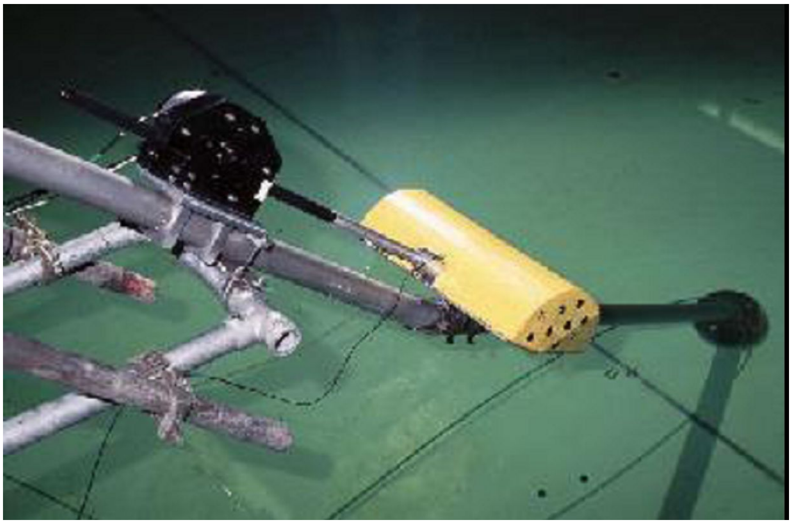

Figure A.67 Constrained half-cylindrical float [49]

A.3.3.4.3 Wave Rider

The wave rider device consists of a buoy that is connected to hydraulic pumps on the ocean floor. Through wave action, hydraulic fluid is pumped to turn a hydraulic turbine to generate electricity. SeaVolt Technologies; formerly Sea Power & Associates are marketing this prototype device. SeaVolt Technologies was formed in 1997 [20].

Figure A.71 SeaVolt Technologies Wave Ride prototype [50]

A.3.3.4.4 Wave Rotor

The wave rotor is a turbine driven by the waves. It consists of two rotors, a Darieus omni direction rotor and a Wells bi-directional rotor allowing the device to operate in currents in varying directions, i.e., up or down or backwards and forwards. Hydrodynamic lift turns the blades relative to the vertical axis. The blades are driven by currents created by the orbital motion of wave driven water particles and are also influenced by tidal currents. The 1/10-scale prototype was developed by both EcoFys in the Netherlands and Danish partner Eric Rosen [52]. The wave rotor is a turbine driven by the waves. It consists of two rotors, a Darieus omni direction rotor and a Wells bi-directional rotor allowing the device to operate in currents in varying directions, i.e., up or down or backwards and forwards. Hydrodynamic lift turns the blades relative to the vertical axis. The blades are driven by currents created by the orbital motion of wave driven water particles and are also influenced by tidal currents. The 1/10-scale prototype was developed by both EcoFys in the Netherlands and Danish partner Eric Rosen [52].

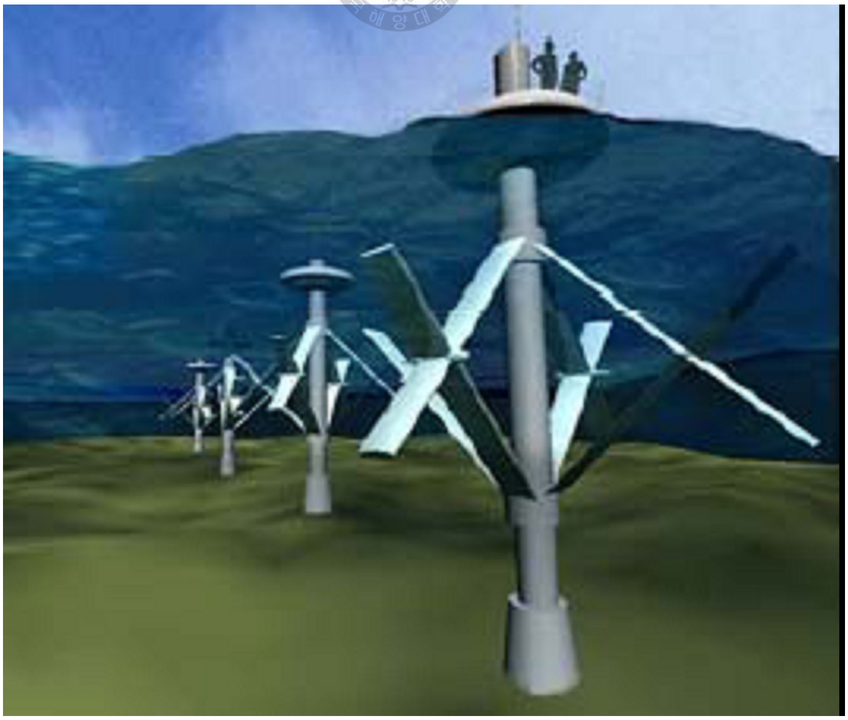

Figure A.72 The Wave Rotor wave energy converter [52]

A.3.3.5 Surge

A.3.3.5.1 Lanchester Sea Clam

The sea clam was developed by Sea Energy Associates, Ltd. under the direction of Norman Bellamy at Coventry Polytechnic in the U.K. The design was based on a similar spine-based device, the Edinburgh Duck. The sea clam consists of a floating concrete spine with a number of bags connected to one side moored at approximately 55 degrees to the incident wave direction. The bag acts like a bellow with wave crest action collapsing the bag and forcing air through a self rectifying Wells air turbine present in the hollow spine. During the trough of the wave, the bag expands by returning air to the bag through the turbine. It was found that if the basic spine structure of the Clam is wrapped back on itself in a circle the unit becomes more efficient and has better pitch- and roll-stability.

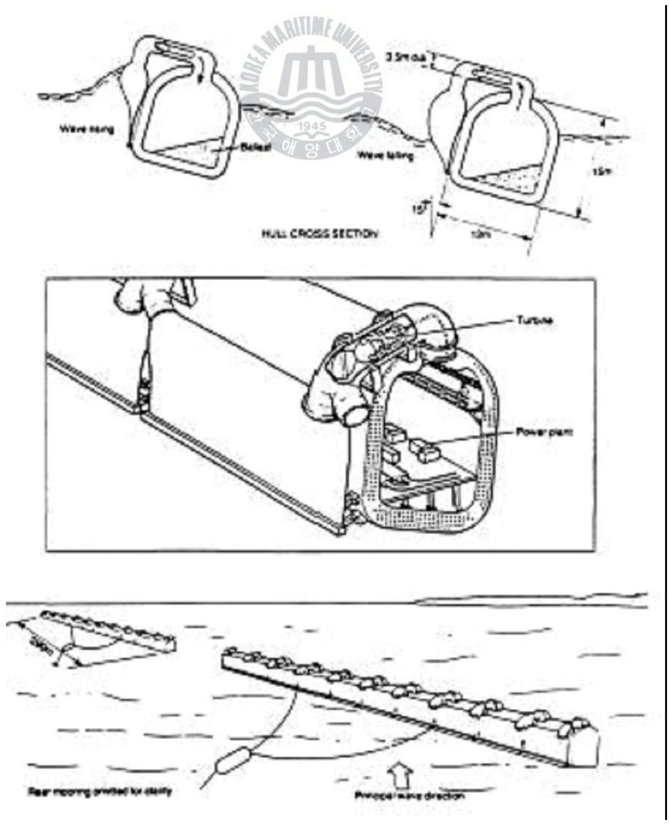

Figure A.73 Sea Clam [24]

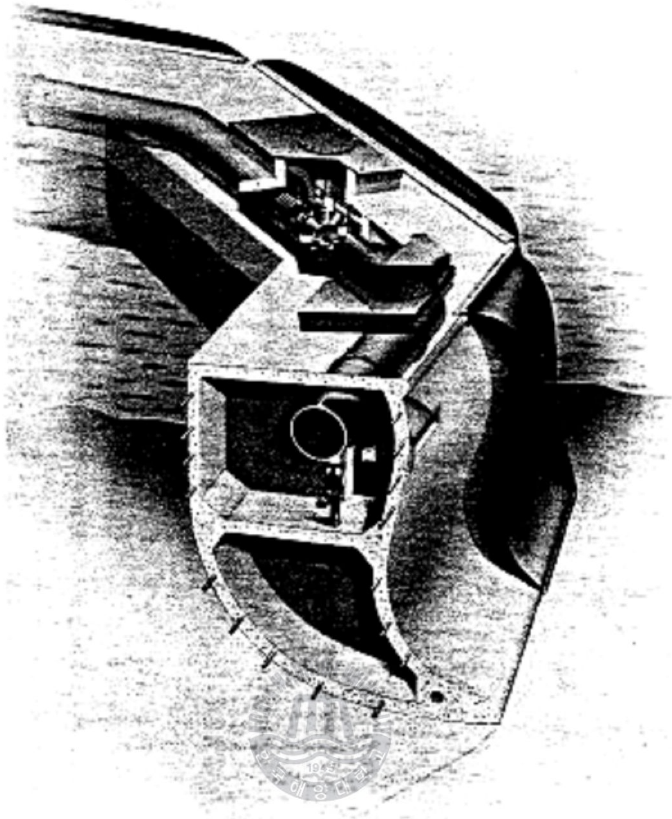

Figure A.74 Circular SEA Clam design-concrete hull.[24]

A.3.3.5.2 PS Frog

In 1986, the design of the PS Frog was started at the Lancaster University UK. This WEC operates on wave pitch and surge. Power extraction was twice as great in the anti-symmetrical mode to the waves as compared to the symmetrical mode such as heaving. Of the six fundamental modes, only heaving, pitching and surging are coupled to the waves and thus pitching and surging is a natural choice for wave energy extraction. The PS Frog generates power by working against a moving mass. The PS Frog's upper paddle shape is the working surface while the lower cylindrical part contains the moving mass, and power generation equipment.

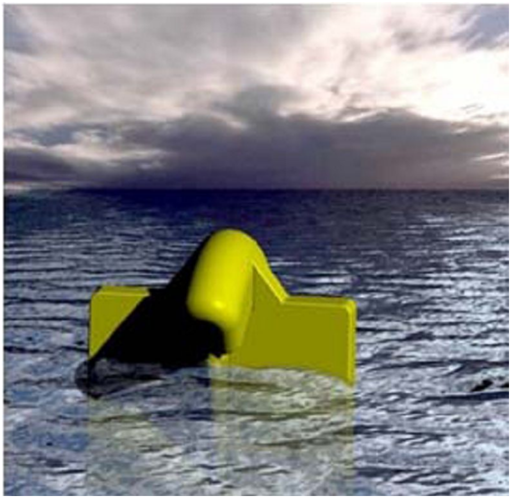

Figure A.75 Artist's impression of the PS Frog of Lancaster University [53]

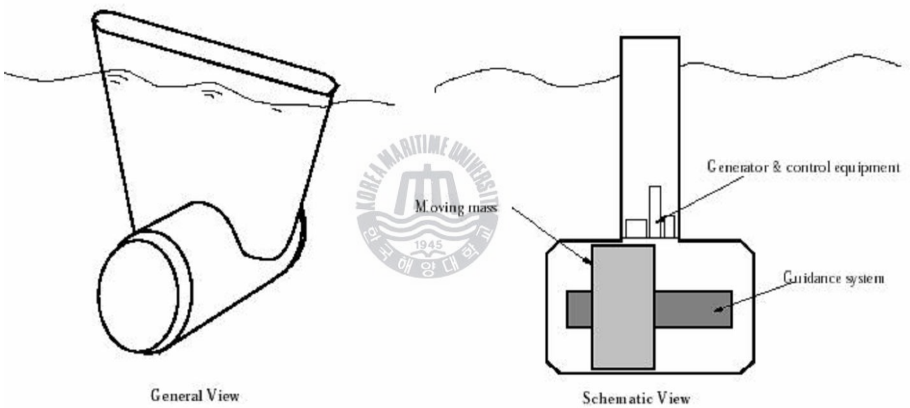

Figure A.76 The first version of the PS Frog with schematic view [11]

The 400-ton moving mass slides back and forth on guide rails, restrained by hydraulic rams connected on either side of the mass. Valves control the flow from the hydraulic rams, shutting the valves off holds the hydraulic rams in place. Opening the valves allows the hydraulic rams to pump high pressure hydraulic fluid, which turns a hydraulic motor coupled to an electric generator. A hydraulic accumulator provides energy storage and smoothing of the hydraulic flow. Switching the valves to a low pressure oil system, the mass experiences little resistance from the hydraulic rams. By controlling the phase relationship of the PS Frog's quasi-resonance relative to the sea waves through valve action, maximum wave energy is captured. . For the newer PS Frog (Mark III) the paddle shape was made shallower by 21m wide, to lower the radiation coefficient while increasing the center of pressure. This reduces the size of the slider mass. The Mark III PS Frog has a 12mm thick welded steel hull (24 mm near the bottom) with an overall weight of the steel structure of 110 ton displacing 1300 ton [11].

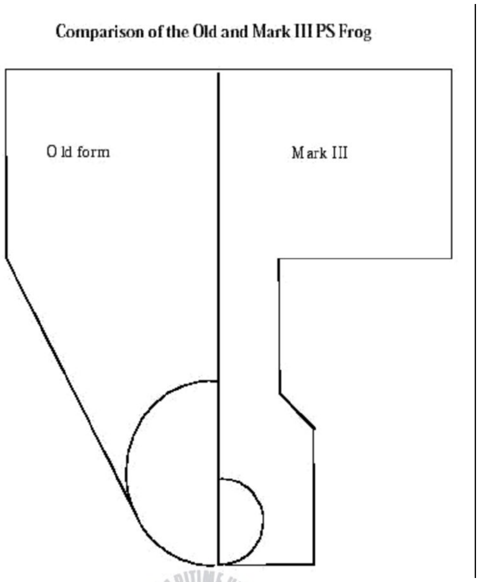

Figure A.77 IPS Frog - Old versus New Mark III form [11]

Electricity is transmitted to the shore through undersea cables. The PS Frog is connected to the sea bed by compliant mooring and can operate at wide range of depths, with 40 m being the optimum [63]. A linear array can be achieved by placing multiple units together. The earlier design was less efficient, as shown in Fig. A.7 The differences between the Frog and PS Frog are discussed in Robert H Bracewell's paper "Frog and PS Frog: A Study of Two Reactionless Ocean Wave Energy Converters" for which he received his Ph.D. in 1990. Essentially the PS Frog was developed to correct inherent problems in the Frog. While the newer PS Frog operates on a pitching and surging action of incident waves, the Frog was a heaving, vertically axis-symmetrical buoy, and 15-20m wide. Thus the power capture width of the Frog was one half that of the PS Frog.

Table A.7 Productivity Analysis of PS Frog [11]

Summary of the Productivity Analysis of PS Frog

Power in Sea	50 kW/m
Device Width	21 m
Directionality	0.94
Mean Power Intercepted	987 kW
Capture Efficiency	66 %
Power Captured	651 kW
Conversion Efficiency	92 %
Electrical Efficiency	88 %
Availability	93 %
Average Power Output	529 kW
Annual Output	4.3 GWh

A.3.3.5.3 Mace

Developed by Developed by Edinburgh University, U.K., the swinging mace is a bottom-hinged vertical spar with enlarged head that swings back and forth on a universal joint due to wave surge. The swinging action drives a ring-cam pump that causes water to be forced in and out of the anchored base to drive a hydraulic ram up and down.

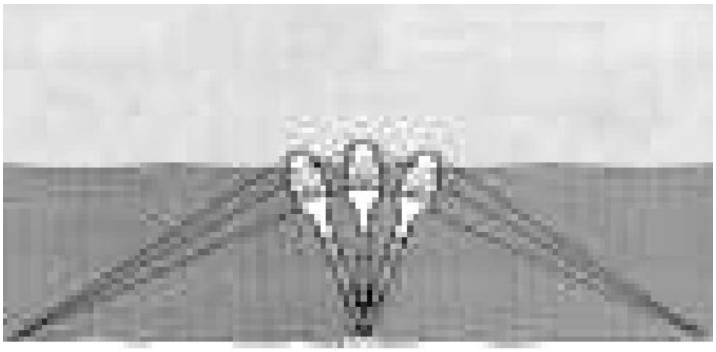

Figure A.78 The Mace wave energy converter [29]

APPENDIX A REFERENCES

[1] Wavegen. (2005a, 06/15/2005). "The Collector & Oscillating Water Column." Retrieved June 16, 2009, from http://www.wavegen.com/not_used/osprey_owc.htm.

[2] Batley, S. (1996). "Power from the waves." Retrieved 06/16/2009, from http://www.iesd.dmu.ac.uk/wind_energy/sustainable_dev/wcwave.html.

[3] Wavegen. (2005a, 06/15/2005). "The Collector & Oscillating Water Column." Retrieved June 16, 2009, from http://www.wavegen.com/not_used/osprey_owc.htm.

[4] Wavegen. (2005b, 06/15/2005). "Islay." Retrieved June 16, 2009, from http://www.wavegen.com/what_we_offer_limpet_islay.htm.

[5] "Energie Perspektiven."(2005). Max-Planck-Institu für Plasmaphysik. Retrieved June 16, 2009, From http://www.ipp.mpg.de/ippcms/ep/ausgaben/ep200203/bilder/0302_stroemung_dia.html.

[6] "Welcome to Energetech."(2005). Energetech Australia Plty Ltd. Retrieved June 16, 2009, from http://www.energetech.com.au/.

[7] Mylonas, E. M. (2002). "Introduction to an Advanced Hybrid (Wave & Wind) Renewable Energy Technology (RET) Multipurpose System." DAEDALUS Informatics Ltd. Retrieved September 17, 2009, from http://www.daedalus.gr/DAEI/PRODUCTS/RET/General/RETWW0.html.

[8] O'Mara, K., and Jennings, P. (1999). "Wave Energy Systems." Murdoch University. Retrieved June 16, 2009, from http://reslab.com.au/resfiles/wave/text.html.

[9] Thorpe, T. W. (1999a). "Economic Analysis of Wave Power Devices." AEA Technology, Oxfordshire, UK. Retrieved September 23, 2009, from http://www.waveenergy.net/Library/Economic%20Analysis%20of%20Wave%20Power.pdf.

[10] Thorpe, T. W. (1999b). "An Overview of Wave Energy Technologies:Status Performance and Cost." Wave Power Moving Towards Commerical Viability, Broadway House, Westminster,London. Retrieved, from http://www.waveenergy.net/Library/An%20Overview%20of%20Wave%20Energy.pdf.

[11] Thorpe, T. W. (1999). "A Brief Review of Wave Energy." Prepared for the UK Department of Trade and Industry. Retrieved June 16, 2009, from http://www.dti.gov.uk/energy/renewables/publications/pdfs/r120w97.pdf.

[12] "Harvesting the power of the ocean."(2005). WAVEenergy. Retrieved September 17, 2009, from http://www.waveenergy.no/.

[13] "Region 1: New England S.D.E. Energy Ltd."(2005). U.S. Environmental Protection Agency. Retrieved September 10, 2009, from http://www.epa.gov/region1/assistance/ceit_iti/tech_cos/sde_edl.html.

[14] "The Collector & Oscillating Water Column."(2005, June 15 2005). Wavegen. Retrieved June 16, 2009, from http://www.wavegen.com/not_used/osprey_owc.htm.

[15] Thompson, P. A., Pridden, D., and Griffiths, J. W. (2003). "Offshore Renewables: Collaborating for a Windy and Wet Future?" Retrieved June 18, 2009, from http://www.owen.eru.rl.ac.uk/documents/BWEA23/BWEA23_Thompson_Wind&Wave_ paper.pdf.

[16] "The Pneumatically Stabilized Platform or PSP - How it works."(2005). Float Incorporated. Retrieved June 16, 2009, from http://www.floatinc.com/How.html.

[17] "Wavemill."(2001). Wavemill Energy Corp. Retrieved June 18, 2009, from http://www.wavemill.com/.

[18] Ross, D. (1995). Power from the Waves, Oxford University Press Inc., New York. "S.D.E. Sea Wave Power Plant."(2005). Shmuel Ovadia. Retrieved September 10, 2009, from http://www.sde.co.il/.

[19] Washio, Y., Osawa, H., and Ogata, T. (2001). "The Open Sea Tests of the Offshore Floating Type Wave Power Device "Mighty Whale" - Characteristics of Wave Energy Absorption and Power Generation." OCEANS, MTS/IEEE Conference and Exhibition, 1, 579-585.

[20] "Offshore Floating Wave Energy Device Mighty Whale."(1998). Wave Energy Research and Development at JAMSTEC. Retrieved June 30, 2009, from http://www.jamstec.go.jp/jamstec/MTD/Whale/.

[21] "Making Wave Energy Work."(2003). ORECon Ltd. Retrieved June 18, 2009, from http://www.orecon.com/.

[22] Seymour, R. J. (1992). Ocean Energy Recovery: The State of the Art, American Society of Civil Engineers, New York, N.Y.

[23] "Backward Duct Buoy."(2003). National Institute of Ocean Technology. Retrieved June 17, 2009, from http://www.niot.res.in/m1/BBDB.htm.

[24] "Sea Power Waves of Nature."(2005). Sea Power AB International. Retrieved June 18, 2009, from http://www.seapower.se/indexeng.html.

[25] "Wave Dragon."(2003). Waveenergy.dk. Retrieved May 26, 2009, from http://www.waveenergy.dk/wave_teknik/2dk_anlaeg/wavedragon/teknik_wavedragon.ht ml.

[26] "A Large Offshore Wave Energy Converter."(2005). Wave Dragon. Retrieved June 18, 2009, from http://www.wavedragon.net/.

[27] O'Mara, K., and Jennings, P. (1999). "Wave Energy Systems." Murdoch University. Retrieved June 16, 2009, from http://reslab.com.au/resfiles/wave/text.html.

[28] Duckers, L. (2000). "Wave Energy." Open University - The Update Supplement for the 'Renewable Energy' book. Retrieved September 10, 2009, from http://technology.open.ac.uk/eeru/t265/update/wave.htm.

[29] "Chapter 3 Energy Alternatives."(2001). The Centre for Sustainable Development, The University of Cambridge. Retrieved June 17, 2009, from http://www7.caret.cam.ac.uk/chapter_3.pdf.

[30] "Pelamis."(2005). Ocean Power Delivery Ltd. Retrieved September 25, 2009, from http://www.oceanpd.com/.

[31] "Recent Developments: Waiting for the Waves."(2003). The IEA Ocean Energy Systems Newsletter Issue 2. Retrieved June 16, 2009, from http://www.ieaoceans.org/newsletters/news2.pdf.

[32] "The Waveberg System for Offshore Wave Energy Harvesting." Waveberg Development Limited. Retrieved September 20, 2009, from http://waveberg.com/index.htm.

[33] Hopfe, H., Enet, F., and Chavez, M. (2003). "The Wave Energy Module (WEM)." Pacific Energy News. Retrieved September 15, 2009, from http://www.spc.org.nc/preface/press%20releases/PEN%20Issue%20Jan%2003.pdf.

[34] "Ocean Wave Energy Converter." Ocean Wave Energy Company. Retrieved September 16, 2009, from http://www.owec.com/.

[35] Ashby, T. (1995). "Cheap Wave Power Hopes Pinned on Infant Technology." Reuters Information Services. Retrieved June 17, 2009, from http://www.iath.virginia.edu/~meg3c/id/id_acrich/Wave_energy.html.

[36] Danielsson, O. (2003). "Design of a Linear Generator for Wave Energy Plant." Retrieved June 16, 2009, from http://www.el.angstrom.uu.se/meny/artiklar/Design%20of%20a%20linear%20generator %20for%20wave%20energy%20plant4.pdf.

[37] "Renewable Energy Out of Ocean Waves."(2002). Archimedes Wave Swing BV. Retrieved June 16, 2009, from http://www.waveswing.com/index/index.html.

[38] "Welcome to the Archimedes Wave Swing Web Site."(2004). Archimedes Wave Swing. Retrieved September 24, 2009, from http://www.waveswing.com/.

[39] "The Power of Waves, the Future of Energy."(2004). Ocean Power Technologies, Inc. Retrieved September 13, 2009, from http://www.oceanpowertechnologies.com/.

[40] Taylor, G. W. (2002). "Using Wave Power for Energy: Issues in Design and Deployment." Ocean Power Technologies, Inc. Retrieved June 18, 2009, from http://www.oceanpowertechnologies.com/pdf/montreaux_energy.pdf.

[41] "AquaEnergy Group Ltd."(2005). AquaEnergy Group Ltd. Retrieved September 13, 2009, from http://aquaenergygroup.com/index.php.

[42] "Marine Energy Challenge." Carbon Trust. Retrieved September 20, 2009, from http://www.thecarbontrust.co.uk/ctmarine2/Page1.htm.

[43] "Wave Power."(2005). EUREKA 2278 WWEC. Retrieved September 13, 2009, from http://www.eureka.be/inaction/viewSuccessStory.do?docid=18099.

[44] Clément, A., McCullen, P., Falcão, A., Fiorentino, A., Gardner, F., Hammarlund, K., Lemonis, G., Lewis, T., Nielsen, K., Petroncini, S., Pontes, M. T., Shild, P., Sjöström, B.-O., Sørensen, H. C., and Thorpe, T. (2002). "Wave Energy in Europe: Current Status and Perspectives." Renewable and Sustainable Energy Reviews, 6, 405-431. Retrieved, from http://www.poemsinc.org/papers/2002WEstat.pdf.

[45] "Point Absorber."(2001). Waveenergy.dk. Retrieved September 18, 2009, from http://www.waveenergy.dk/wave_teknik/2dk_anlaeg/pointabsorber/teknik_pointabsor.ht ml.

[46] "The Wave of the Future is Here."(2002). Ocean Motion International. Retrieved September 16,2009, from http://www.oceanmotion.ws/.

[47] "A Paradigm Shift in the Generation of Energy!"(2004). Independent Natural Resources Inc. Retrieved September 16, 2009, from http://www.inri.us/pages/1/index.htm?gen_time=1083949891616#.

[48] "Ocean Wave Energy Conversion System." SARA Inc. Retrieved June 30, 2009, from http://www.sara.com/energy/energy.html.

[49] Taylor, J., and Mackay, I. (2001). "The Design of an Eddy Current Dynamometer for a Freefloating Sloped IPS Buoy." International Conference on Marine Renewable Energies. Retrieved June 17, 2009, from http://www.mech.ed.ac.uk/research/wavepower/sloped%20IPS/Maritec2001%202.htm.

[50] "SeaVolt Technologies Company Profile." Yahoo! Finance - Industry Center - Diversified Utilities. Retrieved September 13, 2009, from http://biz.yahoo.com/ic/105/105092.html.

[51] "SeaVolt Technologies." SeaVolt Technologies. Retrieved September 13, 2009, from http://www.seavolt.com/product.html.

[52] "Wave Rotor."(2005). EcoFys. Retrieved September 14, 2009, from http://www.ecofys.nl/nl/expertisegebieden/product_systeemontwikkeling/waverotor.htm.

[53] "Marine Energy Challenge." Carbon Trust. Retrieved September 20, 2009, from http://www.thecarbontrust.co.uk/ctmarine2/Page1.htm.